SYNTHESIS AND CHARACTERIZATION OF POLYMERIZABLE PHOSPHOLIPIDS AND RELATED POLYMERS

BY

JUNG-HUA STEVEN KUO

A DISSERTATION PRESENTED TO THE GRADUATE SCHOOL
OF THE UNIVERSITY OF FLORIDA IN PARTIAL FULFILLMENT
OF THE REQUIREMENTS FOR THE DEGREE OF
DOCTOR OF PHILOSOPHY

UNIVERSITY OF FLORIDA

1992

ACKNOWLEDGEMENTS

I would first like to express my deepest appreciation and gratitude to my advisor, Dr. E. P. Goldberg, who offered me the opportunity to work on various exciting biomedical research projects. His guidance, kindness, advice, patience, and continued encouragement has been indispensable. I am also grateful to Dr. A. Jakakrishman, for his assistance and contribution in organic synthesis. Much acknowledgement must be accorded to the members of my supervisory committee, Drs. A. B. Brennan, C. D. Batich, B. M. Moudgil, and R. S. Duran, for their discussions and suggestions. I would like to acknowledge Dr. H. Hattori for his friendship, advice, and assistance; and for his skill in surgery and drawing. I also wish to acknowledge Rudy Strohschein at the chemistry glass shop and all my friends in the macromolecular center for their assistance. I am grateful to P. Martin for the epithelial cell adhesion study and Nina Klingman-Baptist for the vascular endothelial cell and platelet adhesion study.

I am grateful to Dr. Romulo Ochoa for his help with ellipsometric measurements. Appreciation also goes to all my friends and colleagues in the biomedical engineering center for their ever-present assistance. Special thanks go to two great Illinois friends, Dr. Jean Quigg and Wendy Knepp, for their unwaivering encouragement. I also cannot find words which are adequate to thank Drs. Eric Luo, S.-W. Shang and D.-G. Chen for their everlasting friendship and help. Lastly and most important of all, I thank my parents for their understanding and constantly encouragement. This work is dedicated to them.

TABLE OF CONTENTS

ACKNOWLEDGEMENTS ii

ABSTRACT v

CHAPTERS

I. INTRODUCTION 1

II. BACKGROUND 4

2.1 Biomembranes 4
2.2 Polymerizable PLs 6
2.3 Interfacial Phenomena of Biomaterials 9
2.4 PL Surface Modification 10
2.5 Surface Modification Techniques 12
2.6 IOL Implants 14
2.7 Thrombogenicity of Vascular Devices 18
2.8 Summary of Previous Research 24

III. MATERIALS AND METHODS 26

3.1 Synthesis of Bis[(methacryloyloxyethylene)adipoyl]-L-α-phosphatidylcholine (HEMA-PL) 26
3.1.1 Synthesis of (Methacryloyloxyethylene)mono adipate 26
3.1.2 Synthesis of Bis-(methacryloyloxyethylene)-adipic Anhydride 28
3.1.3 Acylation of L-α-glycerophorylcholine (GPPC) 29
3.2 Synthesis of 12-PL 39
3.2.1 Synthesis of 12-(Methacryloyloxy)dodecanoic Acid 31
3.2.2 Synthesis of 12-(Methacryloyloxy)dodecanoic Anhydride 31
3.2.3 Acylation of GPPC 32
3.3 Substrates 32
3.4 Plasma Pretreatment of Substrates 32
3.5 Phospholipid Dispersion 35
3.6 UV Irradiation 35
3.7 Gamma Irradiation 36
3.8 Characterization 36
3.8.1 Contact Angle Measurements 36
3.8.2 Fourier Transform Infra-Red/ Attenuated Total Reflectance (FTIR/ATR) 41
3.8.3 X-ray Photoelectron Spectroscopy (XPS) 41
3.8.4 Scanning Electron Microscopy (SEM) 44
3.8.5 Optical Microscopy 44
3.8.6 Ultraviolet-Visible (UV-VIS) Spectroscopy 44
3.8.7 Synthesis Characterization 44
3.8.8 Ellipsometry 45

3.9 In Vitro 47
3.9.1 Epithelial Cell Adhesion 47
3.9.2 Corneal Endothelium Damage Testing 47
3.9.3 Vascular Endothelial Cell and Platelet Adhesion 49

IV RESULTS AND DISCUSSIONS 50

4.1 Synthesis and Characterization of HEMA-PL 50
4.1.1 (Methacryloyloxyethylene)mono adipate Synthesis and Characterization 50
4.1.2 Bis(methacryloyloxyethylene)-adipic Anhydride Synthesis and Characterization 52
4.1.3 HEMA-PL Synthesis and Characterization 52
4.2 Synthesis and Characterization of 12-PL 55
4.2.1 12-(Methacryloyloxy)dodecanoic Acid Synthesis and Characterization 57
4.2.2 12-(Methacryloyloxy)dodecanoic Anhydride Synthesis and Characterization 57
4.2.3 12-PL Synthsis and Characterization 60
4.3 Phospholipid Dispersion 60
4.4 Surface Modification of PMMA with HEMA-PL by Gamma Radiation 63
4.4.1 Contact Angle(C.A.) Measurements 67
4.4.2 UV-VIS Spectroscopy 67
4.4.3 SEM 71
4.4.4 FTIR/ATR 71
4.4.5 XPS 75
4.4.6 Structure and Stability of HEMA-PL Grafts 79
4.4.7 Graft Thickness Measurements 84
4.4.8 Epithelial Cell Adhesion and Corneal Cell Damage Testing 88
4.4.9 Summary of Surface Modification of PMMA with HEMA-PL 92
4.5 Surface Modification of PMMA with Hema lipid by Plasma/ gamma Method 94
4.5.1 RF Plasma Pretreatment 95
4.5.2 "Plasma/gamma" method 95
4.5.3 Epithelial Cell Adhesion 103
4.5.4 Vascular Endothelial Cell and Platelet Adhesion 107
4.5.5 Summary of Surface Modification of PMMA with HEMA-PL by RF Plasma/gamma Method 109
4.6 Surface Modification of PMMA with 12-PL by UV and Plasma/UV Methohs 110
4.6.1 Graft Characterization 110
4.6.2 Epithelial Cell Adhesion 117
4.6.3 Vascular Endothelial Cell and Platelet Adhesion 119
4.6.4 Summary 123
4.7 Surface Modification of PP and PDMS with 12-PL by UV Radiation 124
4.7.1 Surface Modification of PP with 12-PL by UV Radiation 124
4.7.2 Surface Modification of PDMS with 12-PL by UV Radiation 129
4.8.Miscellaneous Study 140

V. SUMMARIES AND CONCLUSIONS 143

LIST OF REFERENCES 146

BIOGRAPHICAL SKETCH 153

Abstract of Dissertation Presented to the Graduate School
of the University of Florida in Partial Fulfillment of the
Requirements for the Degree of Doctor of Philosophy

SYNTHESIS AND CHARACTERATION OF POLYMERIZABLE PHOSPHOLIPIDS AND RELATED POLYMERS

By

Jung-Hua Steven Kuo

December, 1992

Chairman: Dr. Eugene P. Goldberg
Major Department: Materials Science and Engineering

It is well known that the biocompatibility of biomaterials is strongly influenced by the surfaces of these materials. The surfaces are totally different in structure and property from the bulk. Many attempts have been made to modify the surfaces of biomaterials in order to achieve more biocompatible devices. However, these approaches based on theoretical hypotheses have been unsuccessful because they do not adequately account for the complexity of biological mechanisms.

The goal for this research is to design biomaterials surfaces which better mimic biological membranes using phospholipids. Biomembranes, which contain phospholipids, proteins and polysaccharides, are known for their excellent biocompatibility. Two polymerizable phospholipid monomers (Bis[(methacryloxyethylene)adipoyl]-L-α-phosphatidylcholine (HEMA-PL) and Bis[12-(methacryloyloxy)dodecanoyl]-L-α-phosphatidylcholine (12-L)) were synthesized via improved synthesis pathways and characterized by IR and ^{1}HNMR. HEMA-PL is a novel compound not previously reported.

The present study has successfully demonstrated the feasibility of hydrophilic polyphospholipid surfaces of PMMA, PP, and PDMS by various surface modification techniques. These techniques involved gamma or UV radiation either separately or coupled with water RF plasma pretreatment. The resulting surfaces have been well characterized by contact angle measurements, FTIR/ATR, XPS, SEM, and UV-VIS. HEMA-PL modified PMMA has significantly less epithelial cell adhesion and corneal endothelial cell damage than unmodified PMMA. The ratio for endothelial/platelet cells adhesion for 12-PL modified PMMA was higher than one and platelet cell adhesion was substantially lower than unmodified PMMA. Thus, hydrophilic PL surfaces may improve biocompatibility.

CHAPTER I
INTRODUCTION

Polymeric biomaterials have been clinically used extensively in various applications such as prosthetic devices and surgical implants. Due to contact with living systems, the interfacial properties of these materials play a significant role in biocompatibility. Biocompatible surfaces must have appropriate interaction in biological environments. In the past, many attempts have been made to modify the surfaces of biomaterials in order to achieve more biocompatible devices. These approaches were based on the physicochemical surface science theories such as surface energy, surface chemistry, and morphology (28-32). However, these hypotheses do not successfully predict the behavior of complicated biological systems. The understanding of biological systems is still the most difficult part of designing improved biomaterials.

The goal of this study is to better mimic mother nature. Biological membranes provide the external structure of cells and are obviously biocompatible (1). One primary constituent of these biomembranes is phospholipids (PLs). PLs favor the formation of bilayer membranes in aqueous environments. This tendency derives from the chemical structure of the PL molecules, which contain both hydrophilic and hydrophobic regions. If biomembrane-like structures can be created on material surfaces, foreign body reactions triggered by the immune system may be minimized and the material may be better accepted as part of the biological system. However, naturally occurring PLs do not possess any active sites with which to interact chemically with polymeric substrates. Therefore, the design of modified PL containing reactive groups to polymeric substrates is important with the goal of improved biocompatibility.

The study of polymerizable PLs consisting of photoreactive groups has been reported by several groups (2, 3). However, only a few studies focus on surface

modification of polymers with polymerizable PLs (4). From a surface energy point of view, a monolayer of polymerizable PLs is expected to form at the interface of hydrophobic polymer/water mixtures. Subsequent polymerization can create a PL membrane on the polymer surface.

Several surface modification methods using radiation polymerization have been developed in this laboratory for grafting hydrophilic monomers onto polymer surfaces (5). These radiation techniques include gamma radiation-induced graft polymerization and a "plasma/ gamma" method. Gamma radiation-induced graft polymerization is carried out at the solid/water interface by free radical formation resulting in a chemically bonded hydrophilic graft on the polymer surfaces (6). Another surface modification technique is a plasma/ gamma method which can provide improved graft efficiency on some substrates compared to gamma radiation alone. This method combines Radio Frenquency (RF) plasma pretreatment of substrates followed by gamma radiation-induced graft polymerization. Active sites and increased hydrophilicity are generated on the substrates by RF plasma which increases the monomer concentration available at the interface during gamma polymerization and facilitates the production of more free radical sites on the substrate surface by gamma radiation.

UV radiation is another surface modification technique and has also been used to graft polymerizable PLs, Bis[12-(methacryloyloxy)dodecanoyl]-L-α-phosphatidylcholine (12-PL),onto Poly(methyl methacrylate) (PMMA) surfaces by J. Larson (7). The modified surfaces have been evaluated for improved ophthalmic implant surfaces. However, the yield of 12-PL synthesis was somewhat unsatisfactory.

In this study, a novel polymerizable PL with shorter hydrophobic tails than the 12-PL but retaining the same hydrophilic head was synthesized and grafted on PMMA using either gamma or plasma/gamma methods. The grafts were then compared to PMMA samples grafted with the 12-PL via UV radiation. The synthesis of the 12-PL was modified to increase its yield. The 12-PL was also grafted onto several other polymer

substrates by UV radiation. Some of the polymeric substrates were treated with water vapor plasma prior to the UV grafting. These biomembrane-like surfaces exhibit interesting surface properties but retain the bulk properties of the biomaterial substrate. Such biomembrane surfaces in this study are of particular interest for Intraocular Lens (IOL) implants and vascular implant device applications.

The primary objectives of this study were therefore as follows:

(1) High yield synthesis of novel polymerizable PL and 12-PL monomers which have polymerizable functional groups.

(2) Preparation of polymeric biomaterials with hydrophilic PL surfaces using these polymerizable PL monomers by surface modification methods.

(3) Surface characterization (physical, chemical and biological) of PL surface modifications.

(4) Preliminary evaluation of the biocompatibility of IOL and vascular biomaterials with hydrophilic PL surfaces.

CHAPTER II
BACKGROUND

2.1 Biomembranes

Biomembranes are organized assemblies consisting mainly of lipids, proteins and polysaccharides. The schematic organization of biomembranes by three interpretations is illustrated in Figure 1 (8). The first model (A) is the classical model of Davson and Danielli. Two layers of protein are located on either side of bimolecular leaflet of mixed lipid with its hydrophilic heads directed outward. The fluid-mosaic model (B) has been used to describe arrangements of lipids and proteins (8, 9). The major aspects of this model are that lipids are in bilayer form interact specifically with particular membrane proteins, and membrane proteins can diffuse laterally in the lipid matrix unless restricted by special interactions. The third model (C) features that the bulk of proteins is within the lipid matrix, but polysaccharide chains of glycoprotein and glycolipid constituents project above the surface. Either model B or C is more consistent with free-cleaving images of biomembranes than A. The functions of biomembranes include construction of cell walls, formation of permeability barriers, rejection of toxins, and recognition of cells (10).

PLs, the major class of membrane lipids, are derived from either glycerol or sphingosine. A phosphoglyceride, a PL derived from glycerol, consists of a glycerol backbone, two fatty acid chains, and a phosphorylated alcohol (11). A phosphatidate is a lipid in which the hydroxyl groups at C-1 and C-2 of glycerol are esterified to the carboxyl groups of two fatty acid chains and the C-3 hydroxyl group of the glycerol backbone is esterified to phosphoric acid. Furthermore, the phosphate group of phosphatidate is esterified to the hydroxyl group of one of several alcohols which moieties of

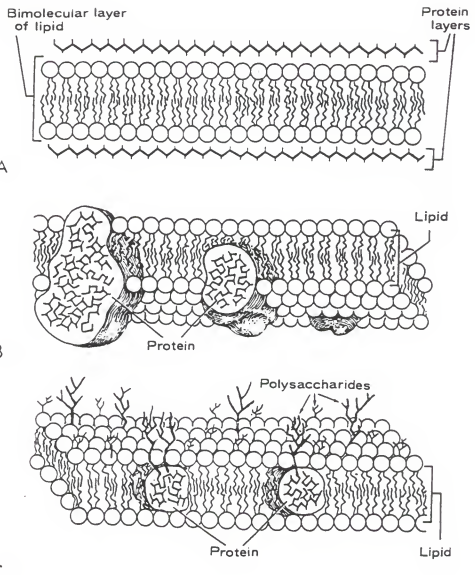

Figure 1. The schematic organization of biomembranes (8)

phosphoglycerides are serine, ethanolamine, glycerol, inositol, and choline (12). The chemical structure of phosphatidylcholine, or lecithin, is shown in Figure 2.

In surface chemistry terminology, PLs which contain both hydrophilic and hydrophobic moieties are called amphiphilic molecules. The hydrophilic unit, which is a polar head group, will have affinity for water whereas the hydrophobic tails will avoid water. The formation of bilayers from PLs in water with head groups on the surface and hydrocarbon tails inside, is a spontaneous process because the Gibbs free energy of the system is reduced by minimizing the number of exposed hydrocarbon chains (13). Lipid vesicles, or so called "liposomes," are closed spherical structures consisting of a lipid bilayer with an aqueous interior and can be formed by sonication of PL suspensions (Figure 3). However, liposomes are often unstable for long term use although there is considerable ongoing research aimed at improving liposome stability and using them as drug carriers (14, 15).

2.2 Polymerizable PLs

Chakrabarti and Khorana were perhaps the first to propose the general concept of polymerizable PLs (2). They proposed that lipids carrying photoreactive groups could covalently link the lipid molecules by UV irradiation. This concept was extended to other amphiphilic molecules carrying polymerizable groups (3). To date, a variety of polymerizable structures have been synthesized such as acryloylic, methacryloylic, diacetylenic,butadienic,vinylic, and maleic (16, 17). Depending on the purpose of the study, the position of polymerizable groups may be in the hydrophilic head group or in the hydrocarbon tails (18). Polycondensation reactions as well as addition type polymerization can also be used to form polymerized amphiphilic molecules (19). The stability of biomembranes increases by crosslinking via polymerization of photoreactive groups (16).

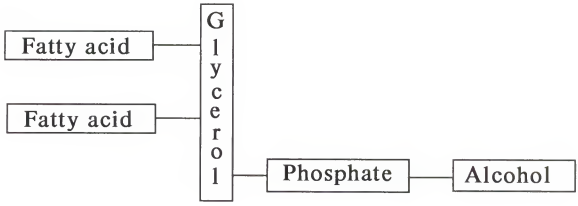

Components of a phosphoglyceride

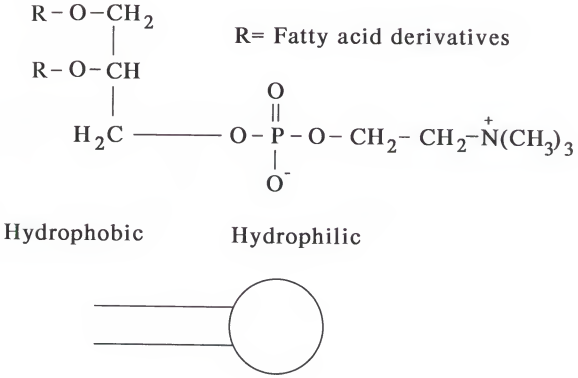

Figure 2. The chemical structure of phosphatidylcholine (12)

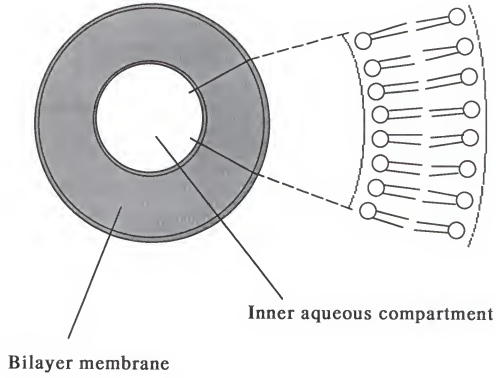

Figure 3. The diagram of a lipid vesicle (12)

Among the different approaches to the synthesis of polymerizable glycerophospholipids, the acylation of glycero-3-phosphorylcholine (GPPC) is most commonly used because of the preformed PL backbone structure (20). The reagents used for acylation of GPPC are fatty acyl chlorides, anhydrides, and mixed anhydrides. Various methods have been introduced for the acylation of GPPC but all have proved to be somewhat unsatisfactory (21, 22). However, Gupta et al. found that N,N-dimethyl-4-aminopyridine, a powerful base catalyst in many organic reactions, was very efficient in the acylation of GPPC. This method offered the following advantages over previous methods: high yields (75-90%), low temperature (ambient), and moderate amounts of fatty acry anhydrides (1.2-1.5 mol per OH group in GPPC) (20).

To investigate biomembrane models, three systems have been most commonly used to study polymerizable PLs : monolayers at the gas/water interface, bimolecular lipid membrane (BLM), and liposomes (18, 23, 24). Physical membrane properties such as stability, permeability, morphology, fluidity, and phase behavior have been extensively studied. Among those three systems, liposomes have been most widely studied. In addition to investigation of biomembrane models, polymerizable liposomes also have a variety of potential applications in controlled drug delivery, photochemical energy transfer, and the novel approach of surface modification of polymers (4).

2.3 Interfacial Phenomena of Biomaterials

Adhesion of biological molecules is probably the most important interfacial phenomenon for biomaterials (25). Because the surfaces of a biomaterial are directly interfaced with biological environments, the surfaces play a crucial role in avoiding adverse interfacial responses. Therefore, the biocompatibility of implant devices depends upon an appropriate interaction between biomaterials and biological environments. Depending on

the particular application of an implant device, adherence of biological molecules may be either a positive or negative attribute (26).

Adsorption of proteins occurs when implant surfaces contact biological media (27). Protein adsorption to implant surfaces can facilitate specific cell attachment to the protein molecules. Adsorbed cells can interact with cell membrane receptor sites, stimulating cellular interactions such as adhesion, spreading, and growth (28). The amount and nature of adsorbed proteins are strongly dependent on the characteristics of the material surface. Horbett suggested that hydrophilic surfaces do not easily adsorb certain proteins in comparison to hydrophobic surfaces (29). However, albumin from human plasma has a preference for hydrophilic surfaces. In contrast, Ishikhara et al. reported that albumin adsorption from human plasma is reduced on PL surfaces (30).

Based upon physicochemical models, there are various hypotheses to predict surface properties of biocompatible implants. Parameters include surface energy, surface chemistry, morphology, ionicity, compliance, dynamic motions, water content, and electrical conductivity (31-35). However, none of these hypotheses adequately predict the adhesion mechanisms of a biological response (36). Nature has its own complicated ways to interact with foreign surfaces and therefore gives an incentive to develop more biomimetic compositions, i.e. polymerizable PLs, for improving the biocompatibility of implant surfaces.

2.4 PL Surface Modification

Polymerized PLs have been studied for solar energy conversion and as drug carriers, but rarely for surface modification.(4) The deposition of phosphatidylcholines with diacetylene in two acyl chains on a variety of substrates can be accomplished by using Langmuir-Blodgett methods (37). After lipid multilayers were established, ultraviolet radiation was used to polymerize the diacetylene groups and link the PLs together with a conjugated chain consisting of alternating single, double, and triple bonds. A stable

hydrophilic surface was produced on a variety of substrates including glass, quartz, Perspex ,Teflon, and steel.

Albrecht et al. suggested that several phosphorylcholine derivatives with hydroxyl-reactive groups were covalently coupled with glass and silica surfaces containing hydroxyl groups by chemical pretreatment (38). The hydroxyl groups were generated on the substrate surface by reaction with mono- and bifunctional reagents. The evidence of covalent modification of the treated surfaces was provided by IR spectroscopy showing the removal of surface hydroxyl group. The modified surfaces were stable at a temperature of 375°C. Polymerized PLs were suggested to display many advantages such as hydrophilic surfaces, nonthrombogenicity, low antigenic potential, low permeability, and chemical stability, as compared to other types of thromboresistant polymers.

PL surface modification of polyethylene film was reported by Regen et al. 12-PL was synthesized and sonicated to form liposome dispersions (4). Polyethylene film immersed in the dispersion, followed by 254 nm ultraviolet radiation and washed with water yielded a hydrophilic surface as measured by water contact angle measurement (35°). A carbonyl band and ester group in the polymerized PL were detected by IR-ATR spectrum. A significantly improved procedure for the synthesis and surface modification polymerization of 12-PL was developed by Larson in this laboratory (7). Hydrophilic PMMA surfaces were produced by UV-initiated polymerization of divinyl PL adsorbed at the water-polymer interface and evaluated for improved ophthalmic implant surfaces. The modified surfaces had low interfacial free energy and negligible tissue adhesion force. Also, uniform coverage of polymerized PL was suggested by angular XPS. Synthesis of poly(2-methacryloyloxyethyl phosphorylcholine) was prepared by Ishihara et al.and it was copolymerized with n-butyl methacrylate (39). The resultant polymer was coated onto acrylic beads and used to study thrombogenicity. They concluded that PL polar groups significantly reduced the adsorption of platelets from human plasma to the modified surface.

2.5 Surface Modification Techniques

In addition to UV radiation and chemical means, there are some other surface modification techniques which can be conducted to incorporate polymerizable PLs onto a substrate surface. Primary objectives for PL surface modifications are to produce stable, chemically bound surface grafts. Two novel surface modification techniques, gamma radiation-induced graft polymerization and a plasma/gamma method, have been developed in this laboratory for grafting hydrophilic monomers onto polymeric substrates (40).

Gamma radiation is electromagnetic energy produced by a radioisotope source. Cobalt-60 is most commonly used because it provides a variety of advantages over the other radioisotope source (41). These advantages include high energy and penetration power, longer half-life, ability to activate relatively stable materials, i.e. free radical formation in polymeric substrates (42, 43). The effects of gamma radiation on polymeric substrates have been well reported (44). The radiolysis of polymers results in chain scission or crosslinking with the formation of free radicals. Polymers will degrade at high doses of radiation, the extent of degradation depending upon polymer structure. Free radicals can interact with oxygen and increase the degradation of polymers in the presence of air (45). The mechanism of free radical formation in various polymers, such as PMMA, PP, PDMS, have been fully discussed in the literature (46-49).

It is well known that gamma radiation can be used to initiate the polymerization of vinyl monomers in an aqueous medium (50). Initiation by gamma radiation can avoid contamination by chemical initiation means which might produce products unsuitable for use in biological environments. The kinetics of radiation polymerization have been reviewed by Chapiro (51). In general, the rate of polymerization is proportional to the square root of the rate of initiation and to the first power of monomer concentration at low dose rates ($< 10^3$ rad/min.).

Gamma radiation-induced graft polymerization can be carried out by chain transfer of growing chains to the polymeric substrate or by direct grafting to polymeric substrate through initiation by free radical formation in the substrate. Unique surface properties can be achieved on the polymeric substrate by gamma radiation with little change in bulk properties at low graft radiation doses. Considerable research has been performed in this laboratory involving the synthesis, characterization, and properties of hydrophilic polymer graftings. The permanent, covalently bound hydrophilic grafting of poly(vinylpyrrolidone) (PVP) on a variety of polymers has been studied in detail and evaluated for many biomedical applications (6).

A novel method termed "plasma/gamma" grafting, has also been recently developed in order to improve gamma radiation-induced graft polymerization on many substrates, especially for metals and glasses (5). This method involves RF plasma pretreatment of substrates, followed by gamma radiation-induced graft polymerization. The graft yield by gamma treatment alone may be low for some substrates because the reaction is a diffusion controlled process conducted at the solid/liquid interface in a dilute monomer medium (40). Grafting efficiency can be increased if additional active sites can be created on substrates by RF plasma pretreatment and if the surface is made more hydrophilic for hydrophilic monomer grafting in aqueous media.

Radio frequency plasma has been widely used to improve the surface wettability of polymers (52, 53). The glow discharge RF plasma is the result of accelerated electrons created by inductively coupled RF current at reduced pressure. The excited species are produced by the collision between accelerated electrons and gas molecules within the plasma chamber. Those excited species might be free radicals, ions, ion radicals, excited atoms and molecules, and UV radiation (54). Furthermore, free radicals can be generated on the polymer surface by energy transfer from those excited species to form highly polar surface layers.

The surface modification of PMMA ,PE, and PDMS by RF plasma pretreatment in water vapor has been investigated (40, 55, 56). The optimum power and treatment time with RF plasma to produce stable oxidized layers has been reported. Also, the oxygen content of the treated surface indicated that plasma pretreatment can generate a variety of oxygen-containing polar groups as determined by XPS analysis. A thin layer of oxidized species has been confirmed by angle-resolved XPS. Plasma surface activation followed by gamma radiation with aqueous NVP yielded more efficient grafting on PMMA and PDMS.

As discussed previously, surface modification of polymeric materials with functionalized PLs can be achieved by various initiation radiation methods. This represents a potentially useful way to design biomaterial surfaces which may combine the unique properties both of biomembranes and synthetic polymers. Biomembrane-like surfaces may have improved biocompatibility and be useful in a wide variety of biomedical applications. Current problems related to IOL implants and vascular devices have been specifically considered in this study.

2.6 IOL Implants

IOLs are ocular implants for restoring vision after cataract surgery. The natural crystalline lens is a unique visual tissue in the eye for visual acuity,as shown in Figure 4. A cataract is an opacification of the crystalline lens by insolublization of proteins (57). Cataracts are a major cause of impaired vision worldwide, affecting about 20 million people in 1990 (58). The formation of cataracts is believed to result from lens damage such as aging oxidation, UV light, diabetes, etc. (59, 60, 61). Congenital and genetic factors also contribute to the formation of cataracts in children (62). Drug therapy and other methods of cataract treatment are under investigation (63). Surgical extraction of the opacified crystalline lens remains the only way to prevent blindness. After cataract surgery, there are three alternatives to maintain visual acuity: spectacle lenses, contact lenses, and IOLs.

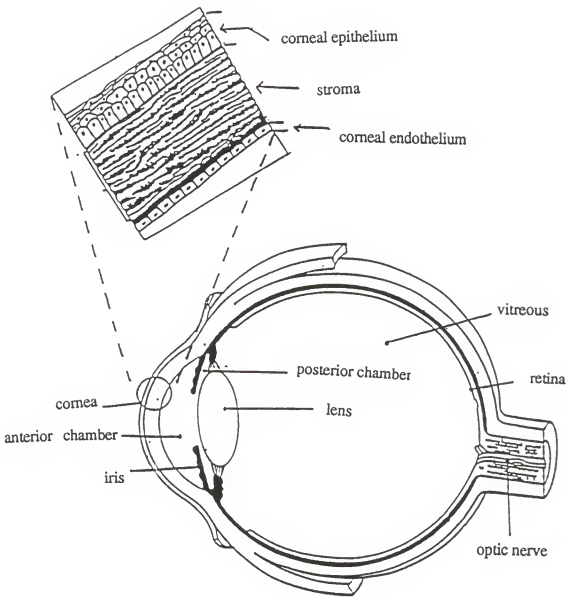

Figure 4. The schematic structure of the human eye (40)

Among these three alternatives, IOLs have proven to be the best treatment because they afford the most natural optical correction and avoid limitations of the other alternatives.

In 1949, Dr. Harold Ridley performed the first posterior chamber lens implantation in a human eye after cataract surgery (64). This idea came to him during World War II when he found that PMMA fragments from shattered aircraft canopies which penetrated into pilot eyes did not cause serious inflammation. Since then, IOL implantation has become one of the fastest-growing medical technologies and many improvements have been investigated. An IOL is commonly composed of an optic and two haptics used for fixation (Figure 5). Basically, there are currently two different optic materials : hard and soft. The material for hard optics is PMMA, whereas soft IOLs may be polydimethylsiloxane (PDMS) or hydrogels such as polyhydroxyethylmethacrylate (PHEMA). The haptics can be made of PMMA, PP, or polyvinylidinefluoride (PVDF) (65).

At present, PMMA remains the most widely used material for IOLs in spite of the fact that soft polymers offer unique properties such as small incision implantation (3.5 mm) (66). PMMA is an amorphous, thermoplastic polymer that has excellent optical clarity and biostability in the eye (67). It also has good mechanical properties such as dimensional stability (68). However, there are some limitations associated with PMMA. A large incision (> 6 mm) is required to insert the IOL due to the rigidity of PMMA. As a result, some patients may need more time to recover from trauma and astigmatism (69, 70). PMMA IOLs can not be sterilized by autoclaving because PMMA is not dimensionally stable at high temperatures. Additionally, it is now believed that some complications in surgery may be induced by the hydrophobic surface of PMMA. Those complications include corneal endothelium damage, abrasion of the iris, inflammation, fibrous exudate, and posterior capsule opacification (71).

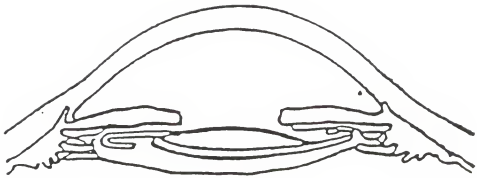

The location of IOL in the eye

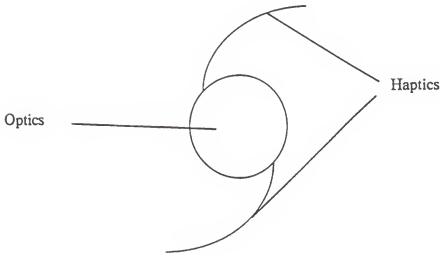

Figure 5. The location and components of IOL

Soft materials such as hydrogels may have improved biocompatibility because of their greater similarity to living tissues. Hydrogels are hydrophilic and have a high water content within their structure. However, the mechanical properties of hydrogels are generally very poor. Failure of hydrogels can be induced by mechanical manipulations (66). Improved hydrophilic materials for IOLs will require better mechanical properties. Hydrophilic surface modification of polymeric substrates can provide desired surface properties but maintain bulk properties and thereby combine the advantages of both hard and soft materials.

In the past decade, novel surface modified PMMA IOLs using NVP and other monomers have been developed using gamma-induced graft polymerization. Such IOLs have been successfully clinically tested, patented, and trademaked as Hydrograft ® surface modification by the University of Florida (72). The Hydrograft surface is hydrophilic and lubricous so corneal endothelium damage and iris abrasion are reduced (73). The surface does not adhere to tissue, surgical debris such as epithelial cells, or inflammatory cells (40). Consequently, Hydrograft IOLs may induce fewer complications than unmodified PMMA IOLs.

PL biomembranes may also have improved biocompatibility for implant surfaces. Larson reported that a PL surface modified PMMA IOL reduced corneal endothelium damage (7). However, no further ophthalmic studies, such as epithelial cell adhesion, have been reported to date. This research was aimed at extending Larson's preliminary study and to develop novel polymerizable PLs used for surface modified implants such as IOLs.

2.7 Thrombogenicity of Vascular Devices

The clinical application of vascular devices in contact with blood has been of great importance in modern medicine. The major restriction in the use of vascular implants is thrombosis of the surface (74). In the past, many researchers have attempted to develop

thromboresistant biomaterials. However, few truly blood compatible biomaterials have been reported because of the complexity of platelet activation and coagulation processes. Also, no generally satisfactory hypotheses have provided an explanation for development of haemocompatible biomaterial surfaces (75-78).

The reduction of blood loss from a wound (haemostasis) is shown in Figure 6. The normal blood vessel is lined with a cell layer of endothelium. Damage to vascular endothelium initiates a clotting cascade involving platelet aggregation and fibrin formation. After bleeding has been arrested, fibrin is degraded by fibrinolytic enzymes (i.e. plasmin). Wound healing involving collagen deposition and endothelial cell repair can then occur (79).

Exposure of blood to biomaterial surfaces can lead to platelet adhesion. Aggregation of platelets rapidly can take place (80). Adenosine diphosphate (ADP), in platelets, is believed to trigger the platelet reactions and cause degranulation of platelet cells. Eventually, activated platelets generate thrombin which results in the formation of a fibrin clot (Figure 7) (81).

Clotting is initiated in an injured vessel by platelet activation as well as by extrinsic and intrinsic pathways. The blood coagulation cascade is shown in Figure 8. The extrinsic pathway is usually not activated by contact with blood and involves a tissue factor which is a specific glycoprotein associated with PLs (82). On the other hand, the intrinsic pathway, the most important for biomaterials, is initiated by the exposure of nonendothelial surfaces. In either pathway, inactive zymogens convert to proteolytic enzymes.

The adsorption of Factor XII (Hageman Factor) upon a biomaterial surface initiates the intrinsic pathway. Factor XII is activated by the adsorption of coagulation proteins including Factor XII itself, Factor XI, prekallikrein, and high molecular weight kininogen (83). After the activation of cofactors, the coagulation cascade will proceed to produce fibrin. The majority of the coagulation reactions take place at the membrane interface.

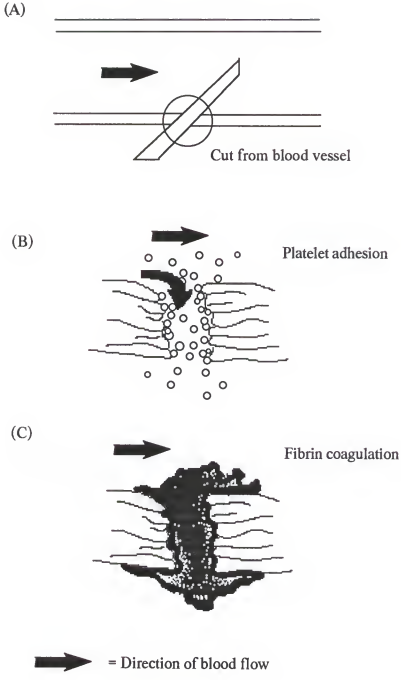

Figure 6. Normal hemostatic mechanism (79)

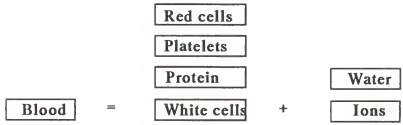

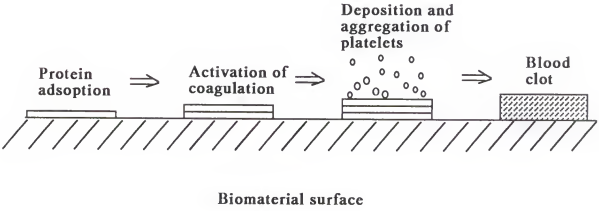

Fgure 7. Blood/Biomaterial interfacial reactions (36)

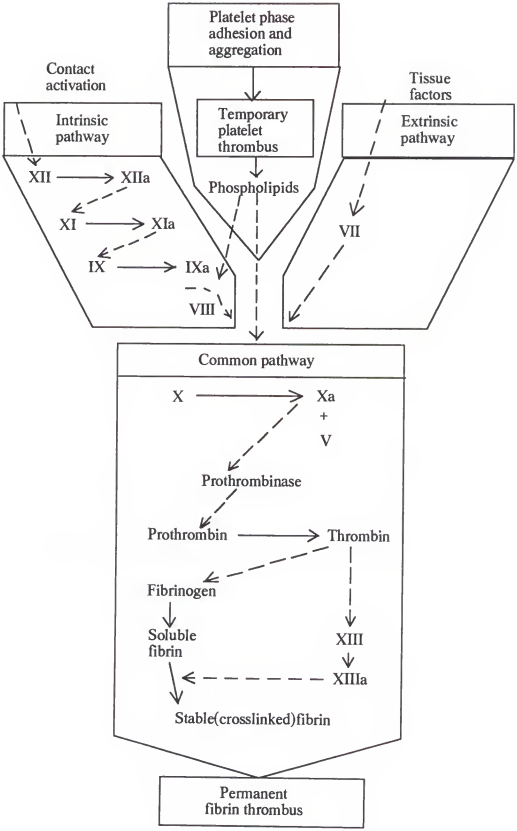

Figure 8. Blood coagulation cascade (82)

Also, activated platelets will adhere to the thin layer of fibrin, aggregate, and speed up thrombus formation (84).

Besides platelets and coagulation proteins, plasma proteins such as albumin, fibrinogen, and g-globulins also contribute to thrombus formation. Plasma proteins immediately adsorb onto the surface of biomaterials after contact with blood. This initial adsorption influences all subsequent events and determines the thrombogenicity of biomaterials. It has been found that adsorption of albumin on a surface tends to inhibit thrombus formation whereas adsorption of fibrinogen and g-globulins enhance thrombosis (85).

Biological membranes consisting of proteins, polysaccharides, and PLs exhibit functional and compositional asymmetry. The outer and inner surfaces of the plasma membranes have different components and enzymatic activities. This asymmetry provides the balance between haemostasis and thrombosis (86). The negatively charged PLs are mostly located in the inner leaflet of the plasma membrane and the zwitterionic PLs are in the outer leaflet (1). For example, the zwitterionically choline-containing PLs are mainly located at the outer cell surface of erythrocytes and quiescent platelets. From in vitro studies, those outer surfaces are inactive in coagulation tests and no significant prothrombin-converting activity can be detected (87, 88). The restricted lateral diffusion of proteins in biomembranes also serves to inhibit the formation of coagulation complexes. Lecithin liposomes have also been shown to adsorb α_2-macroglobulin (an inhibitor of thrombin) by acquiring a negative charge in contact with plasma (89, 90, 91). This evidence further supports the belief that a polymerized PL which is similar to conventional membrane surfaces has haemocompatible potential.

2.8 Summary of Previous Research

In summary, it is clear that a major restriction to the general application of biomaterials are surface properties which may cause adverse biological reactions. Many approaches based on theoretical hypotheses have been unsuccessful because they have not adequately accounted for the complexity of biological mechanisms. An approach for designing improved biomaterials surfaces which better mimic biological membranes using PLs is the basis for this research. PLs which are the major components of biological membranes should have improved biocompatibility. PLs with functional polymerizable groups in the PL chemical structure have been developed to afford stable biomembranes and facilitate surface grafting. PL surfaces on biomaterials can be prepared by various surface polymerization techniques such as UV, gamma, and plasma/gamma initiation. The resulting PL modified biomaterials can be designed to have both hydrophilic membrane-like surfaces and mechanically stable substrates.

Specific applications for PL biomembrane surfaces have focused on IOL and vascular devices in this study. Currently, PMMA is the dominant material for IOLs. The hydrophobic surfaces of PMMA result in various surgical complications such as corneal endothelium damage, inflammation, etc. PL modified surfaces of PMMA are hydrophilic and may prove more biocompatible. For vascular devices, the difficulty of designing nonthrombogenic surfaces is complicated. For red blood cells and quiescent platelets, the extracellar surfaces of the cell membranes are thromboresistant and have a high content of neutrally charged PLs such as lecithins. Hence, biomembrane-like surfaces of polymerized PLs may prove less thrombogenic and exhibit reduced antigenicity.

The specific PLs synthesized in this research involved novel polymeriziable PL and 12-PL, substrates included PMMA, PDMS and PP, and graft polymerization methods involved gamma, plasma/gamma, and UV initiation. The chemical, physical and biological

behavior were investigated with particular attention to potential ophthalmic and blood-contacting devices.

CHAPTER III
MATERIALS AND METHODS

3.1 Synthesis of Bis[(methacryloxyethylene)adipoyl]-L-a-phosphatidylcholine (HEMA-PL)

The synthesis pathway for the novel HEMA-PL is shown in Figure 9. The pathway includes three steps: (1) synthesis of a fatty acid with a polymerizable function group, (2) anhydride formation of the fatty acid, and (3) acylation of glycerophorylcholine with the anhydride.

3.1.1 Synthesis of (Methacryloyloxyethylene)mono adipate

Ophthalmic grade 2-hydroxyethyl methacrylate (HEMA) (7.5 g, 0.0576 mole) (Polysciences, Inc.) was dissolved in 100 ml of anhydrous diethyl ether (Fisher Co.), and the catalyst, 4.6 mL (0.0576 mole) of pyridine (Aldrich Co.,distilled over P_2O_5 (Fisher Co.)) was then added. The solution was cooled to 0°C in an ice bath and stirred using a magnetic stirbar. A solution of 10.6 g (0.0576 mole) of adipoyl chloride (Sigma Co.) dissolved in 100 ml of anhydrous diethyl ether was added dropwise to this solution via a pressure equalized addition funnel. After the addition was complete, the contents were brought to room temperature and stirred for 12 hours. The precipitate was removed by filtration and the supernatant was diluted with 100 ml of distilled water (stirred for 1 hour). The diluted supernatant was poured into a 1 L separation funnel and washed with distilled water until the washings were no longer acidic (tested by pH paper). The ether layer was dried over anhydrous sodium sulfate (Fisher Co.). The sodium sulfate was filtered off and the solvent was removed using a Rotavapor (Brinkmann Instruments Inc.) under reduced pressure. The final purification process was performed on a silica gel column (4 x 75 cm)

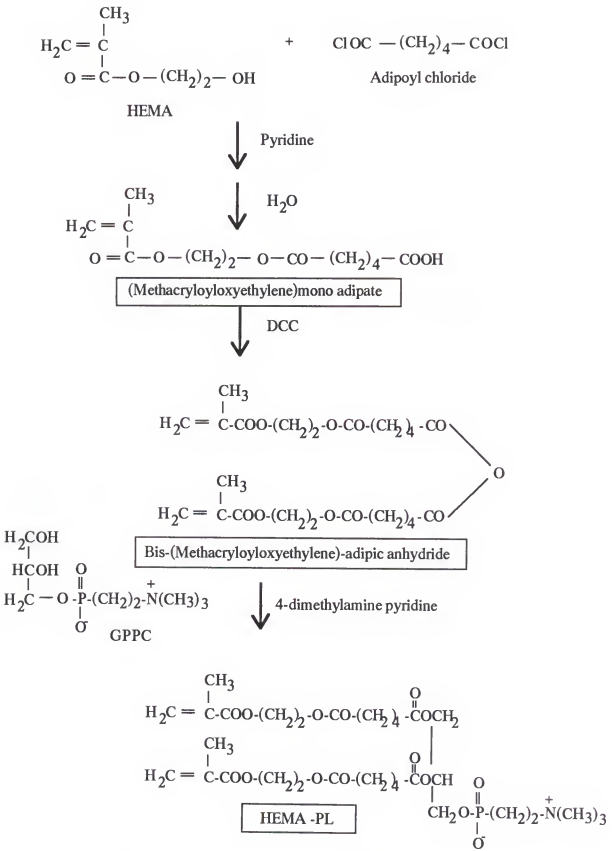

Figure 9. The synthesis pathway of HEMA -PL

in 1:1 chloroform / ethyl acetate (Fisher Co.). The silica gel (Sigma Co.) used for chromatography was Type 60, 70-230 mesh. Thin Layer Chromatography (TLC) in 1:1 chloroform / ethyl acetate was tested for each effluent by silica gel coated plate (T-6145, from Sigma Co.). The effluents which have $R_f = 0.6$ (see Figure 10) were collected and the solvent was removed under reduced pressure. The final product was confirmed by IR and ^1H NMR. The yield was 11.5 g, 82%.

Calculation of Rf value

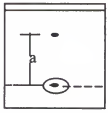

$R_f = a / A$

Figure 10. TLC chromatography

3.1.2 Synthesis of Bis-(methacryloyloxyethylene)- adipic Anhydride

1.3- dicyclohexylcarbodiimde (DCC, Aldrich Co.) (1.7 g, 0.00743 mole) dissolved in 50 ml of dry carbon tetrachloride was added dropwise to a solution of 3.5 g (Methacryloyloxyethylene)mono adipate (0.0135 mole) in 75 ml of dry carbon tetrachloride (Fisher Co., distilled over P_2O_5) via a pressure equalized addition funnel at room temperature. After 12 hours stirring, the precipitates were filtered out and solvent was removed under reduced pressure. The final product was identified by IR and ^1H NMR. The yield of anhydride was 2.97 g, 88%.

3.1.3 Acylation of L-α-glycerophorylcholine (GPPC)

GPPC (Sigma Co., 0.002 mole) in $CdCl_2$ complex form was weighed in a 100 ml round bottom flask and dried by repeated evaporation of benzene (Fisher Co.) under reduced pressure. The dried GPPC was suspended in 50 ml of freshly dried chloroform (distilled over P_2O_5) prior to the addition of 2.5 g of the Bis-(methacryloxyethylene)-adipic anhydride (0.005 mole). Then, 0.51 g (0.005 mole) of 4-dimethylamine pyridine (Aldrich Co.) was added to this solution and degassed with argon. The flask was tightly sealed with a clamp and the contents were vigorously stirred for 30 hours at room temperature in the absence of light. The solvent was removed under reduced pressure and the residue dissolved in 20 ml of 5:4:1 methanol (Fisher Co.)/chloroform/distilled water (volume %). After filtering off the insoluble precipitate, the clear solution was passed through a AG-501-X8(D) ion exchange resin column (1 x 17 cm, Bio-Rad Lab.). The column was further washed with two bed volumes of the same solvent to make sure no residue was left. After removal of the solvent via Rotavapor under reduced pressure, the product was purified by silica gel column chromatography (2 x 30 cm, Type 60, 70-230 mesh) with the following solvent system. The (methacryloyloxyethylene)mono adipate was eluted first using pure chloroform. Then, HEMA lipid was eluted using a 1: 1 (volume %) chloroform / methanol and checked by TLC (R_f = 0.34 with 65:25:4 (volume %) chloroform /methanol / water). The product yield was 0.91 g (51%). IR and ^1H NMR were used to identify the product.

3.2 Synthesis of 12-PL

Figure 11 shows the synthesis pathway for 12-PL. This pathway follows the same steps as HEMA-PL synthesis with the exception that anhydride was formed by the reaction with ethyl chloroformate instead of DCC.

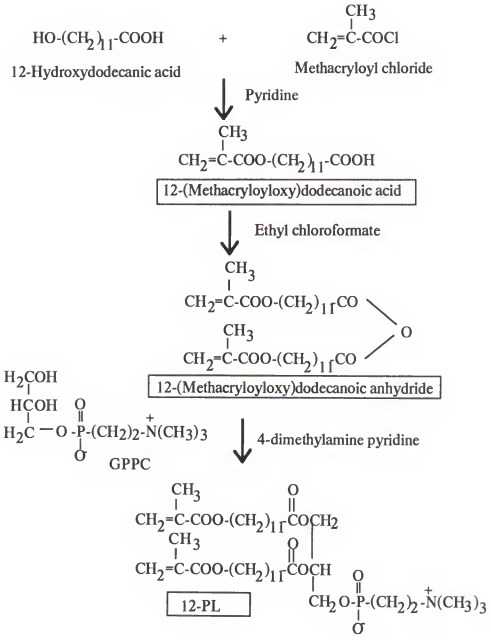

Figure 11. The synthesis pathway of 12-PL

3.2.1 Synthesis of 12-(Methacryloyloxy)dodecanoic Acid

12-hydroxydodecanic acid (0.025 mole, Sigma Co.) was dissolved in 75 ml of dry tetrahydrofuran (THF, Fisher Co.) prior to the addition of 2 ml of distilled pyridine (0.025 mole). The dry THF was distilled by refluxing over sodium metal (Aldrich Co.) and benzophenone (indicator, Fisher Co.) until a violet color was seen. The resulting solution then was cooled in an ice bath, and then 2.9 ml of methacryloyl chloride (0.025 mole, Aldrich Co.) in 25 ml dry THF was added dropwisely via a pressure equalized funnel . The resulting solution was stirred for 12 hours. The precipitates were removed by filtration and the remaining solvent was evaporated under reduced pressure. The residue was dissolved in 150 ml of ether and washed with distilled water. Five percent HCl was added to remove pyridine residue and the solution was neutralized with sodium bicarbonate (Fisher Co.). After washing, the ether layer was dried over anhydrous sodium sulfate. After removing the solvent, the crude product was passed through a silica gel column.(Type 60, 70-230 mesh, 1:2 (volume %) ethyl acetate: hexane (Fisher Co.)). The final product was checked by TLC (R_f = 0.54, 1: 2 (volume %) ethyl acetate: hexane). The solvent was removed and the final product was identified by IR and ^1H NMR. The yield is 7 g, or 89%.

3.2.2 Synthesis of 12-(Methacryloyloxy)dodecanoic Anhydride

To a solution of 2.26 g (0.00795 mole) 12-(methacryloyloxy)dodecanoic acid dissolved in 50 ml of dry THF, 1.5 ml (0.009 mole) of triethylamine (Sigma Co.) was added and cooled by dry CO_2. A solution of 0.9 ml ethyl chloroformate (0.0091 mole, Sigma Co.) in 30 ml dry THF was then added in a dropwise fashion. The mixture was stirred for 1 hour and warmed to room temperature for 30 minutes. The solution was cooled again and a solution of 2.26 g 12-(methacryloyloxy)dodecanoic acid (0.00795 mole) plus 1.5 ml (0.009 mole) of triethylamine dissolved in 50 ml dry THF was added in

a dropwise fashion. The resulting solution was stirred in a dry CO_2 bath for 1 hour and at room temperature for 12 hours. The precipitates were filtered off and the solvent was removed. The residue was dissolved in 150 ml of ether and washed with distilled water. After washing, the ether layer was dried over anhydrous sodium sulfate. The solvent was removed and 3.9 g (yield=90%) of anhydride was identified by IR and ^1H NMR.

3.2.3 Acylation of GPPC

The synthetic steps follow the same procedure of 3.1.3 with the exception that 3.12 g (0.00567 mole) of 12-(methacryloyloxy)dodecanoic anhydride was used in place of bis-(methacryloyloxyethylene)-adipic anhydride. The yield of 12-PL is 1.12 g, 80%.

3.3 Substrates

The polymeric substrates used for surface modification were PMMA (Perspex, ICI Co.), PP (Himont Co.), and PDMS (KE-1935,Shin-Etsu Co., America). The chemical structures and properties are shown in Table 1. Samples were cut into rectangular slabs (1 x1 cm). PMMA IOLs with 6 mm optics were provided by Pharmacia Ophthalmics, Inc. PMMA and PP slabs were cleaned by sonication in a 0.1 % Triton X-100 (Fisher Co.) soap solution for 30 mins, followed by a distilled water rinse, and finally repeated sonication in distilled water for 10 mins (3X). PDMS slabs were cleaned by the above procedure except using 1:1 (volume %) acetone / ethanol solution in each step. PMMA IOLs were sonicated with distilled water for 10 mins. After cleaning, all samples were dried under vacuum and stored in a desiccator until use.

3.4 Plasma Pretreatment of Substrates

The RF plasma system is illustrated in Figure 12. The system consists of a Pyrex "bell jar" reactor, vacuum system, gas inlets, and RF system. The system includes an inductive coil (4 ft, 7 turns of 4 mm copper tubing), generator (13.56 MHz, maximum

Table 1. The chemical structure and physical properties of substrates (67)

	PMMA	PP	PDMS
	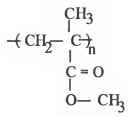	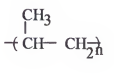	
Density	1.18	.91	1.14
Tg (°C)	105	-19	-123
Modulus (Kpsi)	14.5	165	1.16
Tensile strength (Kpsi)	8	4	0.85
Contact angle (°)	72	90	110
Refrective index	1.49	1.49	1.43
Optical transparency	clear	opaque	clear

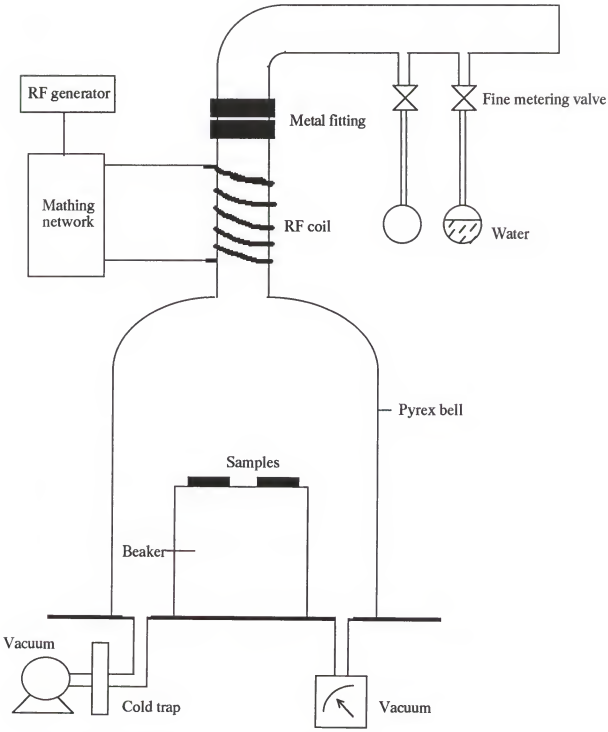

Figure 12. The apparatus of RF plasma system

output = 500 watts, RF plasma Products, HFS 401 S), and matching network which to match the impedance of the plasma discharge to the RF generator. The reflected wattage from the generator can be reduced by controlling the matching network. The vacuum system is composed of a mechanical pump with a liquid nitrogen cold trap and a vacuum gauge. A fine metering valve (Nupro Co.) was used to control gas flow and thus the vacuum pressure. The samples were placed on an inverted glass beaker, 5 cm from the bottom of the reactor.

The reactor was evacuated for 24 hours before mounting the samples. The pressure was pumped down to 30 mTorr for 30 mins after introducing the substrates. By adjusting the water inlet valve, the pressure was maintained at 80 ± 20 mTorr. Then, the RF power was applied and conducted at various operating conditions. The parameters were RF power input, vacuum pressure, and treatment time. After pretreatment, the samples were removed and readied for irradiation.

3.5 Phospholipid Dispersion

Usually, the PLs (HEMA-PL and 12-PL) were stored in chloroform. The weight of PLs would be calculated by pipetting a fixed amount of chloroform solution into a round-bottom flask. After solvent evaporation, distilled water was added to the flask and the suspension sonicated for 20 mins using a 8851 Cole-Palmer ultrasonicator. Typically, the vesicles were well dispersed as monitored by optical microscopy.

3.6 UV Irradiation

The surface modification of the 12-PL was conducted in a Rayonet Photochemical Reactor (RPR-204, Southern New England Ultraviolet Co.). The reactor consisted of four 2537 Å lamps, 120 watt output each, vertically arranged around the inside chamber of the reactor. The vesicle dispersion (5 ml) was pipetted into a 15 ml quartz test tube which contained the clean substrate. Argon was used to purge the dispersion for 5 minutes before

irradiation. The quartz test tube was suspended in the center of the reactor in order to receive uniform irradiation. The schematic sketch of the reactor is shown in Figure 13. After the irradiation, the modified substrate was removed from the dispersion and washed with distilled water three times each day. The washings were checked with UV spectroscopy until no 12-PL was detected. Usually, three days were needed to complete the washing.

3.7 Gamma Irradiation

The gamma-induced graft polymerization of HEMA-PL was carried at room temperature in a 600 Curie ^{60}Co gamma source (Figure 14). HEMA-PL dispersion was added to test tubes containing clean substrate samples as described in section 3.6. The test tubes were placed at a distance of 4 inches from the source center. The dose rate at this distance was 580 rad/min as determined by Fricke dosimetry (41). After irradiation, samples were cleaned according to the method outlined in section 3.6. Summary of the surface modification procedures is presented as a flow chart in Figure 15.

3.8 Characterization

3.8.1 Contact Angle Measurements

Information on the outermost monolayers of a polymer surface can be obtained by contact angle measurements. This method requires relatively simple and inexpensive equipment and is one of the few nondestructive methods to characterize solid/liquid surfaces. The basis for this method is the three phase equilibrium that occurs at the contact point for the solid/liquid/vapor interfaces. Before measuring,the substrates were immersed overnight in water to achieve an equilibrium state. Typically, contact angles were directly measured by the captive air bubble technique illustrated in Figure 16. The substrate was fixed on a glass slide with two rubber bands and the slide was placed across an acrylic

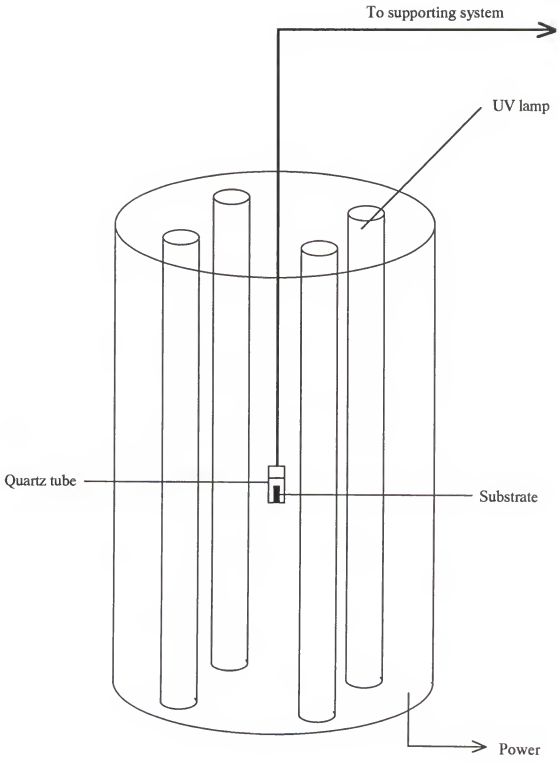

Figure 13. The schematic diagram of UV reactor

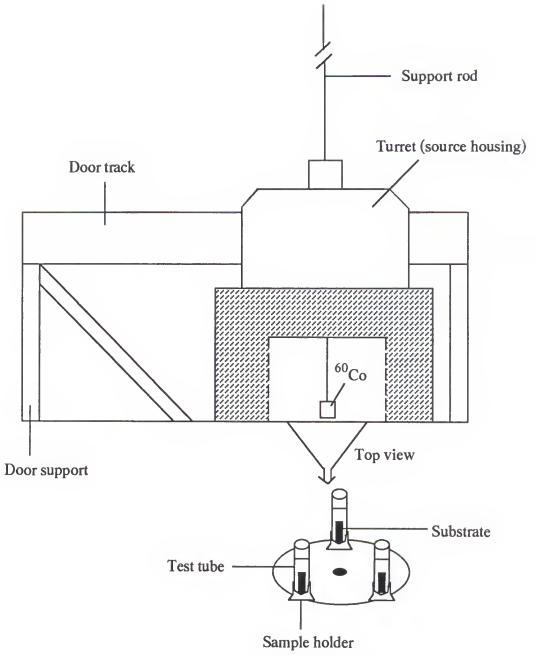

Figure 14. The diagram of gamma source

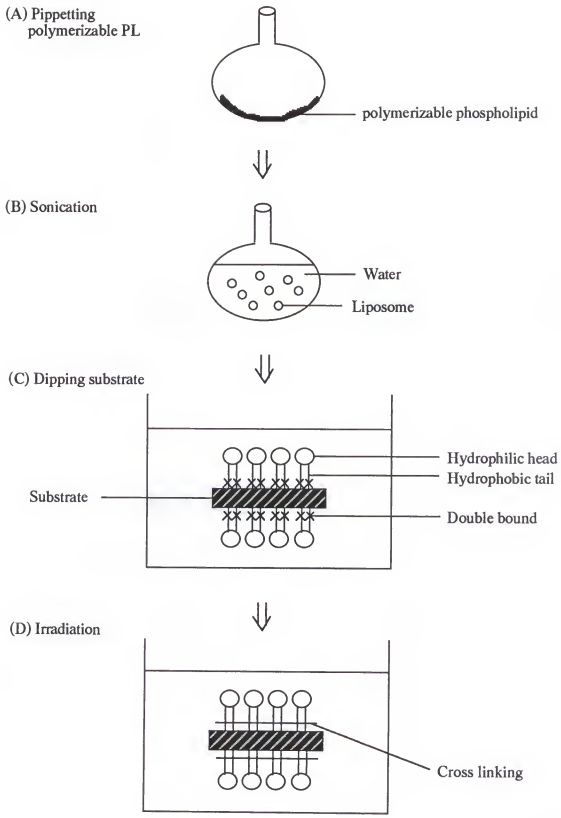

Figure 15. The flow chart of surface modification procedures

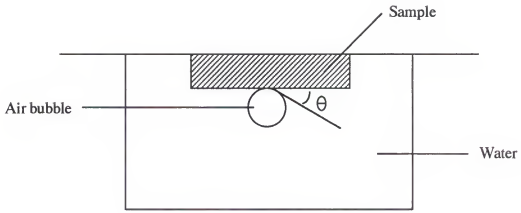

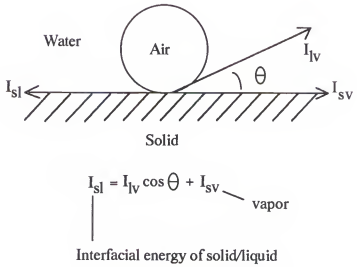

Figure 16. The diagram of the captive air bubble contact angle measurements

chamber filled with distilled water at room temperature. Five air bubbles were then attached on the substrate surface using a microsyringe. The contact angles for each bubble were measured and averaged using a Rame-Hart goniometer (Mountain Lakes, NJ).

3.8.2 Fourier Transform Infra-Red/ Attenuated Total Reflectance (FTIR/ATR)

FTIR/ATR is a powerful and non destructive surface characterization technique. It combines IR spectroscopy and total internal reflection to study the chemical structure and bonding on the surface of a material. IR spectroscopy involves determination of IR radiation absorbed by a sample as a function of the wavelengths. Figure 17 shows the schematic illustration of ATR spectroscopy (90). The IR beam is internally reflected through an optically transparent ZnSe crystal (50 x 10 x 2 mm, entrance and exit face angle = 60^{o}, Spectra Tech) in contact with the samples. Total internal reflection can occur only if the index of ZnSe crystal (n_1= 2.4) is greater than the index of the samples (for polymer, $n_2 < 2.4$) and the relation of the depth of penetration (d_p) with variables of IR beam can be obtained. A Nicolet 60SX spectrometer was used to collect the spectra with 100 scans at a resolution of 4 cm^{-1}.

3.8.3 X-ray Photoelectron Spectroscopy (XPS)

XPS, also known as Electron Spectroscopy for Chemical Analysis (ESCA), is regarded as a very powerful technique for surface characterization. It provides a total elemental analysis (except H and He) as well as some information on the chemical bonding, and composition of the top 10-50 Å of polymer surfaces. The basic principle of XPS is the photoelectric effect (Figure 18). When the samples are bombarded by an X-ray beam, the photon may interact with the atomic orbital electron and totally transfer the energy to the electron. If the photon energy is greater than the binding energy of the orbital electron , the electron is ejected from the atom. By measuring the kinetic energy of the ejected electron, the binding energy can be calculated which identifies the atom. XPS is a surface sensitive

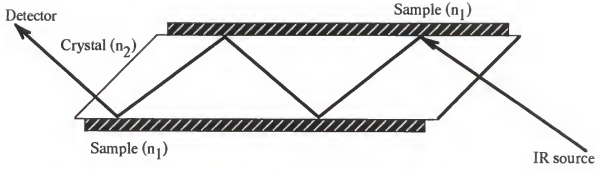

$$d_p = \frac{\lambda}{2\pi n_1(\sin^2\theta - n_2/n_1)^{1/2}}$$

λ = wavelength of IR

n_1 = refractive index of the sample

n_2 = refractive index of the crystal

θ = incident angle

Figure 17. The optical diagram of FTIR/ATR

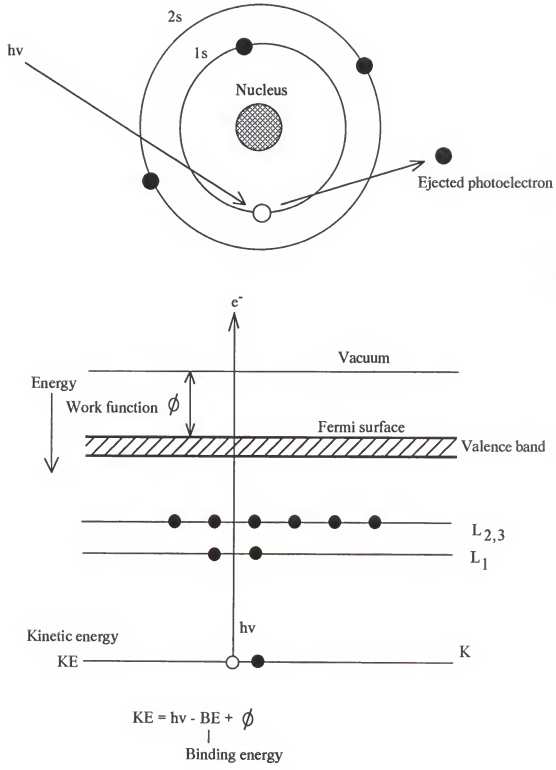

Figure 18. The shematic view of XPS

technique because only electrons emitted from the uppermost surface have a high probability of escaping without energy loss. The XSAM-800 spectrometer from Kratos with an Mg K_a X-ray source (20 KV, 13 mA) was used to obtained the spectra at high vacuum (10^{-7} torr). All of the samples were examined with survey and high resolution scans. The peak areas of energy band were calculated by the standard computer software to represent the atomic concentration for particular chemical elements.

3.8.4 Scanning Electron Microscopy (SEM)

JSM-35CF SEM from JEOL Co. was used to obtain the sample surface topologies. The sample surfaces were coated with gold-palladium (except low voltage SEM) by a Hummer V sputter-coater (Technics, Virginia). Accelerating voltage and magnification were adjusted to reveal the best surface topology.

3.8.5 Optical Microscopy

A Nikon OPTIPHOT microscope and UFX-IIA photomicrographic attachment were used in this study to monitor vesicle dispersion and epithelial cell adhesion.

3.8.6 Ultraviolet-Visible (UV-VIS)Spectroscopy

Perkin-Elmer 552 spectrometer was used to study the UV absorption characteristics of vesicle dispersions and modified samples. Percent absorbance over the range 900-190 nm was obtained to study the potential UV cutoff of the modified samples.

3.8.7 Synthesis Characterization

Infrared (IR) Spectroscopy and Nuclear Magnetic Resonance (NMR) Spectroscopy were used to identify the synthesized compound. IR spectra were obtained with a Perkin-Elmer 283B spectrophotometer with sodium chloride crystals. The liquid compound was cast on the surface of sodium chloride crystals. A GE 300 MHz NMR spectrometer was

used to obtain proton NMR spectra. The compound was dissolved in deuterated chloroform ($CDCl_3$) in a glass tube.

3.8.8 Ellipsometry

A Gaertner L117 Manual Ellipsometer was used to measure the refractive index and the thickness of the grafting. Ellipsometry involves illuminating the surface of a sample with monochromatic incident light of known wavelength. The light is polarized at a fixed angle of incidence and changes in the polarization with reflection are recorded. The schematic diagram of an ellipsometer is shown in Figure 19. A He-Ne laser at 632.8 nm was used as the light source. The light is circularly polarized at the laser output and passes through a polarizer where the polarization of the beam is converted from circular to linear. Then, the linearly polarized beam is further converted to one of elliptical polarization by a quarter-wave compensator. The reflected light passes through an analyzer and an optical interference filter. The beam finally is sensed by a photodetector. When the reflected light is completely linearly polarized, certain azimuth settings (P_1, P_2) are recorded. At these condition, the analyzer then can be rotated to a corresponding position (A_1 and A_2) where no light reaches the detector, indicated by the lowest reading on the extinction meter. By measuring those readings (P_1, P_2, A_1, A_2), the thickness (d) and refractive index (n_1) of the grafting can be determined by solving a series of reflection equations (Fresnel equations and Snells' law) (91). These simultaneous equations were solved for d and n_1 by using a statistical approach and a computer program.

The calculated thickness, $d = d_0 +$ constant $\times m$ ($m = 0, 1, 2, 3$, etc.), is not an unique value. However, the minimum value (d_0) can be obtained for thin polymer grafts, when other measuring techniques are not available.

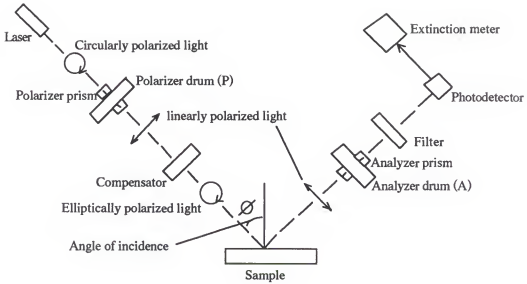

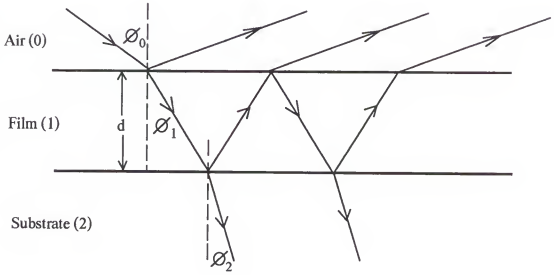

Figure 19. The schematic diagram for the reflection ellipsometry measurements (91)

3.9 In Vitro

3.9.1 Epithelial Cell Adhesion

The procedure for rabbit lens epithelial cell adhesion and cell spreading were developed in this laboratory by P. Martin. The adhesion of lens epithelial cells is believed to be one of the important factors in inflammation (92). The ocular epithelial cells come from New Zealand rabbits. Cells are trypsinized and suspended in Medium 199, 15% fetal bovine serum. After equilibrating test samples in BSS, the cell suspension is applied 2 ml to each sample and 3 ml for each control polystyrene plate. Samples are then incubated at 37°C in a CO_2 atmosphere for 24 hours. Samples are then removed, rinsed in BSS, and placed into 10% neutral buffered formalin. After fixation, samples are stained with crystal violet. Cell adhesions on the samples were then analyzed using a Nikon optical microscope. Two photographs were taken from different portions of each sample.

3.9.2 Corneal Endothelium Damage Testing

The corneal endothelial cell damage can result from abrasive and adhesive interactions with IOL. The method was invented in this laboratory by Reich et. al. (93) Each set of four IOLs were used in this study. The cornea is removed from New Zealand rabbits within 2 hours of enucleation. The cornea is then glued to an aluminum mount using a 9 mm trephine. The mount is placed into a test chamber filled with physiological saline. The testing instrument is shown in Figure 20. An IOL is mounted onto a sample holder and hydrated prior to testing. It is then contacted with the corneal endothelium at 30 lbs for 30 seconds. After contact, the damaged cornea is fixed, dehydrated, and Au-Pd sputter coating. The corneal endothelial cell damage was observed and quantitatively estimated by SEM.

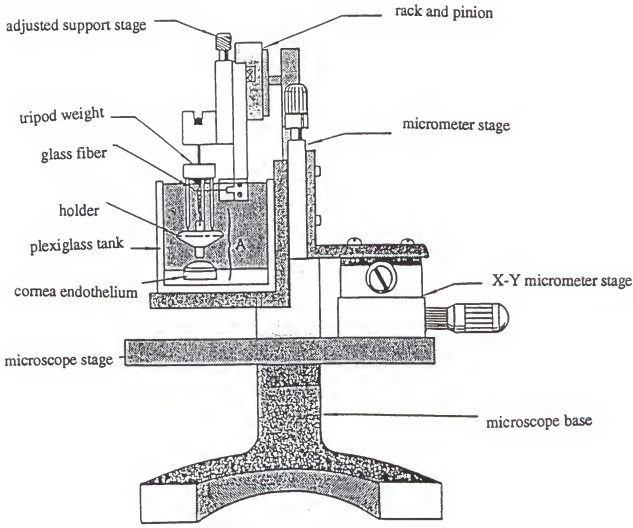

Figure 20. The schematic diagram of corneal endothelial cell damage testing (93)

3.9.3 Vascular Endothelial Cell and Platelet Adhesion

The vascular endothelial and platelet adhesion was conducted by Nina Klingman-Baptist in Dr. Seeger's laboratory at VA Medical Center, Gainesville, Florida. Platelet cells came from human serum and endothelial cells were removed from pigs. The samples were placed in Medium 199 with 20% FCS and incubated for one hour. The medium was removed and new medium with Indium labelled cells, either platelets or vascular endothelial cells, were added to the samples. The samples were incubated for 8 hours at 37 ^{o}C and 5% CO_2 and then counted for radiation labelled cells.

CHAPTER IV
RESULTS AND DISCUSSIONS

4.1 Synthesis and Characterization of HEMA-PL

The incentive for the synthesis of HEMA-PL is to produce a shorter acyl chain compared to 12-PL. The synthesis of HEMA-PL involved three steps: (1) esterification of HEMA with adipoyl chloride, (2) anhydride formation by reaction with DCC, and (3) acylation of GPPC with anhydride. The overall synthesis pathway was shown in Figure 9. The resulting compound from each step was characterized by IR and ^{1}H NMR. HEMA-PL is a novel compound not previously reported.

4.1.1 (Methacryloyloxyethylene)mono adipate Synthesis and Characterization

(Methacryloyloxyethylene)mono adipate was the product of esterification between HEMA and adipoyl chloride followed by water washing and column purification. It was found to be very important to maintain neutrality in the ether/water washing. The product will be a polymerized gel if the washing is acidic. Also, a 1:1 stoichiometric ratio of HEMA / adipoyl chloride should be maintained to prevent side reactions from keeping consuming both functional groups (COOCl) of adipoyl chloride. The yield for this step was 82%. The final product was a light yellow liquid and characterized by IR and ^{1}HNMR: IR (neat): 1720, 1735 (C=O) and 1640 cm^{-1}(C=C) (Figure 21); ^{1}H NMR ($CDCl_3$) : δ : 1.6-1.8 (m, 4H, CH_2CH_2), 1.95 (m, 3H, C=CCH_3), 2.15-2.5 (m, 4H, CH_2COOH), 4.05-4.35 (m, 4H, OCH_2), 5.52 (m, 1H, vinyl), 6.18 (m, 1H, vinyl) (Figure 22).

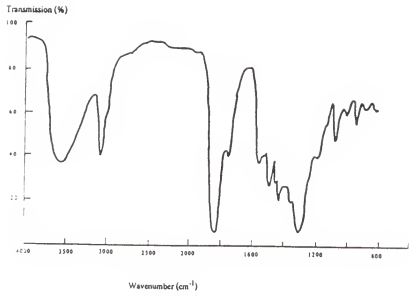

Figure 21. IR spectrum of (Methacryloyloxyethylene)mono adipate

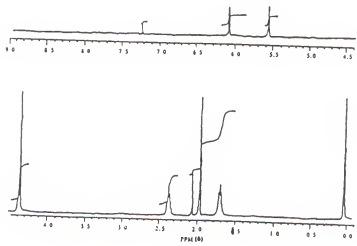

Figure 22. ^{1}HNMR spectrum of (Methacryloyloxyethylene)mono adipate

4.1.2 Bis-(methacryloyloxyethylene)-adipic Anhydride Synthesis and Characterization

The reaction of (methacryloyloxyethylene)mono adipate with DCC produced Bis-(methacryloyloxyethylene)-adipic anhydride (Figure 23). The by-products, DCAU and free fatty acid, did not interfere with the acylation reaction in step 3, therefore the anhydride was not purified (94). As far as product yield was concerned, carbon tetrachloride was found to be a better solvent than THF or chloroform. The yield for this step was 82%. The resulting anhydride was a colorless liquid and characterized by IR and ^{1}HNMR: IR (neat) : 1730,1800 (C=O, anhydride) and 1640 cm^{-1}(C=C) (Figure 24); ^{1}H NMR ($CDCl_3$): δ: 1.6-1.8 (m, 8H, CH_2CH_2), 1.95 (m, 6H, C=CCH_3), 2.35 (m, 4H, CH_2COO) , 2.5 (m, 4H, CH_2COOCH_2), 4.05-4.35 (m, 8H, OCH_2), 5.52 (m, 2H, vinyl), 6.18(m, 2H, vinyl) (Figure 25).

4.1.3 HEMA-PL Synthesis and Characterization

The final step of the HEMA-PL synthesis is the acylation of GPPC with bis-(methacryloyloxyethylene)-adipic anhydride. Water moisture lowers product yield. Therefore, GPPC which is very hygroscopic had to be dried with repeated benzene evaporation and the reaction flask had to be tightly sealed during the acylation reaction. The flask was also covered with aluminum foil to prevent UV degradation of the HEMA-PL. Another possible pathway to synthesize vinyl functional PL was attempted by direct reaction of GPPC in chloroform with 5-fold excess acyl chloride in the presence of pyridine followed by column purification (95). However, Khorana found that side products such as cyclic compounds, demethylated GPPC, and phosphatidic acids were difficult to remove, plus the yield was very low (< 20%) (96). We made many attempts to follow this pathway and did not produce any HEMA-PL. Therefore, the present synthesis method was the most effective one found for HEMA-PL. The final product is a

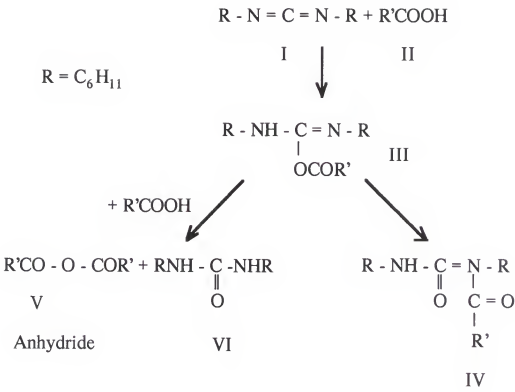

I = DCC, dicyclohexylcarbodiimide
VI = DCU, dicyclohexylurea
IV = DCAU, dicyclohexylacylurea

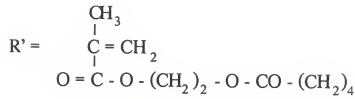

Figure 23. The formation of Bis-(Methacryloyloxyethylene)-adipic anhydride by DCC method

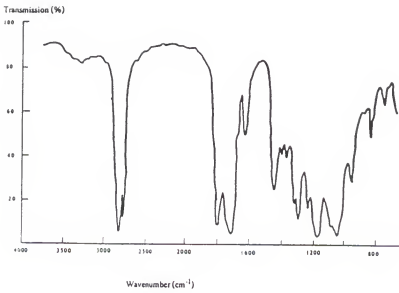

Figure 24. IR spectrum of bis-(methacryloyloxyethylene)-adipic anhydride

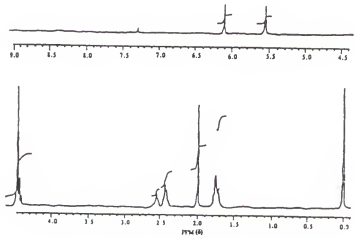

Figure 25. ^{1}HNMR spectrum of bis-(methacryloyloxyethylene)-adipic anhydride

novel previously unreported compound. The yield for this step is 51%. The overall yield of these three steps was 37% (82% x 82% x 51%). HEMA-PL was a colorless liquid and characterized by IR and ^{1}HNMR: IR (neat): 1720 (C=O), 1640 (C=C), and 1060,1090,975 cm^{-1}($^+N(CH_3)_3$) (Figure 26); ^{1}H NMR ($CDCl_3$) : δ: 1.6-1.8 (m , 8H, CH_2CH_2), 1.95 (m, 6H, C=CCH_3), 2.15-2.5 (m, 8H, CH_2COO), 3.28 (br, s, 9H, $^+N(CH_3)_3$), 4.05-4.35(m, 8H,OCH_2), 5.52(m, 2H, vinyl), 6.18(m, 2H, vinyl) (Figure 27).

4.2 Synthesis and Characterization of 12-PL

Figure 11 shows the synthesis of 12-PL. First, esterification of 12-hydroxydodecanoic acid with methacryloyl chloride produced the vinyl moiety at the end of the alky chain. Subsequently anhydride was formed from the above vinyl functional fatty acid by coupling with ECF. Acylation of GPPC with the anhydride yielded 12-PL. This synthesis was a modification of Larson's method which was also a modification of Regen's method (7,97). The present method obtained a better acylation yield (80%) than both previous methods (14% by Larson and 36 % by Regen). In Larson's method, hydroquinone (the inhibitor) was used to prevent polymerization of the anhydride prior to acylation reaction of GPPC but this inhibitor also reduced the acylation yield. Furthermore, GPPC ,which is very hygroscopic, was not completely dried by repeated benzene evaporation. Water moisture lowers the product yield. Finally, both previous methods required 72 hours for complete acylation allowing ample time for side reactions to occur. The present method, no inhibitor was used, GPPC was throughly dried by repeated benzene evaporation and the required time for acylation was reduced to 30 hours. The characterization of resulting compounds was by IR and ^{1}HNMR.

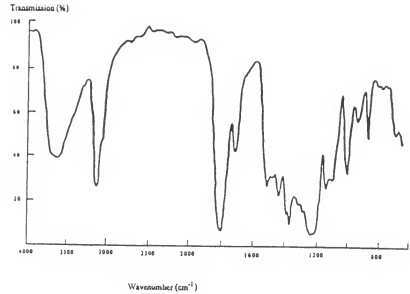

Figure 26. IR spectrum of HEMA-PL

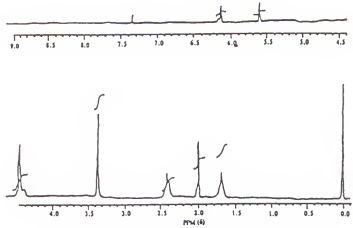

Figure 27. ^{1}HNMR spectrum of HEMA-PL

4.2.1 12-(Methacryloyloxy)dodecanoic Acid Synthesis and Characterization

12-(Methacryloyloxy)dodecanoic acid was produced by the esterification of 12-hydroxydodecanoic acid with methacryloyl chloride. Dry THF was necessary since any water in THF will significantly decrease the reaction yield. After complete reaction, the water washings should be neutral to prevent the product polymerization. The product yield was 89%. The compound was a yellow liquid and characterized by IR and ^{1}HNMR: IR (neat): 1720 (C=O), 1640 cm^{-1}(C=C) (Figure 28); ^{1}HNMR ($CDCl_3$): δ: 1.3 (br, s, 18H, $(CH_2)_9$), 1.95 (m, 3H, $C=CCH_3$), 2.15-2.50 (m, 2H, CH_2COOH), 3.9-4.3 (m, 2H, OCH_2), 5.52 (m, 1H, vinyl), 6.08 (m, 1H, vinyl) (Figure 29).

4.2.2 12-(Methacryloyloxy)dodecanoic Anhydride Synthesis and Characterization

Two moles of 12-(methacryloyloxy)dodecanoic acid reacted with 1 mole of ethyl chloroformate (ECF) yielded 12-(methacryloyloxy)dodecanoic anhydride. The yield in this step was 90%. However, it was found that DCC also could be used to synthesize the anhydride. DCC (1 mmole in 5 ml dry carbon tetrachloride) was added to the 12-(methacryloyloxy)dodecanoic acid (2 mmole in 15 ml dry carbon tetrachloride) via a pressure equalized addition funnel at room temperature. After 12 hours, the precipitates were filtered out and the solvent was removed. This DCC pathway is simpler than the ECF method but has a similar anhydride yield (92%). The anhydride was a dark yellow liquid and characterized by IR and ^{1}HNMR: IR (neat) : 1730, 1800 (anhydride), 1640 cm^{-1}(C=C) (Figure 30); ^{1}HNMR ($CDCl_3$): δ : 1.3 (br, s, 36H, $(CH_2)_9$), 1.96(m, 6H, $C=CCH_3$), 2.2-2.6 (m, 4H, CH_2COOH), 3.9-4.3 (m, 4H, OCH_2), 5.52(m, 1H, vinyl), 6.08(m, 1H, vinyl) (Figure 31).

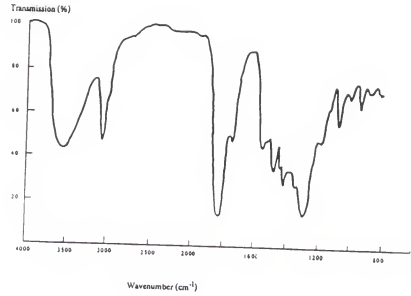

Figure 28. IR spectrum of 12-(methacryloyloxy)dodecanoic acid

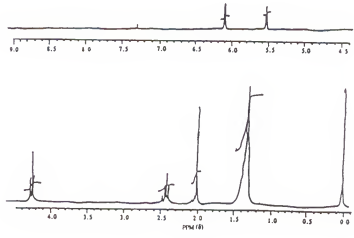

Figure 29. ^{1}HNMR spectrum of 12-(methacryloyloxy)dodecanoic acid

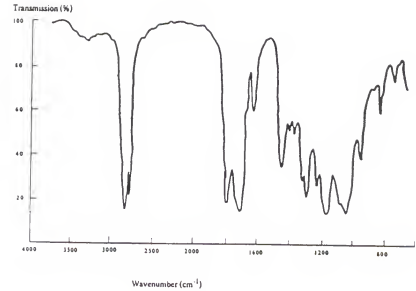

Figure 30. IR spectrum of 12-(methacryloyloxy)dodecanoic anhydride

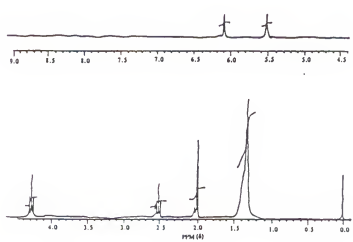

Figure 31. ^{1}HNMR spectrum of 12-(methacryloyloxy)dodecanoic anhydride

4.2.3 12-PL Synthesis and Characterization

The acylation of GPPC with 12-(methacryloyloxy)dodecanoic anhydride yielded 12-PL. As previously stated, no inhibitor was used, GPPC was completely dried by repeated benzene evaporation prior to acylation reaction and the acylation time was reduced to 30 hours to prevent side reactions and reduction in yield. As a result, a much higher yield of 12-PL (80 %) was achieved by pathway as compared to Regen's method (36%) and Larson's method (14%) (97, 7). The overall reaction yield of the three reactions was 64% (89% x 90% x 80%). 12-PL was a yellow liquid and characterized by IR and ^{1}HNMR: IR (neat) : 1720 (C=O), 1640, (C=C), 1090, 1060, 975 cm $^{-1}$ ($^+N(CH_3)_3$) (Figure 32); ^{1}HNMR ($CDCl_3$) : δ: 1.3 (br, s, 36H, $(CH_2)_9$), 1.93 (m, 6H, $C=CCH_3$), 2.2-2.45 (m,4H, CH_2COOH), 3.38 (br, s, 9H, $^+N(CH_3)_3$), 3.75-4.5 (m,13H, CH_2O), 5.52 (m, 2H, vinyl), 6.08(m, 2H, vinyl) (Figure 33).

4.3 Phospholipid Dispersions

PL monomers are amphiphilic, unlike most hydrophilic monomers (NVP, HEMA, etc.) which are soluble in water. Sonication of a PL in water creates a PL dispersion which may have bilayer vesicles due to surface energy considerations. The hydrophilic head can be exposed on both the exterior and encapsulated interior of vesicles while hydrophobic tails may be oriented toward the inside of the vesicles. After sonication, dispersion particle size was determined by optical microscopy. UV-VIS spectra was used for characterization.

The particle size range for HEMA-PL was 30-100 microns in diameter, as shown in Figure 34. Although prolonged sonication can reduce the vesicle size, no significant effect of particle size on surface properties (contact angle and surface atomic concentration of N and P in XPS) was observed in this study as long as the dispersion was homogeneous and

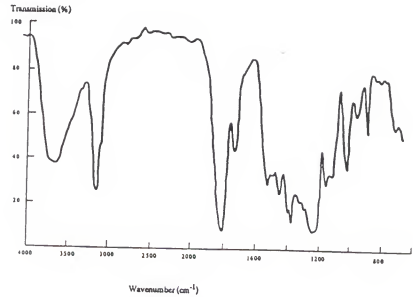

Figure 32. IR spectrum of 12-PL

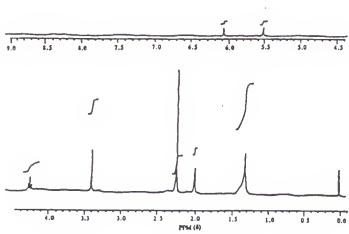

Figure 33. ^{1}HNMR spectrum of 12-PL

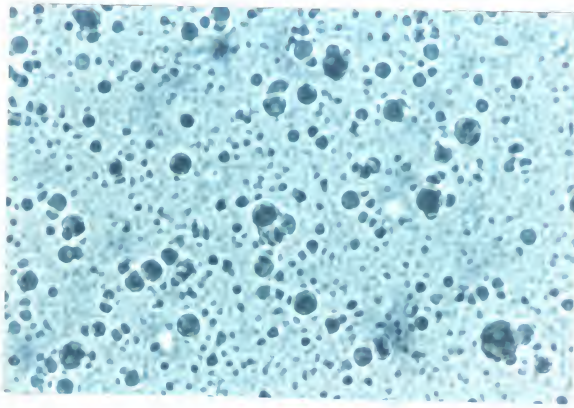

Figure 34. The photograph of HEMA-PL dispersion (2%, 100x)

well dispersed. The UV-VIS spectra of HEMA-PL at 2.5% concentration in water is shown in Figure 35. The HEMA-PL has a strong UV absorbance below 300 nm as expected considering the chemical structure which contains UV absorbant functional groups (C=O, C=C etc.). A distinguishing absorption peak at 280 nm was observed from the UV-VIS spectra . The absorbance at 280 nm vs. HEMA-PL concentration at 2.5-0.3125% was plotted in Figure 36. A straight line relationship was observed from the plot. When the concentration of HEMA-PL was above 2.5%, the absorbance at 280 nm reached 5 which was the maximum reading for this UV-VIS spectrometer. Below 0.3125%, the absorbance at 280 nm was close to zero. However, this absorption peak at 280 nm disappeared for HEMA-PL dispersions after gamma radiation which is shown in Figure 37. Therefore, this absorption peak at 280 nm might be the polymerizable vinyl function groups. For 12-PL, the particle size range was 45-150 microns in diameter. A characteristic UV-VIS absorption peak was observed at 300 nm (7).

4.4 Surface Modification of PMMA with HEMA-PL by Gamma Radiation

UV radiation had been used to graft 12-PL monomer on the PMMA surfaces. Hydrophilic surfaces of 12-PL modified PMMA have been confirmed by J. Larson (7). In this study, UV radiation was also used to graft HEMA-PL monomer on the PMMA surfaces. However, although the solution of HEMA-PL gelled after UV radiation, the modified PMMA surfaces remained hydrophobic (C.A. 71^0). In contrast, gamma radiation was found to graft HEMA-PL monomer onto the PMMA to produce hydrophilic surfaces. The energy in gamma radiation is more powerful than UV radiation thus can create more free radicals on the PMMA surfaces. The concentration of the HEMA-PL and the gamma dose were varied and evaluated in this study.

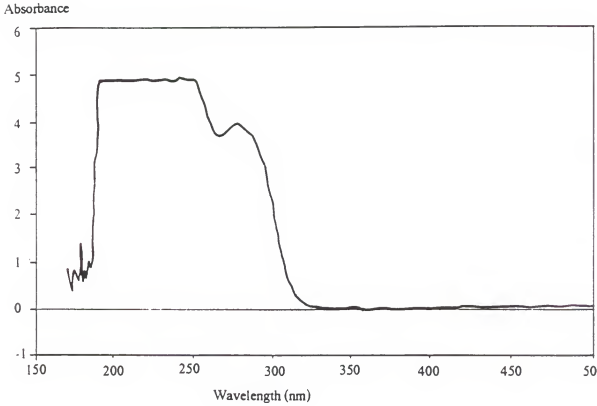

Figure 35. UV-VIS spectrum of HEMA-PL dispersion (2.5%)

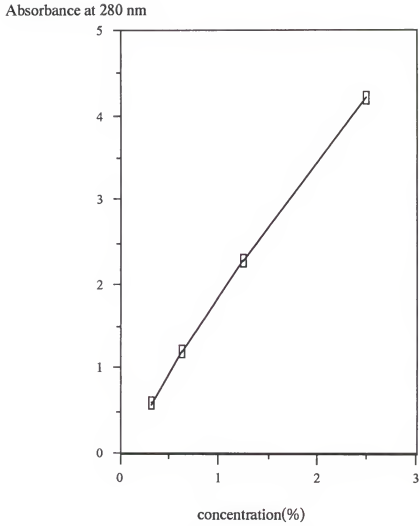

Figure 36. UV-VIS absorbance at 280 nm vs. HEMA-PL dispersion concentration from 0.3125-2.5%

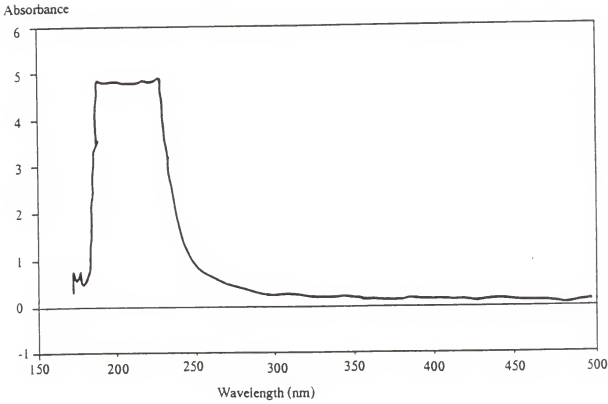

Figure 37. UV-VIS spectrum of HEMA-PL dispersion (2.5%) after 0.1 Mrad gamma radiation

4.4.1 Contact Angle (C.A.) Measurements

For characterizing hydrophilic surfaces, C.A.s were measured under water in the equilibrium state. The reasons for the under water method are that most biological environments are aqueous and the measurements are more accurate at equilibrium hydration. The C.A.s of modified PMMA vs. different concentrations from 1 to 10% of HEMA-PL dispersions at a dose of 0.07Mrad are shown in Figure 38. The C.A. of the HEMA-PL modified PMMA was near 20^0 for each modified condition as compared to unmodified PMMA (72^0). This indicated that the surface of modified PMMA had become very hydrophilic in the concentration range 1 to 10% and the interfacial free energies of the surfaces were very low.

The effect of gamma dose in the range of 0.03 to 0.15 Mrad at 1% of HEMA-PL dispersions on the C.A. of modified PMMA is shown in Figure 39. The C.A. for each condition also was in the 20 range as compared to unmodified PMMA (72^o). Even at a very low gamma dose (0.03 Mrad), the surfaces of modified PMMA were hydrophilic. As the gamma dose was reduced to less than 0.03 Mrad, the C.A. of modified PMMA was 75^o. Therefore, the minimum dose required to graft HEMA-PL on PMMA was 0.03 Mrad. The HEMA-PL solutions after gamma radiation from 0.03 to 0.15Mrad became viscous even at the low end of the concentration range. The UV-VIS spectrum of 2.5 % HEMA-PL solution at 0.07 Mrad was shown in Figure 37.

4.4.2 UV-VIS Spectroscopy

UV-VIS spectroscopy was used to characterize optical properties. The UV-VIS spectra of PMMA and modified PMMA at 2% HEMA-PL and 0.07Mrad are shown in Figure 40. In the visible region (above 400 nm) , PMMA was optically transparent and the transmission was above 90%. After surface modification, the transmission was slightly

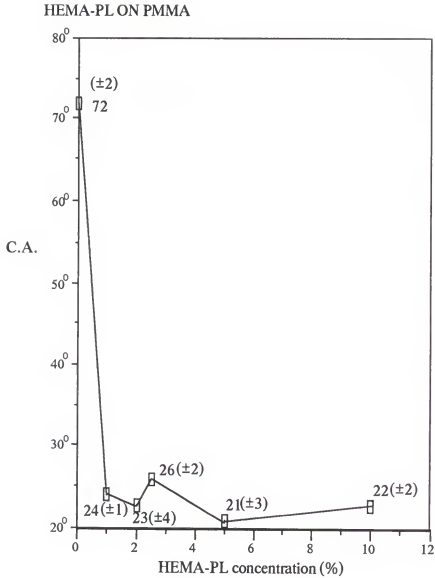

Figure 38. Contact angles of modified PMMA vs. HEMA-PL concentration at 0.07 Mrad

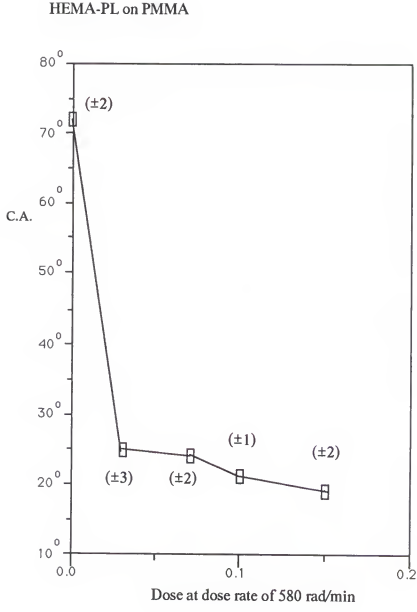

Figure 39. C.A.s of modified PMMA vs. gamma dose at 1% of HEMA-PL dispersion

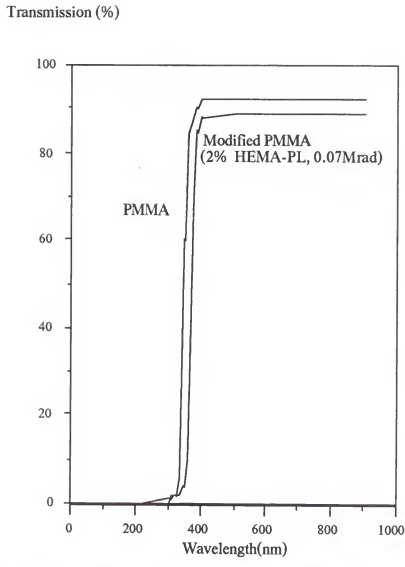

Figure 40. UV-VIS spectra of PMMA and HEMA-PL modified PMMA (2%, 0.07 Mrad)

attenuated, but the two spectra were very similar. The optical properties of PMMA were not significantly affected. For 12-PL, an extra absorption peak at 320 nm was detected by Larson's study (7). This may be due to the different chemical structure between HEMA-PL and 12-PL.

4.4.3 SEM

The surface morphology of surface modified PMMA was examined by SEM. In order to avoid surface damage and artifacts, low voltage SEM (LVSEM), at 0.5 KV was used. No gold coatings were applied to these samples. Figure 41 is a LVSEM SEM of unmodified PMMA. The surface was very smooth and homogeneous. A micrograph of HEMA-PL modified PMMA at 2% and 0.07Mrad obtained using LVSEM is shown in Figure 42. The surface morphology showed no change after surface modification, remaining smooth and homogeneous. Further, no adsorbed liposomal structures were observed. For 12-PL modified PMMA by UV radiation, a full coverage of liposomes on the surface was observed in SEM of a sample with a gold coating before heptane extraction (7). After heptane extraction, the surface was smooth and without any adsorbed liposomes

4.4.4 FTIR/ATR

FTIR/ATR spectrum can reveal chemical information about the surface of materials a depth of 1-10 microns. The FTIR/ATR spectrum of unmodified PMMA and peak assignments are given in Figure 43. The FTIR/ATR spectrum of HEMA-PL modified PMMA at 2% and 0.07 Mrad is shown in Figure 44. The spectra were almost identical since the major absorption peaks such as C=O would overlap for both PMMA and HEMA-PL, and the other characteristic peaks for HEMA-PL such as $^{+}N(CH_3)_3$ were too weak to

Figure 41. SEM of unmodified PMMA

Figure 42. SEM of HEMA-PL modified PMMA (2%, 0.07Mrad)

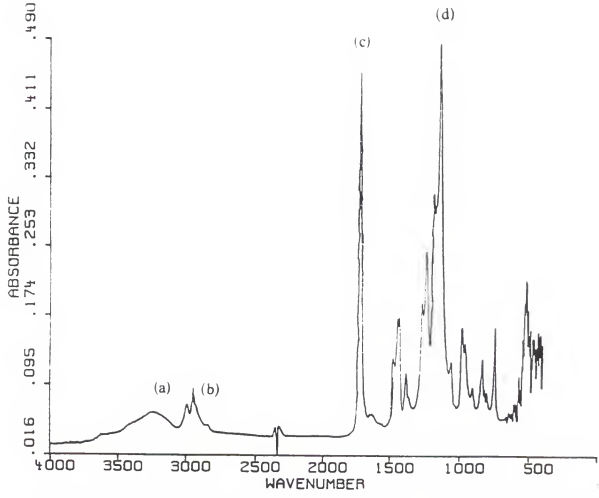

	ν (cm^{-1})	assigment
(a)	2950	- CH_2 - assym. stretch
(b)	2844	- CH_2 - ssym. stretch
(c)	1750	$-\overset{O}{\overset{\|}{C}}-O-$ stretch
(d)	1110-1082	- C - O - C stretch

Figure 43. FTIR/ATR spectrum of unmodified PMMA

HEMA-PL on PMMA

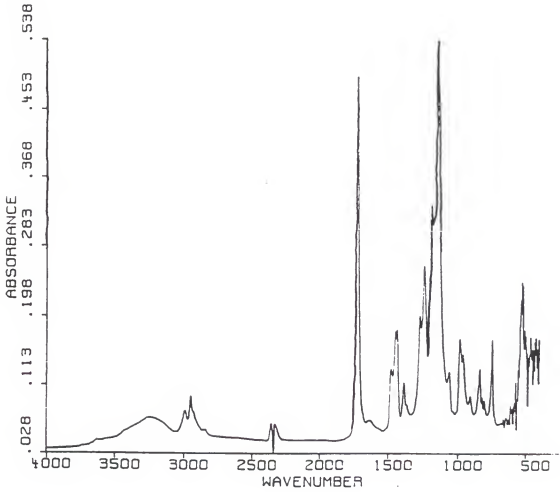

Figure 44. FTIR/ATR spectrum of HEMA-PL modified PMMA (2%, 0.07 Mrad)

detect by FTIR/ATR. Therefore, the FTIR/ATR spectra could not confirm the presence of the HEMA-PL on the PMMA surfaces, especially very thin graft surfaces.

4.4.5 XPS

XPS is a very powerful surface analytical technique for examining the top 50 Å of a surface. The XPS spectrum of unmodified PMMA is shown in Figure 45. As expected, only C1S and O1S peaks were detected and the relative atomic concentrations of C1S and O1S were in reasonable agreement with the theoretical ratio, 71%(C1s): 29%(O1s). The small peak of C1S at 288 eV is also characteristic of the ester group of PMMA.

Figure 46 shows a typical XPS spectrum of a PMMA surface modified with HEMA-PL under 2% and 0.07 Mrad. XPS indicated that a polyHEMA-PL graft was achieved as evidenced by the extra N1S (401 eV) and P2P (135 eV) peaks. Also, the atomic concentration ratio of N1S and P2P was very close to 1:1 as expected from the chemical structure of HEMA-PL. Table 2 summarizes the results of XPS under different graft conditions. At a constant dose (0.07Mrad), the atomic concentration of N1S at the surface slightly increased when the concentration of HEMA-PL monomer was increased from 1 to 2%. In contrast, the increasing trend of N1S was more clear when gamma dose was increased from 0.03 to 0.15 Mrad at a constant concentration of HEMA-PL monomer (1%). At a constant dose (0.07 Mrad), the atomic concentration of P2P increased with increasing monomer concentration in the range of 1 to 10%. At constant monomer concentration (1%), the atomic concentration of P2P also increased with increasing gamma dose from 0.03 to 0.15 Mrad.

From the chemical structure of HEMA-PL, the theoretical atomic concentration of N1S and P2P is 2.12%. XPS for all of the reported grafting conditions yielded somewhat lower N1S and P2P values than theory. The surface distribution and chain orientation of polyHEMA-PL molecules on PMMA surfaces is not very clear. Neverthless, the HEMA-

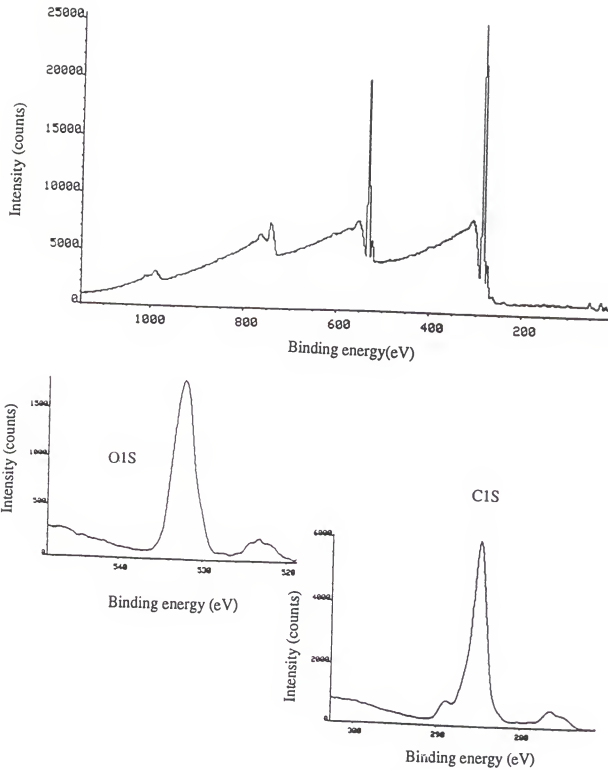

Atomic concentration (%): C1S= 78.3, O1S= 21.7

Figure 45. XPS spectrum of unmodified PMMA

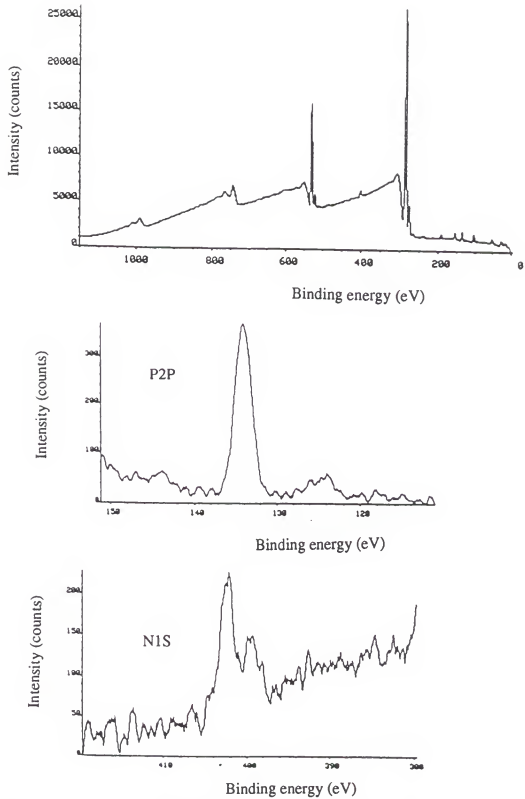

Figure 46. XPS spectrum of HEMA-PL modified PMMA (2%, 0.07 Mrad)

Table 2. Summary of XPS results of modified PMMA with HEMA-PL under different grafting conditions

HEMA-PL concentration (%)	Dose(Mrad)	Atomic concentration(%)			
		C1S	O1S	N1S	P2P
10	0.07	77.8	19.2	1.1	1.9
5	0.07	77.5	20.4	1.0	1.1
2.5	0.07	78.0	20.0	1.1	0.9
2	0.07	78.1	19.9	1.0	1.0
1	0.07	79.1	19.6	0.7	0.6
1	0.15	77.9	19.5	1.7	0.9
1	0.1	78.2	20.3	0.9	0.6
1	0.07	79.1	19.6	0.7	0.6
1	0.03	80.1	19.2	0.4	0.3
Theoretical atomic concentration (%)		68.1	27.7	2.1	2.1

PL modified PMMA produced by these grafting conditions have hydrophilic surfaces as indicated by contact angle measurements. Thus, the HEMA-PL conformation expresses the hydrophilic portion of the molecule at the surface. This is reasonable because the grafting was conducted in the water.

4.4.6 Structure and Stability of HEMA-PL Grafts

C.A. measurements strongly suggested that the hydrophilic HEMA-PL grafts have hydrophilic heads as the graft surface with the two hydrophobic tails closer to the PMMA interface. The theoretical molecular structure and thickness of a monolayer HEMA-PL is shown in Figure 47. The monolayer thickness was calculated by the bond length and angle at each element assuming that each bond is planar zig-zag. HEMA-PL contains vesicles in the solution and molecules at the PMMA interface. Vesicle polymerization is likely due to vinyl groups of one HEMA-PL molecular reacting with an other vinyl group on an adjacent HEMA molecule (2). It is unlikely that significant intramolecular monomer reactions will occur due to stereochemical arrangement.

The actual structure of the HEMA-PL grafts on PMMA is not clear. It is theorized that free radical formation by gamma radiation on PMMA surface occurs as shown in Figure 48 (46). A proposed mechanism for gamma radiation induced grafting polymerization of HEMA-PL is shown in Figure 49. An alternative would be strong physisorption of crosslinked HEMA-PL liposomes onto the PMMA surfaces (Figure 50). However, no adsorbed HEMA-PL liposomes were observed on the modified surfaces using LVSEM. Thus, the only reasonable mechanism is the adsorption of the hydrophobic tails of HEMA-PL on the hydrophobic PMMA surfaces by Van der Waals forces.

The graft stability is very important for any use and also helps verify that covalent bonding occurred with the substrate. Two tests were performed to determine graft stability and whether covalent bonding occurred. First, HEMA-PL modified PMMA was rinsed

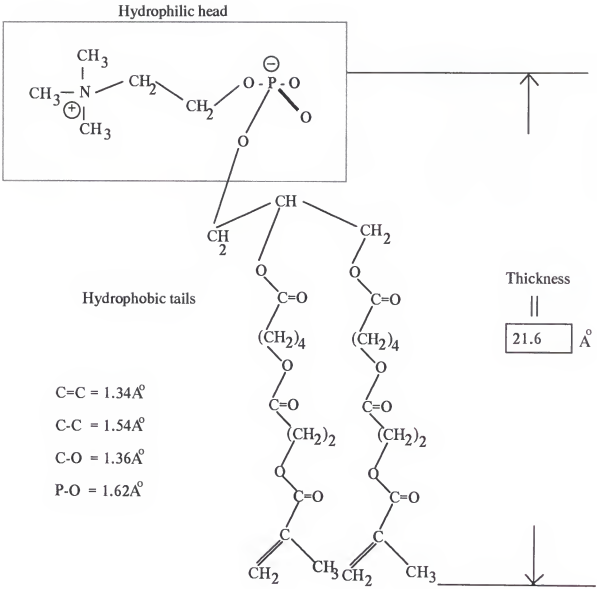

Figure 47. Theoretical HEMA-PL monolayer molecular structure

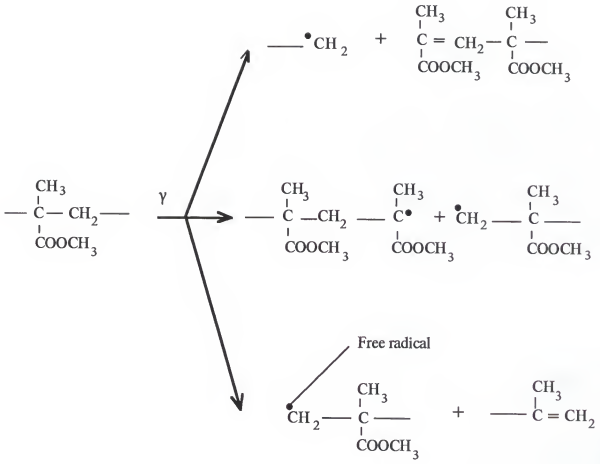

Figure 48. Free radical formation with PMMA by gamma radiation (44)

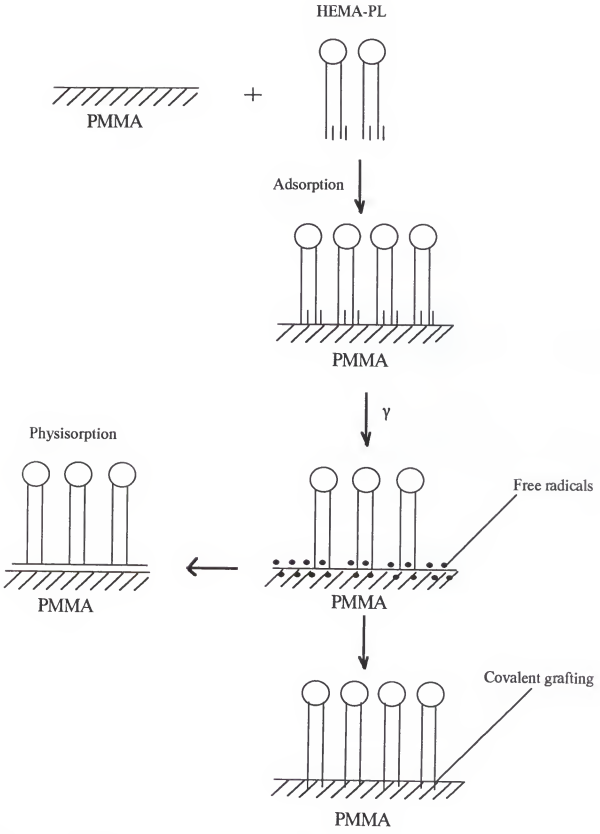

Figure 49. Mechanism for poly HEMA-PL grafts by gamma radiation induced polymerization

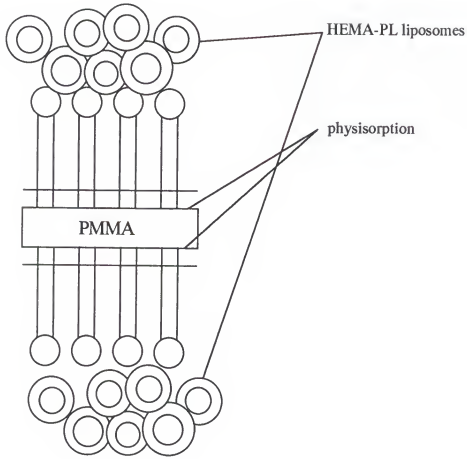

Figure 50. HEMA-PL liposome adsorption on modified PMMA surfaces

with heptane for 2 days. As in Larson's previous study, heptane was used to extract 12-PL liposomes from modified PMMA surfaces (7). Polymerized HEMA-PL is insoluble in heptane but any physisorbed species on PMMA interface will be extracted. After 2 days washing in heptane, the samples were rehydrated in water for 3 days. The surfaces regained their hydrophilicity with C.A.s of 25^{O}. The surfaces remained homogeneous under optical microscopy. For a second test, the heptane extracted HEMA-PL modified PMMA samples were placed in a $60\ ^{0}C$ and the C.A.s were monitored weekly (Figure 51). The surfaces remained hydrophilic with C.A. in the low 20's for 7 weeks. The XPS obtained after 7 weeks is shown in Figure 52. HEMA-PL chemical moieties, P and N, were detected and the atomic concentrations of N1S and P2P were very close to initial values. The polyHEMA-PL graft thus were very stable suggesting covalent bonding rather than physisorption.

4.4.7 Graft Thickness Measurements

A comasie blue PL staining technique was attempted to determine the thickness of the polyHEMA-PL grafts. However, the grafts must be less than 3-5 microns since optical microscopy could not detect them. Ellipsometry using a He-Ne laser at 632.8 nm was therefore used to measure the thickness and the refractive index of dry polyHEMA-PL grafts. The result of ellipsometry for HEMA-PL modified PMMA at 2% and 0.07 Mrad is shown in Table 3. The average thickness of the grafts is 410Å and the refractive index is 1.475. Theoretical molecular monolayer thickness is 21.6 Å suggesting that a multilayer graft (about 18 layers) of polyHEMA-PL on PMMA was created by the gamma radiation method. The refractive index of the graft was slightly lower than unmodified PMMA. The multilayer arrangement of HEMA-PL grafts is not very clear at this point. From a thermodynamic point of view, the second layer of HEMA-PL hydrophobic tails will orient towards water due to the interaction between the hydrophilic heads and the first layer of

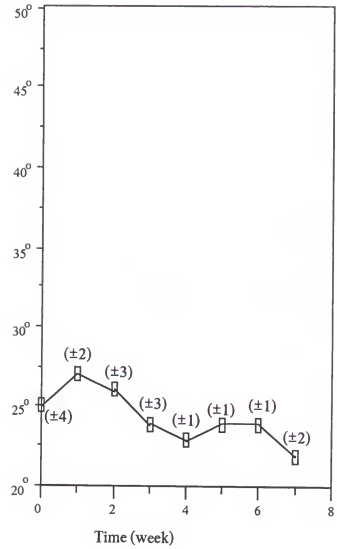

Figure 51. Stability test of HEMA-PL modified PMMA (2%, 0.07 Mrad) after heptane extraction

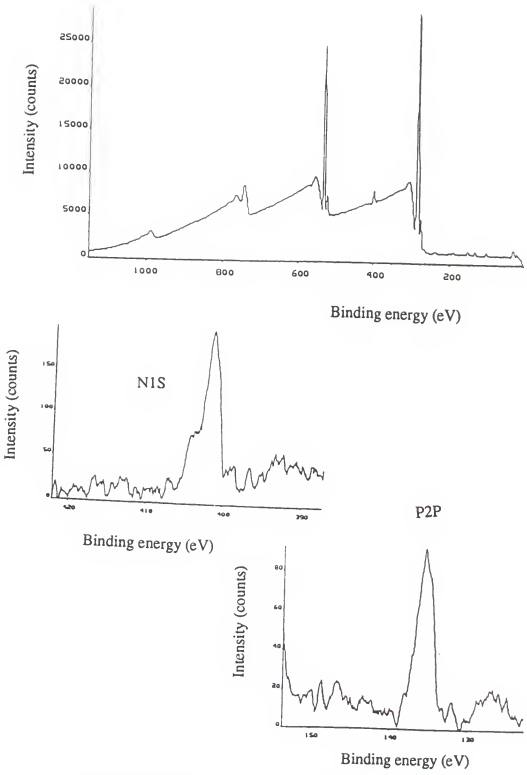

Atomic concentration (%) : C1S= 78.3, O1S= 19.6, N1S = 0.8, P2P = 1.2

Figure 52. XPS spectrum of HEMA-PL modified PMMA (2%, 0.07 Mrad) after 7 weeks of stability test

Table 3. Graft thickness measurement of HEMA-PL modified PMMA (2% , 0.07 Mrad) by Ellipsometry

	Angles (degree)					Graft thickness (Å)
	P_1	A_1	P_2	A_2	Refractive index	
S1	45.9	9.6	135.6	170.5	1.478	400
S2	45.8	9.7	135.5	170.6	1.472	420
S3	45.9	9.7	135.5	170.6	1.475	410
			Average		1.475	410

S1,2,3= HEMA-PL modified PMMA (2%, 0.07 Mrad)

Refractive index of PMMA = 1.490

hydrophilic heads. The next layer will be the interaction between the second and third layers of hydrophobic tails. The possible multilayer arrangement is shown in Figure 53. The resulting surface will be hydrophilic as confirmed by the low C.A.s. However, the association between hydrophilic heads is a polar bond rather than a covalent bond. The structure of poly-HEMA-PL multilayer grafts need to be further investigated. For comparison, LB films were made with a compression trough. This method usually gives perfectly controlled arrangement of surface active molecules (16). Unfortunately, several attempts with HEMA-PL monomer did not produce HEMA-PL films on PMMA substrates.

4.4.8 Epithelial Cell Adhesion and Corneal Endothelial Cell Damage Testing

Cell interactions are important for biomaterials and can be either a positive or negative attribute. For IOLs, cellular deposits on PMMA can induce inflammations, capsular opacification and IOL dislocation caused by the fibrous proliferation of epithelial cells (98). For example, transient fibrinous membranes form on the anterior surface of IOLs during the early post-operative period after cataract surgery (99). These membranes are the result of lens-induced uveitis from the proliferation of epithelial cells and accompanied by inflammations (100). Thus, the inhibition of epithelial cell adhesion on IOL surfaces is important for successful implantation. Figure 54 presents the results of epithelial cell adhesion to unmodified PMMA surfaces. The cells spread and grew over the entire surface with some cells overlapping each other. In contrast, epithelial cells did not adhere to the HEMA-PL modified PMMA at 2% and 0.07 Mrad (Figure 55). The surfaces of HEMA-PL modified PMMA may reduce the possibility of post-operative complications.

Corneal endothelial cell damage is a good method to study cell damage due to contact with implant devices. Corneal endothelial cell damage by surgical manipulation is a

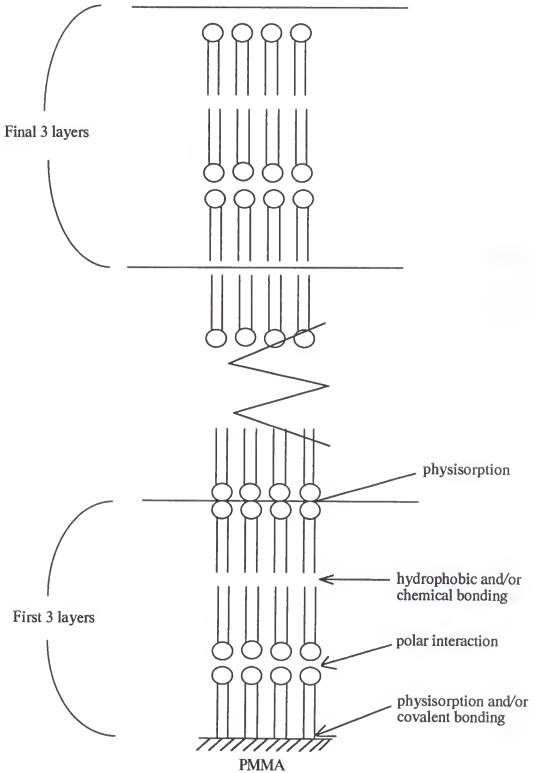

Figure 53. The possible multilayer arrangement of polyHEMA-PL

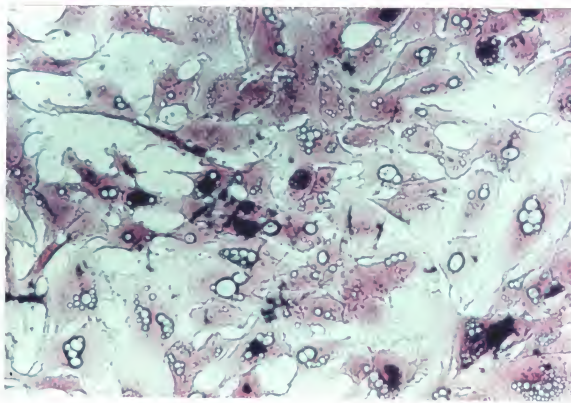

Figure 54. The epithelial cell adhesion for unmodified PMMA (20x)

Figure 55. The epithelial cell adhesion for HEMA-PL modified PMMA (2%, 0.07 Mrad) (20x)

serious problem because they cannot regenerate. The transplantation of a cornea is indicated when damage is serious. Therefore, a protective layer on IOLs is essential during and after IOL implantation. PMMA IOLs were used in this test because they more closely approximate real conditions. The SEM micrograph of corneal endothelial cell damage induced by touching unmodified PMMA IOL is shown in Figure 56. The extent of damage was estimated by the number of cells with white rough spots inside the IOL edges. The small hole located at the bottom of the micrograph represented the junction between optics and haptics. For unmodified PMMA, a significant amount of damage (80%) was observed. From J. Sheet's report, the damage was due to hydrophobic surfaces of PMMA (6).

Similar experiments were carried out for surface modified PMMA IOLs with polyHEMA-PL grafts by gamma radiation at 2% and 0.07 Mrad (Figure 57). The corneal endothelial cells of HEMA-PL modified PMMA IOLs had significantly less damage (5-10%). The only damage spots were located on the edge of the IOL. The hydrophilic polyHEMA-PL graft PMMA may act as a lubricating layer which minimizes the friction between the corneal endothelial cell and IOL surfaces during surgical manipulation. The reduction in corneal endothelial cell damage for 12-PL modified PMMA stubs by UV radiation was also reported by Larson (7).

4.4.9 Summary of Surface Modification of PMMA with HEMA-PL

Surface modified PMMA with hydrophilic polyHEMA-PL was accomplished by gamma radiation induced graft polymerization at concentrations from 1 to 10% and dose from 0.03 to 0.15 Mrad. C.A. measurements and XPS confirmed the grafting of the polyHEMA-PL. Low C.A.(20's) of the HEMA-PL modified PMMA (1 to 10% and 0.03 to 0.15 Mrad) indicated that the modified surfaces are hydrophilic. In the XPS analysis, N and P were observed on the surface modified PMMA with polyHEMA-PL (1 to 10% and

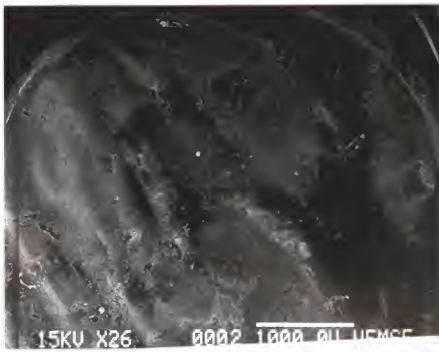

Figure 56. SEM of damaged corneal endothelial cells by unmodified PMMA

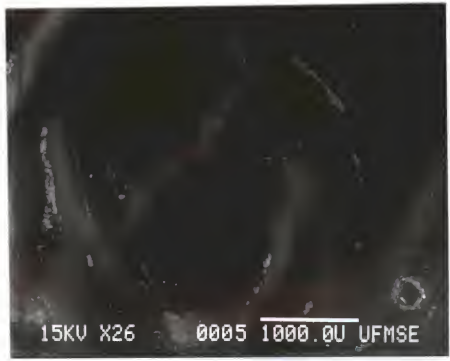

Figure 57. SEM of damaged corneal endothelial cells by HEMA-PL modified PMMA (2%, 0.07Mrad)

0.03 to 0.15 Mrad). As predicted from the chemical structure of HEMA-PL, the atomic concentration ratios of N/P at most grafting conditions were close to one. From SEM, the PMMA surface morphology did not change due to surface modification. From UV-VIS spectrum, the transmission was not significantly attenuated by the HEMA-PL grafting. Due to the overlap of major adsorption bands between HEMA-PL and PMMA substrate, FTIR/ATR spectra did not detect the HEMA-PL grafts. From the ellipsometry measurements, the polyHEMA-PL graft was not a monolayer. Grafts thickness is 410 Å and the refractive index is slightly lower than unmodified PMMA. Surface modified PMMA with HEMA-PL (2% and 0.07 Mrad) was found to have significantly less epithelial cell adhesion and corneal endothelial cell damage than unmodified PMMA.

4.5 Surface Modification of PMMA with HEMA-PL by "Plasma/gamma" Method

A RF plasma/gamma method has been developed in this laboratory for improving graft efficiency. This method involves pretreatment of PMMA with water RF plasma. Ali has reported that water RF plasma pretreatment of polymeric and metal substrates (PMMA, PDMS and stainless steel) produces polar oxygen-containing functional groups on the surface which can enhance interfacial compatibility between substrate and aqueous solution. Furthermore, this can facilitate the free radical formation during gamma radiation. After pretreatment, gamma radiation was used to graft hydrophilic monomers onto the pretreated substrates. In this study, several water RF plasma pretreatment conditions for PMMA were investigated. The HEMA-PL monomer was then grafted on the pretreated PMMA by gamma radiation. Overall, the grafting efficiency was improved compared to gamma radiation alone (40). The surface properties (C.A., XPS etc.) HEMA-PL modified PMMA with water RF plasma pretreatment were characterized.

4.5.1 RF Plasma Pretreatment

The surface oxidation of PMMA by RF plasma pretreatment was characterized by C.A. and XPS. Figure 58 presents the plot of C.A. of RF plasma pretreated PMMA vs plasma treatment time at constant plasma power (50W) and vacuum pressure (0.1 torr). The C.A. of pretreated PMMA dropped down to the lower 20's after 3 mins treatment and levelled off as treatment time increased. Thus, the surfaces of pretreated PMMA were hydrophilic after only 3 minutes of treatment. In order to avoid damage to the PMMA surface caused by plasma bombardment, plasma pretreatment conditions of 3 mins at 50 W and 0.1 torr were used in this study.

The oxidation mechanisms of PMMA by water RF plasma have been reported by Clark (101). He pointed out that UV radiation emitted from the plasma may produce free radicals both on the surface and within the first 10 microns of the substrate. The surface free radicals react with water and resulted in hydroperoxide, hydroxyl, and carbonyl groups on the PMMA surface. Table 4 summarizes the result of the XPS analysis after the water RF plasma pretreatment at varying treatment times. The atomic concentrations of O1S for pretreated PMMA (3 to 10 mins) were slightly higher than unpretreated PMMA. Also, the surfaces of pretreated PMMA were hydrophilic based on C.A. measurements.

4.5.2 " Plasma/gamma" Method

After water plasma pretreatment of PMMA at 3 mins, 50W, and 0.1torr, gamma radiation was used to graft HEMA-PL on the pretreated PMMA surfaces. Table 5 presents the C.A. measurements at various grafting conditions. All of the average contact angles at different grafting conditions were in the 20's indicating that the surfaces were hydrophilic. However, this low C.A. can be attributed to just the hydrophilic water RF plasma pretreatment of PMMA. XPS analysis though confirms the presence of the N and P peaks for the HEMA-PL grafts. Figure 59 shows the typical XPS spectrum of HEMA-PL

power = 50W

Vacuum pressure = 0.1 torr

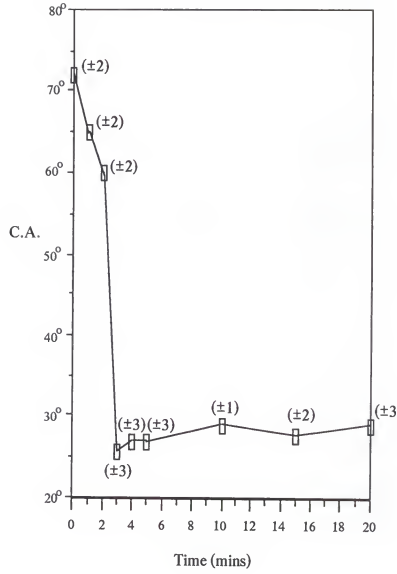

Figure 58. C.A. of water RF plasma pretreated PMMA at different treated time

Table 4. XPS of water RF plasma pretreated PMMA at different treated time

Water plasma treated time (mins)	Atomic concentration(%)	
	C1s	O1s
0	78.3	21.7
3	74.2	25.8
5	74.5	25.5
10	74.3	25.7

Power = 50 W, Pressure = 0.1 torr

Table 5. C.A.s of water RF plasma pretreated PMMA grafted with HEMA-PL at indicated conditions

Grafting conditions		C.A.
Concentration (%)	Dose(Mrad)	(degree)
1	0.15	23 ±2 (20)
1	0.10	21 ±1 (22)
1	0.07	22 ±1 (24)
1	0.03	21 ±3 (25)
5	0.07	22 ±4 (21)

( ) = C.A.s of unpretreated PMMA at indicated grafting conditions

Water RF plasma pretreatment conditions : 3 mins, 50 W, 0.1 torr

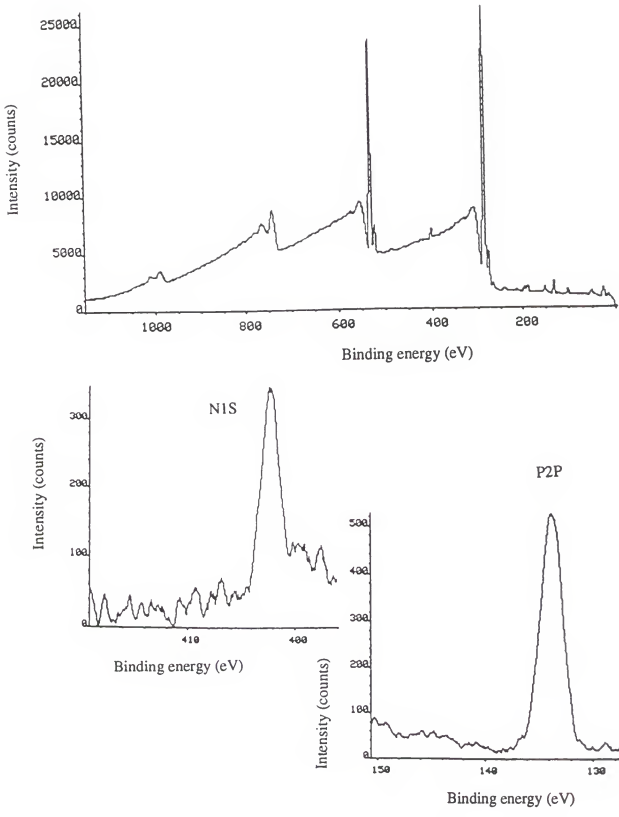

Figure 59. XPS spectrum of HEMA-PL modified PMMA by the plasma/gamma method (2%, 0.07 Mrad)

modified PMMA by the plasma/gamma method. As expected, N1S and P2P atomic concentrations corresponding to the HEMA-PL graft were detected. Also, the atomic concentration ratio of N1S vs P2P was 1:1 as predicted from the chemical structure of HEMA-PL.

Table 6 presents the comparison of N1S and P2P atomic concentrations of HEMA-PL modified PMMA surfaces with and without the water RF plasma pretreatment. For the same grafting conditions, substantially higher atomic concentrations of N1S and P2P were seen on PMMA surfaces modified by the RF plasma/gamma method as opposed to PMMA modified without plasma treatment. Furthermore,the atomic concentrations of N1S and P2P on pretreated PMMA surfaces (1% HEMA-PL, 0.15 Mrad) were very close to the theoretical value (2.1%). The P2P atomic concentration of modified PMMA with pretreatment (5% HEMA-PL, 0.07 Mrad) was even higher than the theoretical value. On the other hand, at the same grafting condition, all of the N1S and P2P atomic concentrations prepared by gamma radiation on unpretreated PMMA surfaces were lower than the theoretical values. Therefore, RF plasma/gamma method enhances grafting atomic concentrations on the surface. The thickness of the polyHEMA-PL grafts obtained by the plasma/gamma method at 2% and 0.07 Mrad was determined from ellipsometery (Table 7). The plasma/gamma method produced thinner grafts (272Å) than the gamma method alone (410Å), but the thickness is still much higher than the theoretical values for a monolayer (21.6Å). This again implies that a multilayer graft (about 12 monolayers) has found. The refractive index of the graft made by plasma/gamma method was also slightly lower than the PMMA substrate.

Based on C.A. measurements, the surfaces of PMMA became hydrophilic after water RF plasma treatment at 3 mins, 50W and 0.1torr. The hydrophilic head of HEMA-PL may have a high affinity to the hydrophilic pretreated surfaces so that hydrophobic tails should orient away from the surface. Therefore, after gamma radiation, the

Table 6. XPS of HEMA-PL modified PMMA with and without water RF plasma treatment at indicated grafting conditions

HEMA-PL concentration (%)	Dose (Mrad)	Atomic concentration (%)			
		N1s untreated PMMA	P2p	N1s plasma pretreated PMMA	P2p
1	0.15	1.7	0.9	2.3	1.9
1	0.10	0.9	0.6	1.1	1.3
1	0.07	0.7	0.6	0.7	1.3
1	0.03	0.4	0.3	0.5	0.6
2	0.07	1.0	1.0	1.4	1.7
5	0.07	1.0	1.1	2.1	3.4

Theoretical atomic concentration (%) N1s = 2.1 P2p = 2.1

Table 7. Graft thickness measurement of HEMA-PL modified PMMA by the plasma/gamma method at 2% and 0.07 Mrad by Ellipsometry

	Angles (degree)				Refractive index	Graft thickness (Å)
	P_1	A_1	P_2	A_2		
S1	46.5	9.8	134.5	170.4	1.474	253
S2	46.8	10.7	135.5	170.6	1.470	270
S3	46.9	9.7	135.3	170.6	1.468	294
			Average		1.471	272

S1,2,3= HEMA-PL modified PMMA by the plasma/gamma method (2%, 0.07 Mrad)

Refractive index of PMMA = 1.490

modified surfaces should be hydrophobic. However, the HEMA-PL modified PMMA by the plasma/gamma method was hydrophilic (C.A.s in 20's). Apparently, the interaction between the hydrophilic surfaces and the hydrophilic heads of HEMA-PL was suppressed by the interaction between the water medium and the hydrophilic heads. Furthermore, due to surface energy consideration, the hydrophobic tails of HEMA-PL are not likely to orient towards water. Hence, the hydrophilic heads of HEMA-PL still orient towards the surrounding water although the water and the final surfaces were hydrophilic. The possible structure of polyHEMA-PL on pretreated PMMA is shown in Figure 60. Whether covalent bonding or physisorption occurred in the interface is still not known.

4.5.3 Epithelial Cell Adhesion

Epithelial cell adhesion was conducted to confirm the influence of water RF pretreatment on PMMA and the result is illustrated in Figure 61. The epithelial cells covered the water RF plasma surfaces (3 mins, 50W, and 0.1torr) to the same degree as they covered unmodified PMMA. Water RF plasma pretreatment alone cannot reduce the adhesion of epithelial cells even though the surfaces were hydrophilic. However, the surfaces of HEMA-PL PMMA at 2% and 0.07 Mrad by the plasma/ gamma method did not have any adhered epithelial cell as shown in Figure 62. The spot in the center of photograph was unwashed residue. Thus, hydrophilic surfaces alone are not able to inhibit epithelial cell adhesion, but hydrophilic HEMA-PL grafting on PMMA by either methods mentioned were able to inhibit cell adhesion.

Cunanan et al. reported that materials with low or high interfacial free energies have lower epithelial cell adhesion than materials with intermediate free energies (102). Hydrophilic polyHEMA-PL grafts on PMMA surfaces have low interfacial free energies and have significantly less epithelial cell adhesion than unmodified PMMA. However, hydrophilic PMMA prepared by water RF plasma had the same epithelial cell adhesion as

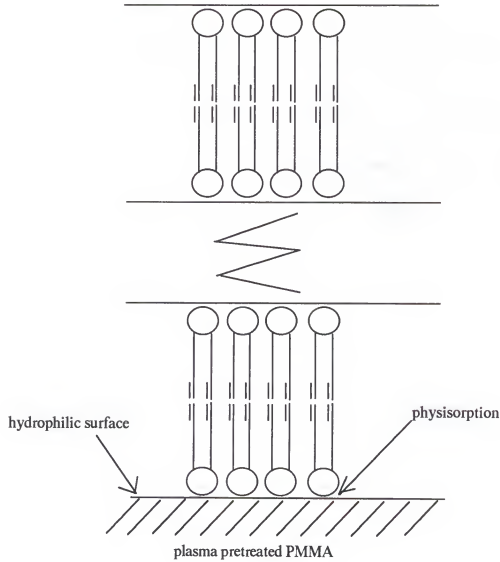

Figure 60. The possible structure of HEMA-PL on water RF-plasma treated PMMA

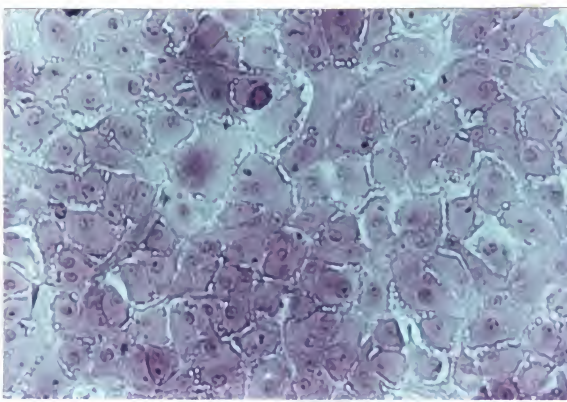

Figure 61. The epithelial cell adhesion for water plasma pretreated modified PMMA (20x)

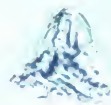

Figure 62. The epithelial cell adhesion for HEMA-PL modified PMMA by the plasma/gamma method (2%, 0.07 Mrad) (20x)

unmodified PMMA. This observation apparently contradicted the free energy hypothesis proposed by Knight. Therefore, the lower interfacial free energy was only a necessary but not a sufficient condition for lower epithelial cell adhesion. Another possible explanation for this phenomenon is that RF plasma roughens the PMMA substrate by molecular collisions between the plasma medium and the substrate. Increased surface roughness generally favors cell or protein adhesion (25). Epithelial cells did not adhere to HEMA-PL modified PMMA by the plasma/gamma method indicating that the surfaces were fully covered by the polyHEMA-PL grafts.

4.5.4 Vascular Endothelial Cell and Platelet Adhesion

Thromboresistance is the critical factor in vascular implants. In a normal blood vessel, a living lining of endothelium separates the blood from potentially thrombogenic tissue (103). Therefore, endothelial cell adhesion tests are important to determine if a natural protective layer forms on implant surface. Also, platetet adhesion onto surfaces can initiate platelet activation leading to coagulation. Thus, preventing platelet adhesion on implant surfaces can reduce the thrombogenicity of vascular devices.

Table 8 presents the results of endothelial and platelet adhesion for unmodified PMMA and HEMA-PL PMMA modified at 5% and 0.07 Mrad by the plasma/gamma method. HEMA-PL PMMA modified by the plasma/gamma method had less endothelial and platelet adhesion than unmodified PMMA. Also, the ratio of endothelial cell to platelet cells for HEMA-PL modified PMMA by plasma/gamma method was less than 1.

Kazuhiko Ishihara et al. have reported that the number of adherent platelets decreased in platelet-rich plasma for polymers with phosphorylcholine polar groups (39). Also, activation of platelets and formation of fibrin were completely suppressed. The outside polar groups on polyHEMA-PL grafts are phosphorylcholine and thus exhibited lower platelet adhesion. However, surfaces covered with endothelial lining are generally

Table 8. The result of endothelial cell and platelet adhesion for PMMA and HEMA-PL modified PMMA by the plasma/gamma method

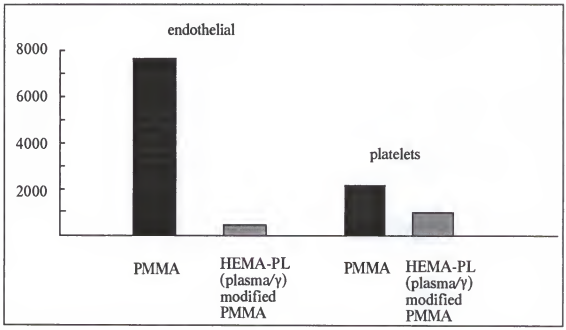

	endothelial cells (1)	plateletes (2)	ratio (1)/(2)
PMMA	7617 ± 1019	2473 ± 555	3
Modified PMMA*	380 ± 286	1233 ± 296	<1

* : water RF plasma pretreatment (50w, 3 min., 0.1 torr) + 5 % HEMA-PL, 0.07 Mrad

considered to be ideal nonthrombogenic surfaces. HEMA-PL modified PMMA by plasma/gamma method apparently did not have more endothelial adhesion than unmodified PMMA. Although endothelial adhesion on polymer surfaces is crucial for thromboresistant biomaterials, the coagulation mechanism is dynamic and complex. Also, the flow of blood significantly effects the stability of endothelial cell lining (104). Therefore, this in vitro study only provides information on the interaction between the specified cells and the grafts. Further in vivo tests are needed to evaluate HEMA-PL modified PMMA. At least, polyHEMA-PL surfaces had lower platelet adhesion than unmodified PMMA surfaces.

4.5.5 Summary of Surface Modification of PMMA with HEMA-PL by "plasma/gamma" Method

Hydrophilic polyHEMA-PL grafts on PMMA surfaces were created by water RF plasma pretreatment of PMMA followed by gamma radiation. Water RF plasma at 3 mins treatment time, 50W and 0.1 torr was chosen to prepare hydrophilic surfaces of PMMA. The resulting PMMA surface was hydrophilic with a low C.A. (26^0). After gamma radiation of pretreated PMMA, HEMA-PL modified PMMA had higher N1S and P2P atomic concentrations than PMMA modified by gamma radiation alone (same grafting conditions). The graft thickness (272Å) of HEMA-PL modified PMMA by plasma/gamma method was thinner than the graft (410Å) prepared in the absence of water RF plasma pretreatment. The HEMA-PL grafts produced by both methods were multilayer. Also, the refractive index of the polyHEMA-PL graft was lower than the PMMA substrate. PMMA modified by water RF plasma pretreatment alone was unable to inhibit epithelial cell adhesion although the surfaces were hydrophilic. However, PMMA modified with HEMA-PL by RF plasma/gamma method did not stick epithelial cells. For vascular application, HEMA-PL modified PMMA by plasma/gamma method was found to have less endothelial cell and platelet adhesion than unmodified PMMA. However, the ratio of endothelial vs platelet cells was less than 1.

4.6. Surface Modification of PMMA with 12-PL with Water RF Plasma Pretreatment

Based on chemical structure, 12-PL have longer hydrophobic tails than the HEMA-PL. The difference in hydrophobic tail length might result in different graft characteristics on modified PMMA surfaces even though the hydrophilic heads were the same. For instance, hydrophilic poly12-PL grafts on PMMA surfaces were prepared by UV radiation and not by gamma radiation. The 20% 12-PL dispersion did not become viscous after 0.15 Mrad gamma radiation, but a gel-like liquid did form at 0.02% dispersion after 2 hours of UV radiation. Also, a lower concentration of 12-PL than the HEMA-PL was needed to achieve grafting on PMMA .

Surface modification of PMMA with 12-PL by UV radiation has been studied by Larson (7). The 12-PL modified PMMA was shown to present a low interfacial free energy surface with significant mitigation of adhesion to tissue. However, limited grafting conditions had been reported due to the difficulty of the synthesis. In this study, a much improved synthesis pathway has been conducted. A novel plasma/UV method was developed to improve the grafting process. Like the plasma/gamma method, PMMA substrates were pretreated with water RF plasma to produce polar surfaces. After pretreatment, UV radiation was used to graft 12-PL on pretreated substrates. Also, rabbit epithelial cell adhesion and vascular endothelial cell and platelet adhesion were studied.

4.6.1 Graft Characterization

The poly12-PL grafts on PMMA by plasma/UV method was characterized by C.A. measurements, XPS, and ellipsometery. Water RF plasma pretreatment conditions were chosen as 3 mins, 50W and 0.1torr. After UV radiation, 12-PL vesicles formed white polymerized gels suspended in the water. Table 9 presents the results of C.A. measurements of 12-PL modified PMMA with and without water RF plasma pretreatment. The resulting 12-PL modified PMMA with and without water RF plasma pretreatment had

Table 9. C.A.s of 12-PL modified PMMA with or without plasma pretreatment under different grafting conditions

12-PL concentration (%)	UV time (hrs)	C.A. (degree) pretreatment	unpretreatment
0.1	2	19±3	20±2
0.1	1	23±2	18±4
0.05	2	21±1	19±2
0.05	1	21±2	23±2
0.02	2	24±2	25±3
0.02	1	23±1	25±2

Water RF plasma pretreatment conditions = 50W, 0.1 torr, 3 mins.

low C.A.s at each grafting condition. This indicated that the hydrophilic head groups of 12-PL are located on the outside of the modified surfaces. The minimum grafting conditions are chosen as 0.02% dispersion and UV exposure time of 1 hour.

The XPS results for 12-PL modified PMMA are shown in Table 10. The XPS spectrum of 12-PL modified PMMA by the plasma/UV method at 0.1% and 2 hours is presented in Figure 63. As expected from the chemical structure of 12-PL, extra N1S and P2P peaks were detected on the modified PMMA surfaces with and without water RF plasma pretreatment (0.02 to 0.1% and 1 to 2 hrs) confirming the presence of the poly12-PL graft. Furthermore, the atomic concentrations of N1S and P2P on modified PMMA by the plasma/UV method were higher than on modified PMMA without pretreatment. The atomic concentration of N1S and P2P of modified PMMA by the plasma/UV method (0.1%, 2 hrs) closed to theoretical values (1.9%). The plasma/UV method increased the density of N1S and P2P atomic concentrations compared with an untreated PMMA substrate. The atomic concentrations of N1S and P2P for 12-PL modified PMMA by the plasma/UV method at 0.1% and UV 2 hours even exceeded theoretical values (1.9%). The theoretical monolayer structure of 12-PL at the PMMA/water interface is shown in Figure 64. The 12-PL monolayer theoretical thickness (23.3Å) was higher than the one for HEMA-PL (21.6 Å). Again, the planar zig-zag of each bond was assumed for the monolayer thickness calculation of 12-PL.

The thickness of poly12-PL grafts on PMMA with and without pretreatment at 0.1% and UV 2 hours were determined by ellipsometery (Table 11). The poly12-PL graft without plasma pretreatment of PMMA (586Å, about 25 layers) was thicker than the graft obtained by the plasma/UV method (443Å, about 19 monolayers). Water RF plasma pretreatment of PMMA reduced the thickness of the grafts. This trend was consistent with PMMA modified with HEMA-PL by the plasma/gamma method. However, the graft thickness of 12-PL by the plasma/UV method (443Å) was a little higher than the one for

Table 10. XPS of 12-PL modified PMMA with or without plasma pretreatment under different grafting conditions

12-PL concentration (%)	UV time (hrs)	Atomic concentration(%) N1s pretreatment	P2p pretreatment	N1s unpretreatment	P2p unpretreatment
0.1	2	2.8	3.1	1.6	1.7
0.1	1	1.5	1.9	0.6	0.7
0.05	2	1.5	1.7	0.9	1.2
0.05	1	1.5	1.1	0.5	0.4
0.02	2	0.9	0.8	0. 6	0.3
0.02	1	0.9	0.6	0.4	0.3

Water RF plasma pretreatment conditions = 50W, 0.1 torr, 3 mins.
Theoretical atomic concentation of poly12-PL, N1s =1.9%, P2p = 1.9%

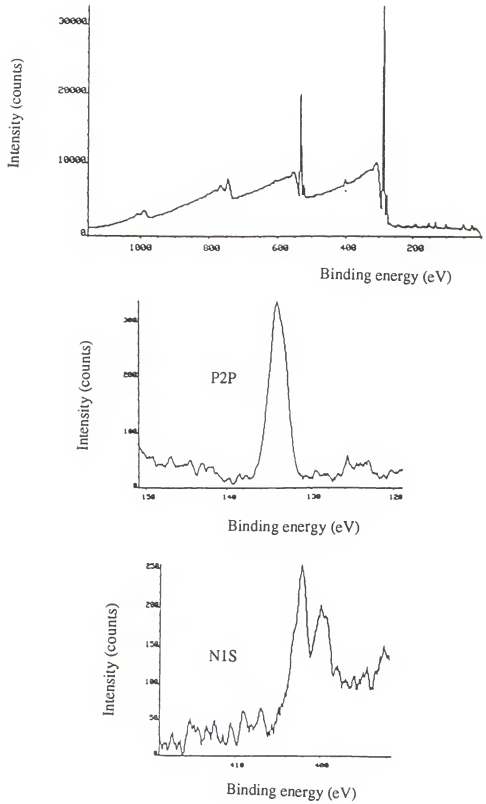

Figure 63. XPS spectrum of 12-PL modified PMMA by the plasma/ UV method (0.1%, UV time of 2 hours)

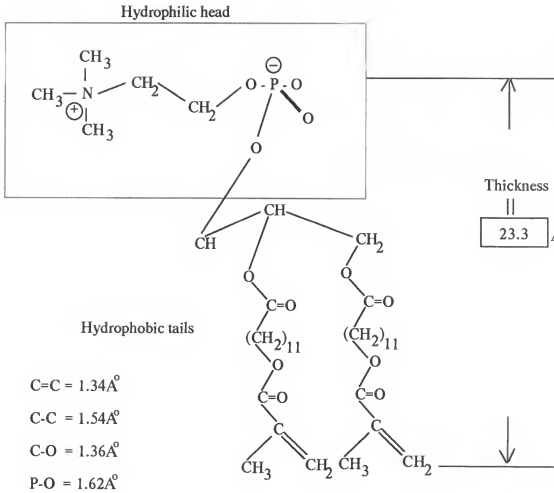

Figure 64. Theoretical monolayer structure of 12-PL

Table 11. Graft thickness measurement of 12-PL modified PMMA with and without plasma pretreatment by Ellipsometry

	Angles (degree)				Refractive index	Graft thickness (Å)
	P_1	A_1	P_2	A_2		
S1	45.6	9.8	135.6	170.2	1.473	440
S2	45.7	9.7	135.3	170.6	1.471	460
S3	45.3	9.7	135.5	170.6	1.474	430
			Average		1.473	443
S4	47.8	8.9	134.6	170.5	1.478	580
S5	47.7	8.9	134.5	170.7	1.479	592
S6	47.8	8.8	134.5	170.7	1.478	585
			Average		1.478	586

S1,2,3= 12-PL modified PMMA by the plasma/UV method at 0.1% and UV time of 2 hours

S4,5,6= modified PMMA by UV radiation alone at 0.1% and UV time of 2 hours

Refractive index of PMMA = 1.490

HEMA-PL (272Å). Also, the poly12-PL graft by both methods did not provide monolayer coverage on PMMA.

The stability mechanisms of 12-PL on polymeric substrates by UV radiation have been explained by Regen et al. (4). They suggested that the stability of the 12-PL grafts is achieved in three ways: extended hydrophobic interactions between hydrophobic tails and hydrophobic polymeric substrate, insolubility of the newly formed cross-linked network of vesicles, and covalent linking of 12-PL to alkyl radicals generated on the polymeric surface. The first two ways involve physisoption on the interface while the last involves the covalent bond. To date, the characterization of chemical bonding at the interface of the polymeric substrate is still the most difficult subject. However, the evidence of free radical generation by UV radiation on polymeric substrates such as polyester, PMMA, polyethylene and polyethylene terephthalate has been reported (51). Therefore, it is likely that the bonding between the poly12-PL and the PMMA substrate is covalent bonding. In fact, one reason for the water RF plasma pretreatment of PMMA is to enhance the possibility of free radical generation during UV radiation.

Regen et al. (4) analyzed the phosphorous content of the poly12-PL grafts and converted it to the packing density of lipid molecules on the PE substrate. They concluded that the packing density of poly12-PL ($1.4 \times 10^{14}/cm^2$) equaled the theoretical value. This indicated that all of the available surface has been covered by poly12-PL. Also, a homogeneous, smooth 12-PL modified PMMA surface by UV radiation was observed by Larson (7). In our study, different areas of modified PMMA were examined by C.A. measurements and optical microscopy suggesting that this is a uniform grafts.

4.6.2 Epithelial Cell Adhesion

The result of epithelial cell adhesion of modified PMMA with 12-PL by UV radiation alone at 0.1% and UV 2 hours is shown in Figure 65. The spardic epithelial cell

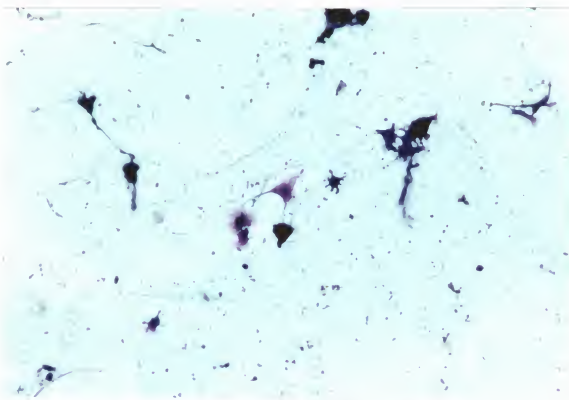

Figure 65. The epithelial cell adhesion for 12-PL modified PMMA by UV radiation (0.1%, UV time of 2 hours) (20x)

can be seen around the modified surface. Also, those adhered epithelial cells were constrained and did not spread out over the occupied areas. Furthermore, the 12-PL modified PMMA surfaces had less epithelial cell adhesion than unmodified PMMA (Figure 54). Figure 66 presents the results of cell adhesion of modified PMMA with 12-PL by plasma/UV method at 0.1% and UV 2 hours. Like 12-PL modified PMMA without plasma pretreatment, small amounts of epithelial cells were observed on the surface. As discussed before in Figure 61, plasma pretreatment of PMMA did not reduce the amount of epithelial cell adhesion. The PMMA modified with 12-PL by UV or plasma/UV methods ended up with PL coverage on the surface. The cells interacted with the complete PL membrane surface. Therefore, poly12-PL graft surface had some degree of interaction resulting in epithelial cell adhesion.

Epithelial cell adhesion on modified PMMA with HEMA-PL or 12-PL was different. For HEMA-PL grafts on a PMMA surface, almost no epithelial cells adhered to the surface. However, 12-PL grafting on PMMA had some epithelial cell adhesion on the surface although those cells did not spread out beyond the adhered areas. The difference between those PLs was that 12-PL has longer hydrophobic tails than HEMA-PL. The difference in chemical structure of PLs caused this difference of epithelial cell adhesion even though the polar group of two PLs were the same. The epithelial cell adhesion on biomaterials was a kind of foreign-body reaction. The inflammations after IOL implantation were possibly triggered by cellular deposits (71). In this study , the reduction of epithelial cell adhesion on modified PMMA surface by PLs apparently may hopefully reduce the chance of inflammation.

4.6.3 Platelet and Endothelial Cell Adhesion

The results of platelet and endothelial cell adhesion for 12-PL modified PMMA with and without water RF plasma pretreatment (0.1% and UV 2 hours) are presented in Table

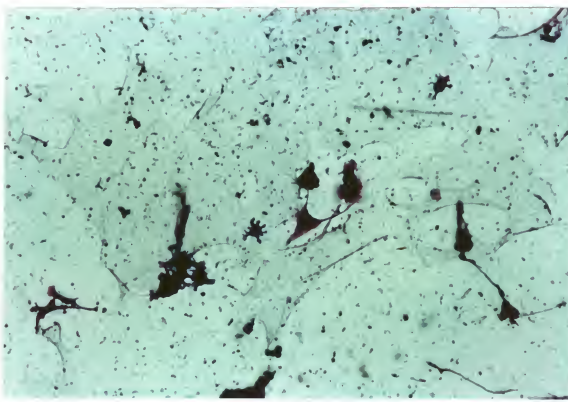

Figure 66. The epithelial cell adhesion for 12-PL modified PMMA by the plasma/UV method (water pretreated PMMA at 3 mins, 50W, 0.1torr) (0.1%, UV time of 2 hours) (20x)

12. For 12-PL modified PMMA without pretreatment, the number of adhered endothelial cells was much higher than the incidence on unmodified PMMA. However, the number of adhered platelet cells was very close to the results obtained for unmodified PMMA. The ratio of endothelial to platelet cells was higher than 1. For 12-PL modified PMMA with pretreatment, the amount of endothelial cell adhesion was also higher than one for unmodified PMMA. Furthermore, platelet adhesion was lower than for unmodified PMMA and also lower than for 12-PL PMMA modified without plasma pretreatment. The ratio of endothelial to platelet cells was also higher than 1 and even higher than that for modified PMMA without plasma pretreatment.

The PMMA modified with 12-PL by the plasma/UV method provided an ideal biomaterial surface for vascular applications. The platelet adhesion was reduced and endothelial cell adhesion was enhanced by the hydrophilic polyPL surface compared with unmodified hydrophobic PMMA. Surprisingly, modified PMMA without plasma pretreatment had higher platelet adhesion than that achieved with plasma pretreatment although the surfaces were covered with the same poly-12-PL grafts. Nevertheless, the ratio of endothelial to platelet cell adhesion was higher than 1 for each method . For polyHEMA-PL surfaces (Table 8), endothelial adhesion was much less than for poly12-PL surfaces although it reduced platelet adhesion. The difference in endothelial adhesion between these two PLs might be due to the length of hydrophobic tails.

Albrecht et al. reported that polymeric PLs in vitro did not participate as a cofactor in coagulation and the restricted lateral diffusion of proteins along a polymeric surface will also inhibit the formation of coagulation complexes. Also, platelet reactivity in vitro is not affected by polymeric PLs (38). Furthermore, Ishihara reported that polymers which had phosphorylcholine polar groups reduced in vitro platelet adhesion (39). The same tendency was noted when Ca^{+2} readded platelet-rich plasma came in contact with the PL modified polymers. The Ca^{+2} ions were required for the activation of platelets accompanying

Table 12. The result of endothelial and platelet adhesion for PMMA and 12-PL modified PMMA by the plasma/UV method and UV radiation only

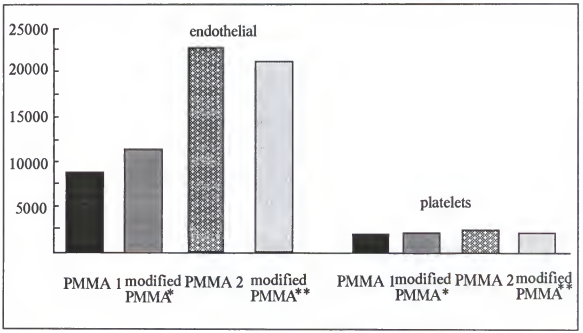

		endothelial cells (1)	plateletes (2)	ratio
PMMA 1		7617 ± 1019	2473 ± 555	3
Modified	*	12370 ± 2711	3027 ± 1682	4

* : 0.1 % 12-PL, UV 2 hs.

PMMA 2		23640 ± 6050	5320 ± 1270	4
Modified	**	21760 ± 11250	3970 ± 2250	5

** : water plasma pretreatment (50w, 3 min., 0.1 torr)+ 0.1 % 12-PL, UV 2 hs.
PMMA 1, PMMA 2 : PMMA cultured in different batch

thrombus formation (39). The above observations coincided with our platelet adhesion results of poly12-PL and polyHEMA-PL surfaces on PMMA. Furthermore, more endothelial adhesion to poly12-PL surfaces than unmodified PMMA surfaces confirmed that a natural non-thrombogenic endothelial lining might form on poly12-PL surfaces. Hence, hydrophilic poly12-PL surfaces may improve hemocompatibility of biomaterials for vascular application.

4.6.4 Summary

Surface modification of PMMA with 12-PL was accomplished by UV and plasma/UV methods at concentrations of 0.02% to 0.1% and UV time from 1 to 2 hours. In the plasma/UV method, PMMA was pretreated with water RF plasma (3 mins, 50W and 0.1 torr) and irradiated in a 12-PL monomer dispersion by UV radiation. PMMA modified with 12-PL by plasma/UV method had higher N1S and P2P atomic concentrations than without plasma pretreatment of PMMA as determined by XPS. At the concentration of 0.1% and UV time 2 hours, 12-PL modified PMMA by plasma/UV method produced higher N1S and P2P atomic concentrations than theoretical values (1.9%). Low C.A.s of modified PMMA by both methods were observed, which indicated the presence of hydrophilic surfaces. The graft thickness of poly12-PL by the plasma/UV method (443Å) was less than that achieved without plasma pretreatment (586Å). Poly12-PL grafts on PMMA prepared by both methods at 0.1% and UV time 2 hours had significantly less rabbit epithelial cell adhesion than unmodified PMMA although some spardic cells constrained in fixed areas were observed. Also, the ratios of endothelial/ platelet cells adhesion for 12-PL modified PMMA by both methods at 0.1% and UV time 2 hours were higher than 1. This might favor the endothelial adhesion on the 12-PL modified PMMA. Furthermore, platelet cell adhesion of 12-PL modified PMMA prepared by both methods

was substantially lower than unmodified PMMA. Hydrophilic poly12-PL grafting on PMMA by UV or plasma/UV methods may have potential to be nonthrombogenic surfaces.

4.7 Surface Modification of PP and PDMS with 12-PL by UV Radiation

In addition to PMMA, 12-PL was grafted on PP and PDMS. PP is a common material for the IOL haptics. PDMS is a potential material for soft IOLs. PP and PDMS are hydrophobic, so surface modification of these materials is imperative. 12-PL monomer in an aqueous medium will attach onto the surface with hydrophilic head groups oriented towards water. UV radiation then polymerized adsorbed 12-PL monomers to form a stable graft. The objective of using PP and PDMS was to investigate the versatility of using the aforementioned surface modification method for 12-PL grafting.

4.7.1 Surface Modification of PP with 12-PL by UV Radiation

The hydrophilicity of modified PP with a 12-PL graft by UV radiation was measured by C.A. measurements and the results are shown in Table 13. The surface of 12-PL modified PP at 0.1% and UV time 1 and 2 hours were hydrophilic as compared to unmodified PP. Figure 67 presents the FTIR/ATR spectrum of unmodified PP with accompanying peaks assignment. After surface modification with 12-PL by UV radiation, the resulting ATR spectrum of 12-PL modified PP at 0.1% and UV time 2 hours is shown in Figure 68. In addition to the peaks shown in Figure 67, an extra carbonyl peak (1720 cm^{-1}) was observed. This peak might come from the oxidation mechanism of PP by UV radiation. In order to test this possibility, unmodified PP was placed in pure water and irradiated with UV for 2 hours. The resulting ATR spectrum, shown in Figure 69, did not contain a carbonyl peak. Apparently, the carbonyl peak is not due to UV oxidation of PP film. This carbonyl peak should come from the chemical moieties of 12-PL and therefore confirmed the presence of the graft. This carbonyl peak was not detected for 12-PL

Table 13. C.A.s of 12-PL modified PP by UV radiation at 0.1% and UV time of 1 and 2 hours

12-PL concentration (%)	UV time (hrs)	C.A. (degree)
0.1	2	23±2
0.1	1	24±1
Unmodified PP		93±2

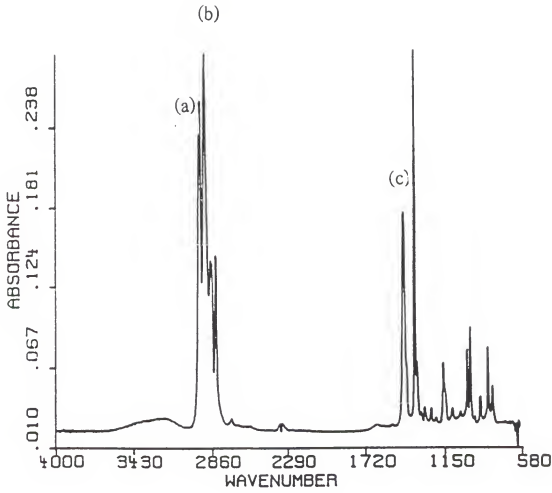

	$\nu(cm^{-1})$	Assignment
(a)	2930	$-CH_3$ stretch
(b)	2864	-C-H stretch
(c)	1460	$-CH_3$ deformation

Figure 67. FTIR/ATR spectrum of unmodified PP

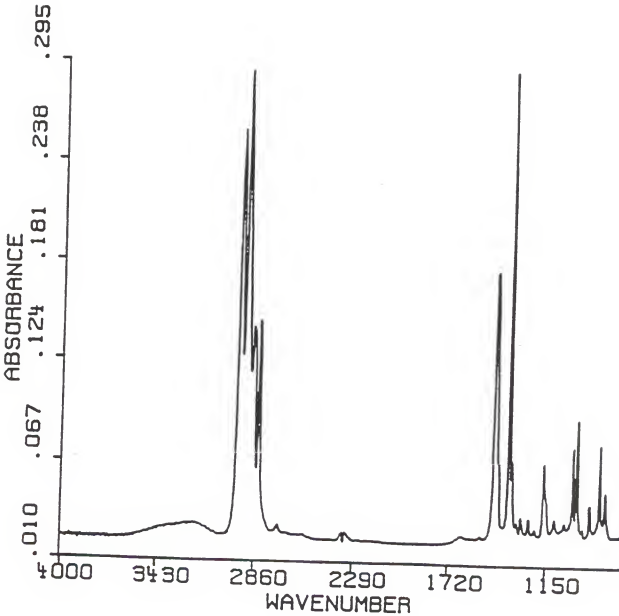

Figure 69. FTIR/ATR spectrum of unmodified PP after UV radiation of 2 hours

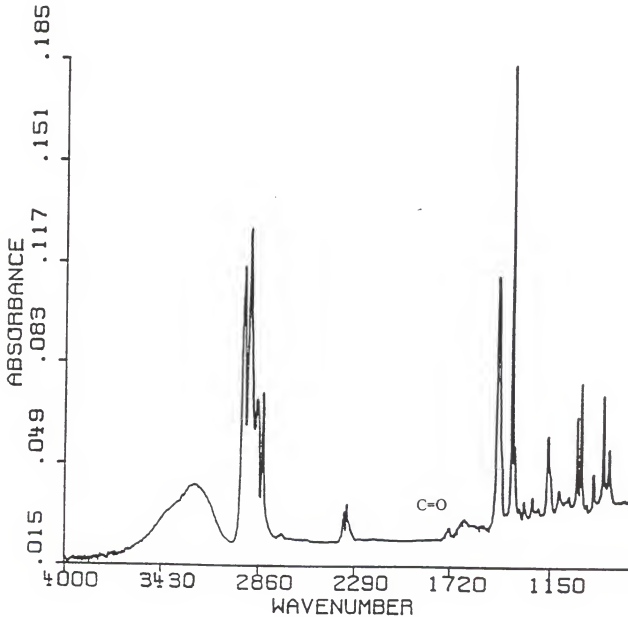

Figure 68. FTIR/ATR spectrum of 12-PL modified PP by UV radiation (0.1%, UV time of 2 hours)

modified PP at 0.1% and UV time 1 hour. The grafting may be too thin to be observed by FTIR/ATR.

The XPS spectrum of unmodified PP is presented in Figure 70. A small amount of oxygen was detected along with Carbon. This indicated that the PP film has a small degree of oxidation although it could not be detected by FTIR/ATR. After surface modification, the resulting XPS spectrum of 12-PL modified PP at 0.1% and UV time 2 hours is shown in Figure 71. The extra N and P elements were detected based on the chemical structure of 12-PL. The XPS atomic concentrations for 12-PL modified PP at 0.1% and UV time 1 and 2 hours are presented in Table 14. The ratio of N1S to P2P atomic concentrations for 12-PL modified PP at 0.1% and UV time 1 hour was close to 1 as expected from chemical structure of 12-PL. P2P atomic concentration was higher for a UV time 2 hours than 1 hour at 0.1% concentration. However, the N1S and P2P atomic concentration for these modified PP were still lower than theoretical values (1.9%). The P2P atomic concentration (1.4%) of 12-PL modified PP at 0.1% and UV time 2 hours was much higher than the N1S atomic concentration (0.5%).

The same 12-PL graft by UV radiation was conducted by S. Regen on PE substrate (4). PE and PP belong to the polyolefin family. Similar grafting results should be expected for both PE and PP. XPS and FTIR/ATR did confirm the presence of poly12-PL grafts. Since the samples floated in the 12-PL dispersion, they were weighted with a metal clamps to keep them submerged during UV radiation. After surface modification, the areas in contact with the clamp was cut off and the remaining PP film was used for analysis.

4.7.2 Surface Modification of PDMS with 12-PL by UV Radiation

PDMS is a potential material for soft IOLs. However, the hydrophobic surface of PDMS can cause some complications after surgery just like PMMA. Hence, hydrophilic surface modification of PDMS should improve their biocompatibility. C.A. measurements

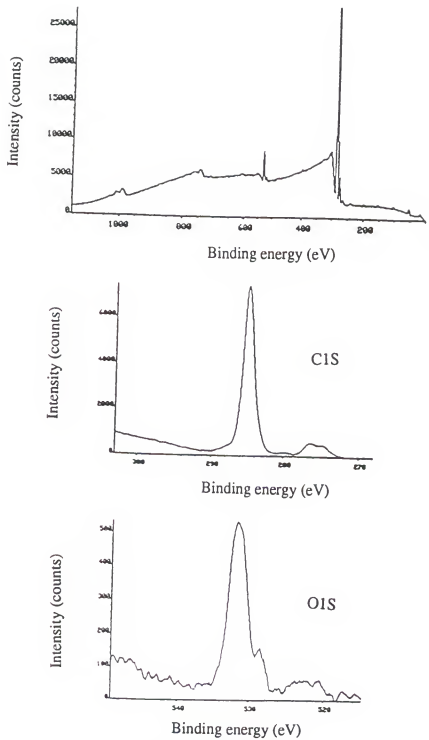

Atomic concentration (%) :C1S = 94.2, O1S = 5.8

Figure 70. XPS spectrum of unmodified PP

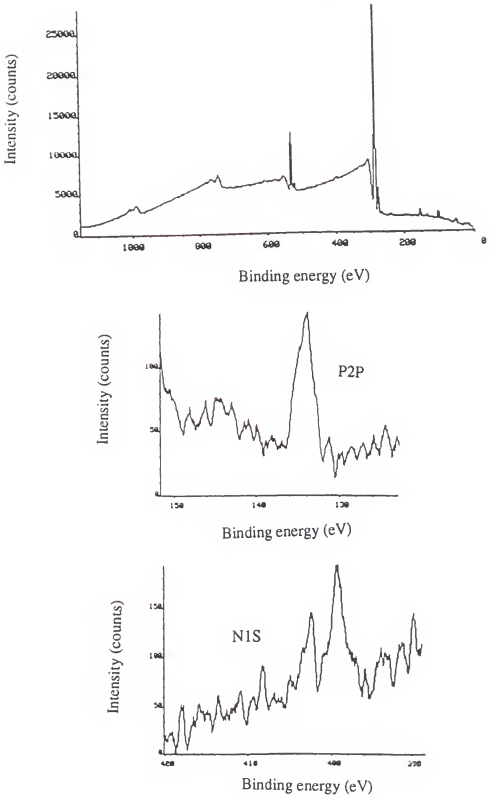

Figure 71. XPS spectrum of 12-PL modified PP by UV radiation method (0.1%, UV time of 2 hours)

Table 14. XPS of 12-PL modified PP by UV radiation at 0.1% and UV time of 1 and 2 hours

12-PL concentration(%)	UV time (hrs)	Atomic concentration (%) C1s	O1s	N1s	P2p
0.1	2	84.0	14.1	0. 5	1.4
0.1	1	85.1	14.2	0.3	0.4
12-PL theoretic atomic concentration		75.4	20.8	1.9	1.9

of PDMS and PDMS modified with 12- PL at 0.1% by UV radiation is shown in Table 15. The 12-PL modified PDMS at 0.1% and UV time 1 and 2 hours had lower C.A.s ($20s^0$) than unmodified PDMS. The surfaces of PDMS modified with 12-PL by UV radiation at these specified grafting conditions were hydrophilic. The FTIR/ATR spectrum and peak assignments of PDMS are presented in Figure 72. After surface modification, the resulting spectrum for the samples treated at 0.1% and 2 hours is shown in Figure 73. The carbonyl peak at 1730 cm^{-1}, corresponding to 12-PL, was observed. As discussed in previous section, a possible explanation for the presence of this carbonyl peak is oxidation by UV radiation. The resulting FTIR/ATR spectrum of PDMS under UV radiation for 2 hours is presented in Figure 74. No carbonyl peak was detected in the spectrum. Oxidation by UV radiation did not produce the carbonyl peak. Therefore, the carbonyl peak is due to the grafting of 12-PL by UV radiation. The carbonyl peak cannot be observed for 12-PL modified PDMS at 0.1% and UV time 1 hour.

The XPS spectrum of PDMS is presented in Figure 75. As expected, three elements (C,O,Si) were detected and the ratio of each element's atomic concentration were close to theoretical values. After surface modification, the results of XPS are summarized in Table 16. Extra N1S and P2P, corresponding to 12-PL,were detected on the surfaces of modified PDMS at 0.1% and UV time 1 and 2 hours. The ratio of N1S to P2P atomic concentration was close to 1 at 0.1% and UV time 2 hours. However, the atomic concentration of N1S and P2P for 12-PL modified PDMS were lower than the theoretical values (1.9%). One possible reason for the lower N1S and P2P atomic concentrations for modified PDMS is that Si-O chains of PDMS are very flexible so that the hydrophobic methyl groups may migrate to the top layer in the high vacuum environment.

Table 15. C.A.s of 12-PL modified PDMS by UV radiation at 0.1% and UV time of 1 and 2 hours

12-PL concentration (%)	UV time (hrs)	C.A. (degree)
0.1	2	19±2
0.1	1	21±1
Unmodified PDMS		89±2

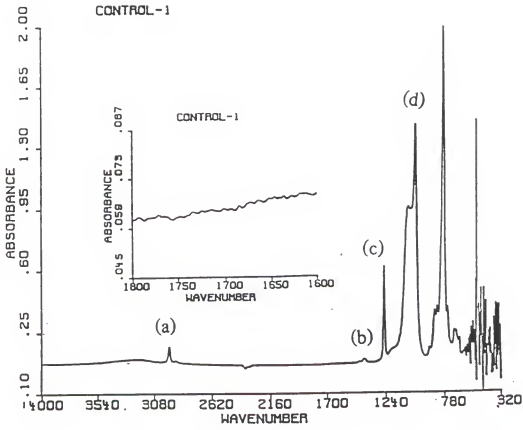

	$\nu(cm^{-1})$	assignment	
(a)	2961	$-CH_3$	stretch
(b)	1412	$-CH_3$	bend
(c)	1256	$-Si-CH_3$	stretch
(d)	1006	-Si-O-Si	stretch

Figure 72. FTIR/ATR spectrum of unmodified PDMS

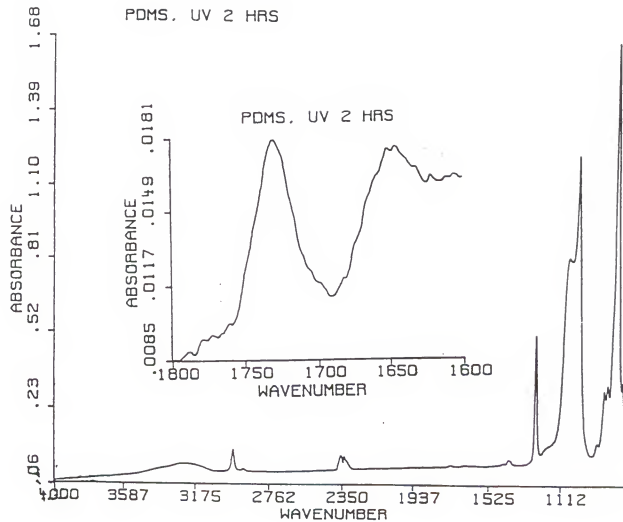

Figure 73. FTIR/ATR spectrum of 12-PL modified PDMS after UV radiation (0.1%, UV time of 2 hours)

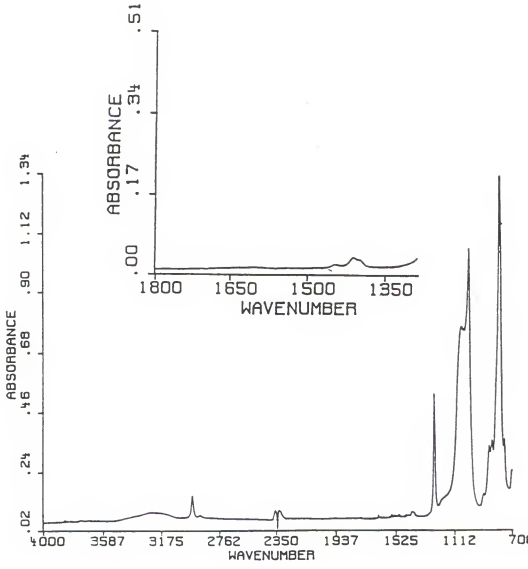

Figure 74. FTIR/ATR spectrum of unmodified PDMS after UV radiation of 2 hours

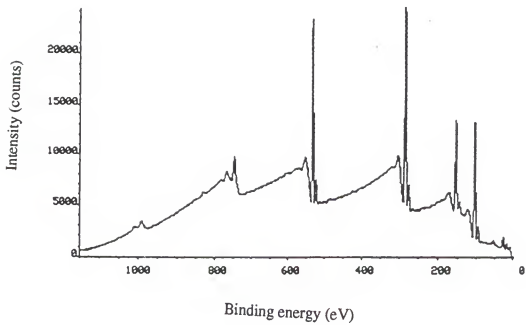

Atomic concentration (%) : C1S = 33.1, O1S = 22.3, Si2P = 44.6

Figure 75. XPS spectrum of unmodified PDMS

Table 16. XPS of 12-PL modified PDMS by UV radiation at 0.1% and UV time of 1and 2 hours

12-PL concentration(%)	UV time (hrs)	Atomic concentration (%) Si2p	C1s	O1s	N1s	P2p
0.1	2	37.9	39.0	21.8	0.7	0.7
0.1	1	35.1	42.5	21.2	1.0	0.3
12-PL theoretical atomic concentration		0	75.4	20.8	1.9	1.9

4.7.3 Summary

Surface modification for PP and PDMS with 12-PL by UV radiation at 0.1% and UV time 1 and 2 hours produced hydrophilic surfaces as indicated from low C.A.s. The carbonyl peak at 1720 cm^{-1} which corresponds to the chemical structure of 12-PL was observed in FTIR/ATR for modified PP and PDMS at 0.1% and UV time 2 hours. For XPS, extra N1S and P2P atomic concentrations, from poly12-PL grafts, were observed for modified PP and PDMS. This surface modification method with 12-PL by UV radiation provided the versatility for a variety of polymeric substrates such as PMMA, PP and PDMS.

4.8. Miscellaneous Study

Hydrophilic monomer, NVP, has been widely used to graft onto PMMA by gamma radiation induced polymerization in our laboratory (38). It is interesting to know whether HEMA-PL can graft on NVP modified PMMA. First, PMMA was grafted with 10% NVP by gamma radiation at 0.15 Mrad. After washing with water, the surface of NVP modified PMMA was characterized by C.A. and XPS. The C.A. for the NVP modified PMMA was 21^0. Atomic concentrations of N1S was 4.7%. No extra phosphous was observed for NVP modified PMMA. Then, NVP modified PMMA was grafted again with HEMA-PL at 2% and 0.1 Mrad. The C.A. for the modified PMMA was 23^0. Atomic concentration of N1S was reduced from 4.7% to 1.8% while extra 2.4% P2P was observed. The extra phosphorus confirmed the polyHEMA-PL grafts. Also, the atomic concentrations of N1S and P2P were very close to each other while theoretical values were 2.1%. Furthermore, the resultant PMMA surfaces were hydrophilic indicating that the hydrophilic heads of HEMA-PL were oriented towards water. Hydrophilic double grafting, NVP followed by HEMA-PL, on PMMA using gamma radiation was performed. As discussed before,

HEMA-PL also could graft on water RF plasma pretreated PMMA which was hydrophilic after pretreatment. However, the mechanism of HEMA-PL grafted on NVP modified PMMA needs to be further studied.

Copolymerization of NVP with HEMA-PL by gamma radiation in this study was also tried to modify PMMA surfaces. Three different concentration ratios of NVP vs. HEMA-PL (2:1, 1:1, and 1:2) at total 6% were studied. After sonication, the initial milky suspension turned clear. This indicated that NVP increased the solubility of HEMA-PL in water. After gamma radiation at 0.15 Mrad, the modified PMMA was characterized by C.A. and XPS. The resultant solutions at each concentration ratio after gamma radiation became milky and viscous. C.A. for modified PMMA at 2:1 and 1:2 (NVP: HEMA-PL) were 70^0 and 73^0 respectively. However, C.A. for the modified PMMA at 1:1 (NVP:HEMA-PL) was 32^0. For XPS, 5.3% N1S and 1.6% P2P were observed for modified PMMA at 1:1(NVP:HEMA-PL, total 6%) and 0.15 Mrad. For NVP grafting alone, it is impossible to obtain phosphorus. Also, it was unlikely to have such high 5.3% of N1S if HEMA-PL was all grafted on PMMA. Therefore, NVP and HEMA each contributed to the hybrid grafts on modified PMMA. Total concentrations of 3% with ratios of 2:1, 1:1, and 1:2 (NVP:HEMA-PL) at 0.15 Mrad were also used. However, hydrophobic surfaces were observed since C.A.s were 71^0, 72^0. As indicated from previous discussions, lower HEMA-PL concentration (0.5%, 0.15) can be used to modify PMMA. However, the concentration of NVP to obtain graft at 0.15 Mrad is higher than 3%. This may be due to the difference in reactivity ratio of NVP and HEMA-PL.

Also, PMMA pregrafted with NVP (10%, 0.15 Mrad) was modified by copolymerization of NVP with HEMA-PL at 2:1, 1:1, and 1:2 ratio (NVP:HEMA , total 6%) by gamma radiation at 0.1 Mrad. At 2:1 and 1:2 ratio (NVP:HEMA-PL), no extra phosphorus was observed for the modified PMMA in XPS although C.A.s were 23^0 and 24^0. Low C.A.s were due to the NVP pregraft. At 1:1 ratio of NVP vs. HEMA-PL, extra 1.4% P2P and 5.5% N1S were observed in XPS. Again, the phosphorus was due to

HEMA-PL and the nitrogen was mostly due to NVP. C.A. of the modified PMMA was 21^0.

CHAPTER V
SUMMARIES AND CONCLUSIONS

The present study successfully demonstrated the feasibility of grafting hydrophilic polyPL surfaces onto PMMA, PP, and PDMS by various surface modification techniques to improve their biocompatibility. These techniques involved gamma or UV radiation either separately or coupled with water RF plasma pretreatment of the substrates. Two polymerizable PL monomers (HEMA-PL and 12-PL) were synthesized via improved synthesis pathways and characterized by IR and ^{1}HNMR . HEMA-PL is a novel compound not previously reported. The synthesis of HEMA-PL was composed of three steps:(1) esterification of HEMA with adipoyl, (2) anhydride formation by reaction with DCC, and (3) acylation of GPPC with the anhydride. The overall yield of these three steps was 37% (82% x 82%x 51%). The synthesis of 12-PL also involved three steps: fatty acid formation with vinyl groups, anhydride formation, and acylation of GPPC with the anhydride. This synthesis was a modification of Larson's method in that no inhibitor was used, GPPC was thoroughly dried by repeated benzene evaporation and the required time for acylation was reduced to 30 hours. As a result, a much higher yield of 12-PL (64%) has been achieved as compared to Regen's (36%) and Larson's (14%) methods.

Surface modified PMMA with HEMA-PL was accomplished by gamma radiation induced graft polymerization with 1 to 10% HEMA-PL dispersion and with 0.03 to 0.15 Mrad. Low C.A.(20s) of HEMA-PL modified PMMA indicated that the modified surfaces are hydrophilic. In XPS analysis, extra nitrogen and phosphorus were observed on the modified surfaces confirming the polyHEMA-PL grafts. The atomic concentration ratios of N/P at most grafting conditions were close to one. SEM indicated no change in surface morphology. UV-VIS transmission was not significantly attenuated by the grafts. FTIR/ATR spectra did not detect the grafts due to the overlap of carbonyl peaks between

HEMA-PL and PMMA. Ellipsometry measurements calculated a graft thickness of 410 Å and a refractive index slightly lower than PMMA. The polyHEMA-PL graft is thus composed of 18 monolayers. HEMA-PL modified PMMA at 2% concentration and 0.07 Mrad has significantly less epithelial cell adhesion and corneal endothelial cell damage than unmodified PMMA.

The plasma/gamma method was also used to modify PMMA surfaces with HEMA-PL. This method involves pretreatment of PMMA with water RF plasma followed by gamma radiation. Water RF plasma at 3 minutes treatment time, 50W and 0.1 torr was chosen to prepare hydrophilic surfaces of PMMA. After gamma radiation of pretreated PMMA, modified PMMA had higher nitrogen and phosphorus atomic concentrations than PMMA modified by gamma radiation alone at same grafting conditions. The resulting PMMA surfaces were hydrophilic with low C.A.s ($20s^0$). The graft thickness (272 Å) of HEMA-PL modified PMMA by this method was thinner than the graft (410Å) prepared without plasma pretreatment. The refractive index of the polyHEMA-PL graft was slightly lower than the PMMA substrates. The grafts by this method were also multilayers (12 monolayers). PMMA modified by water RF plasma pretreatment alone was unable to inhibit epithelial cell adhesion although the surfaces were hydrophilic. However, HEMA-PL modified PMMA by the plasma/gamma method had no epithelial cell adhesion and had less endothelial cell and platelet adhesion than unmodified PMMA. The ratio of endothelial vs platelet cells was less than 1.

Surface modification of PMMA with 12-PL was created by UV and plasma/UV methods at concentrations of 0.02 to 0.1% and UV times from 1 to 2 hours. In the plasma/UV method, PMMA was pretreated with water RF plasma (3 mins, 50W, and 0.1 torr) and irradiated in a 12-PL monomer dispersion by UV radiation. The resulting surfaces by both methods were hydrophilic with low C.A.s (20s). In XPS analysis, PMMA modified by the plasma/UV method had higher nitrogen and phosphorus atomic concentrations than without pretreatment of PMMA. At the concentration of 0.1% and UV

time of 2 hours, modified PMMA by the plasma/UV method produced higher N1S and P2P atomic concentrations than the theoretical values (1.9%). The graft thickness of modified PMMA by the plasma/UV method (443Å, 19 monolayers) was less than that achieved without plasma pretreatment (586Å, 25 monolayers). Poly12-PL grafts on PMMA prepared by both methods at 0.1% and UV time of 2 hours had less epithelial cell adhesion than unmodified PMMA although some spardic cells constrained in fixed areas were observed and the ratios of endothelial/ platelet cell adhesion were higher than one. Furthermore, platelet cell adhesion of modified PMMA prepared by both methods was substantially lower than unmodified PMMA. Hydrophilic poly12-PL grafting on PMMA has a potential as a nonthrombogenic surface.

12-PL modified PP and PDMS by UV radiation at 0.1% and UV 1 and 2 hours produced hydrophilic surfaces as indicated from low C.A.s. The carbonyl peak at 1720 cm^{-1} which corresponds to the chemical structure of 12-PL was observed in FTIR/ATR for modified PP and PDMS at 0.1% dispersion and UV time of 2 hours. For XPS, extra nitrogen and phosphorus atomic concentrations were observed for modified PP and PDMS.

In conclusion, high yield synthesis of novel polymerizable PL (HEMA-PL and 12-PL) and grafting these PLs onto PMMA, PP, and PDMS was accomplished. Hydrophilic polyPL surfaces improve implant biocompatibilty.

LIST OF REFERENCES

1. J.A. Hayward and D. Chapman, "Biomembrane Surfaces as Models for Polymer Design: The Potential for Haemocompatibility," Biomaterials, 5, 135-142, 1984.

2. P. Chakrabarti and H.G. Khorana, "A New Approach to the Study of Phospholipid-Protein Interactions in Biological Membranes. Synthesis of Fatty Acids and Phospholipids Containing Photosensitive Groups," Biochemistry, 14, No. 23, 5021-5033, 1975.

3. J.E. Rothman and J. Lenard, "Membrane Asymmetry," Science, 195, 743-753,1977.

4. S.L. Regen, P. Kirszensztejn, and A. Singh, "Polymer-Supported Membranes. A New Approach for Modifying Polymer Surfaces," Macromolecules, 16, 335-338, 1983.

5. E.P. Goldberg, A. Yahiaoui, and J.W. Burns, "Combined Glow Discharge Plasma and Gamma-Radiation Polymerization Method for Modifying Surfaces," Patent application (1991).

6. J. Sheets, "Hydrophilic Polymer Coatings to Prevent Tissue Adhesion," Ph.D. Dissertation, University Of Florida, 1983.

7. J. Larson, "Hydrophilic Surface Modifications of Poly(Methyl Methacrylate)," M.S. Thesis, University of Florida, 1984.

8. W. Bloom and D.W. Fawcett, A Textbook of Histology, W.B. Saunders Company, Philadelphia, 1975.

9. S.J. Singer and G.L. Nicolson, "The Fluid Mosaic Model of the Structure Of Cell Membranes," Science, 175, 720-731, 1972.

10. J.H. Fendler, Membrane Mimetic Chemistry, John Wiley and Sons, New York, 1984.

11. M.S. Bretscher, "Membrane Structure: Some General Principles," Science, 181, 622-629, 1973.

12. L. Stryer, Biochemistry, W.H. Freeman and Company, New York, 1981.

13. G.L. Gaines, Insoluble Monolayers At Liquid-Gas Interfaces, Interscience, New York,1966.

14. S.L. Regen, A. Singh, G. Oehme and M. Singh, "Polymerized Phosphatidylcholine Vesicles: Stabilized and Controllable Time-Release Carriers," Biochemical and Biophysical Research Communications, 101, No.1, 131-136,1981.

15. E. Hasegawa, K. Eshima, Y. Matsushita, H. Nishide, and E. Tsuchida, "Stabilization and Degradation: Synthesis of Polymerizable Glycerophosphocholines and Their Polymerized Vesicles," Polymer Bulletin, 14, 31-38,1985.

16. H. Bader, K. Dorn, B. Hupfer, H. Ringsdorf, "Polymeric Monolayers and Liposomes as Model for Biomembranes. How to Bridge the Gap Between Polymer Science and Membrane Biology," Advances in Polymer Science, 64, 1-62, 1985.

17. H.H. Hub, B. Koch, and H. Ringsdorf, "Polymerizable Phospholipid Analogues-New Stable Biomembrane and Cell Models," Angew.Chem., 19, 938-940,1980.

18. H. Bader, H. Ringsdorf, and J. Skura, "Liposomes from Polymerizable Glycolipids," Angew. Chem., 20, 91-92, 1981.

19. K. Fukuda, Y. Shibasaki, H. Nakahara, "Binary Mixed Monolayers of Poly(vinyl stearate) and Simple Long-Chain Compounds at the Air/Water Interface," J. Macromol. Sci.-Chem.,15, 999,1981.

20. C.M. Gupta, R. Radhakrishman, and H.G. Khorana, " Glycerophospholipid Synthesis: Improved General Method and New Analogs Containing Photoactivable Groups," Proc. Natl. Acad. Sci. U.S.A.,Vol.74, No.10, 4315-4319, 1977.

21. R. Aneja and J.S. Chadha, "Acyl-Chloro-Deoxyglycerophosphorylcholines: Structure of the So-Called Cylic Lysolecithins," Biochim.Biophys. Acta, 239, 84-91, 1971.

22. Y. Lapidot, I. Barzilay,J. Hajda, "Synthesis of Diacyl-DL-(and L)-α-glycerolphosphates," Chem.Phys. Lipids, 3, 125-134,1969.

23. H.T. Tien, Bimolecular Lipid Membranes, Theory, and Practice, Dekker, New York, 1974.

24. A. Blume, "A Comparative Study of the Phase Transitions of Phospholipid Bilayers and Monolayers," Biochim. Biophys. Acta, 557,32-44, 1979.

25. H.P. Jennissen, "General Aspects of Protein Adsorption," Makromole.Chem., Macromol. Symp., 17, 111-134, 1988.

26. R.E. Baier, E.G. Shafrin, W.A. Zisman, "Adhesion: Mechanisms that Assist or Impede It," Science, 162, 1360, 1968.

27. J.D. Andrade, "Principles Of Protein Adsorption" in Surface And Interfacial Aspects of Biomedical Polymers ,Vol.2, p.1, Plenum Press, New York, 1985.

28. H. Tanzawa, S. Nagaoka, J. Suzuki, S. Kobayashi, Y. Masubuchi, T. Kikuchi,"Cell Adhesion and Growth on the Surface of Synthetic Hydrogels" in Biomedical Polymers. Polymeric Materials And Pharmaceuticals For Biomedical Use, p.189, Academic Press Inc., New York, 1980.

29. T.A. Horbett, "Protein Adsorption To Hydrogels" in Hydrogels In Medicine And Pharmacy, Vol.1, p.127, CRC Press, Boca Raton, 1987.

30. K. Ishihara, N.P. Ziats, B.P. Tierney, N. Nakabayashi, and J.M. Anderson, "Protein Adsorption from Human Plasma Is Reduced on Phospholipid Polymers," The 17th

Annual Meeting of the Society For Biomaterials, May 1-5, Scottsdale, Arizona, 1991.

31. E. Ruckenstein and S.V. Gourisankar, "A Surface Energetic Criterion of Blood Compatibility of Foreign Surfaces," J. Colloid Interface Sci., 101, 436, 1984.

32. B.D. Ratner, "Surface Structure of Polymers for Biomedical Applications," Makromol. Chem. Macromol. Symp., 19, 163, 1988.

33. B.D. Ratner, A.B. Johnston, and T.J. Lenk, "Biomaterial Surfaces," Journal Of Biomedical Materials Research: Applied Biomaterials, 21, No. A1, 59, 1987.

34. M.S. Jhon and J.D. Andrade, "Water and Hydrogels," J. Biomed. Mater. Res., 7, 509, 1973.

35. H. Yasuda, A.K. Sharma, and T. Yasuda, "Effect of Orientation and Mobility of Polymer Molecules at Surfaces on Contact Angle and Its Hysteresis," J. Polym.Sci. Polym. Phys. Ed., 19, 1285, 1981.

36. L. Vroman, "Protein/Surface Interaction" in Biocompatible Polymers, Metals and Composites, Technomic Publishing Co. Inc., Lancaster, Pennsylvania, 1983.

37. K.B. Blodgett, "Films Built by Depositing Successive Monomolecular Layers on a Solid Surface," J. Am. Chem. Soc., 57, 1007, 1935.

38. O. Albrecht, D.S. Johnston, C. Villaverde, and D. Chapman, "Stable Biomembrane Surfaces Formed by Phospholipid Polymers," Biochimica et Biophysica Acta, 687, 165, 1982.

39. K. Ishihara, R. Aragaki, T. Ueda, A. Watenable, and N. Nakabayashi, "Reduced Thrombogenicity of Polymers Having Phospholipid Polar Groups," Journal Of Biomedical Materials Research, 24, 1069, 1990.

40. A. Yahiaoui, "Surface Modification of Intraocular Lens Polymers by Hydrophilic Graft Polymerization for Improved Ocular Implant Biocompatibility," Ph.D. Dissertation, University Of Florida, 1990.

41. J.E. Wilson, Radiation Chemistry of Monomers, Polymers and Plastics, Marcel Dekker Inc., New York, 1974.

42. A. Charlesby, Atomic Radiation of Polymers, Pergamon Press, Oxford, 1960.

43. M. Tsuda, and S. Oikawa, "Theoretical Aspects of the Radiation Effects of Polymers," J. Polym. Sci. Polym. Chem. Ed., 17, 3759, 1979.

44. H. Wilski, "The Radiation Induced Degradation of Polymers," Radiat. Phys. Chem., 29, 1-14, 1987.

45. B. Ranby, and J.F. Rabek, Photodegradation, Photo-oxidation and Photostabilization Of Polymers: Principles and Applications, Wiley & Sons, New York, 1975.

46. A.R. Shultz, P.I. Roth, and J.M. Berge, "Radiation Degradation of Polymethaacrylates. Dose Rate and Medium Effects," J. Polym. Sci., Part A, 1, 1651, 1963.

47. M. Imai, L.-G. Xu, K. Ametani, and M. Tutiya, "Gamma-Irradiation of PP in Vacuum and in Air," J. Polym. Sci. Polym. Chem. Ed., 27, 1763, 1989.

48. M.G. Omerod, and A. Charlesby, "The Radiation Chemistry of Some Polysiloxanes: An ESR Study," Polymer, 4, 459, 1963.

49. H. Menhoffer, and H. Hensinger, "Radical Formation in Polydimethylsiloxanes and Polydimethyldiphenylsiloxanes Studied by the ESR Spintrap Technique," Radiat.Phys. Chem., 29, 243,1987.

50. A. Todd, "The Mechanisms of Radiation-Induced Changes in Vinyl Polymer,"J. Polym. Sci., 42, 223, 1960.

51. A. Chapiro, Radiation Chemistry Of Polymeric Systems, Wiley- Interscience, New York, 1962.

52. H. Yasuda, Plasma Polymerization, Academic Press Inc., New York, 1985.

53. J.R. Hollahan and A.T. Bell, Techniques And Applications Of Plasma Chemistry, Wiley & Sons, New York, 1974.

54. D.R. Johnson, Y. Osada, A.T. Bell, and M. Shen, "Studies of the Mechanisms and Kinetics of Plasma-Initiated Polymerization of Methyl Methacrylate," Macromolecules, 14, 118, 1981.

55. T.G. Vargo, J.A. Gardella, and L. Salvati, "Multitechnique Surface Spectroscopic Studies of Plasma Modified Polymers. III H_2O and O_2/H_2O Plasma Modified PMMA," J. Polym. Sci. Polym. Chem. Ed., 27, 1267, 1989.

56. R.G. Nuzzo, and G. Smolinsky, "Preparation and Characterization of Functionalized PE Surfaces," Macromolecules, 17, 1013, 1984.

57. R.C. Augusteyn, "Protein Modification in Cataract. Possible Oxidative Mechanisms." in Mechanisms of Cataract Formation In The Human Lens, Ed. G. Duncan, p.71, Academic Press, New York, 1981.

58. J.J. Harding, "Cataract Epidemiology," Current Opinion in Ophthalmology, 1, 10, 1990.

59. R. De Natale, J. Flammer, M. Zulanf, T. Bebie, "Influence of Age on the Transparency of the Lens in Normals," Ophthalmological, 197, 14, 1988.

60. S. Zigman, T. Yulo, and J. Schultz, "Possible Roles of Near UV Light in the Cataractous Process," Exp. Eye Res., 15, 201, 1973.

61. P. Vidal and J. Cabezas-Cerrato, "The Stable Products of the NonenzymaticGlycation of Pig Crystallines: New Findings Related to the Pathogenesis of Diabetic Cataracts", Diabetes Res., 8, 183, 1988.

62. K.S. Morgan, "Congenital And Infantile Cataracts," Current Opinion in Opthalmology, 1, 20, 1990.

63. S. Masket, "Pathogenesis and Pathophysiology of Cataracts," Current Opinion in Ophthalmology, 1,5, 1990.

64. J.W. Morgan, Modern Cataract Surgery and Artificial Lens Implants, D. Armstrong Co., Inc., Houston, 1983.

65. N.S. Jaffe, "The Outlook for Intraocular Lenses Through 1990," J. Cataract Refract. Surg., 12, 267, 1986.

66. A.C. Neumann, and B. Cobb, "Advantages And Limitations of Current Soft Intraocular Lenses," J. Cataract Refract. Surg., 15, 257, 1989.

67. J. Brandrup, and E.H. Immergut , Eds., Polymer Handbook, John Wiley & Sons, New York, 1979.

68. Encyclopedia of Modern Plastics, McGraw Hill, New York, 1991.

69. C.C. Cory, "Prevention and Treatment of Postimplantation Astigmatism," J. Cataract Refract. Surg.,15,58, 1989.

70. W.T. Parker, and G.S. Clorefine, "Long-term Evolution Of Astigmatism Following Planned Extracapsular Cataract Extraction," Arch. Ophthalmol, 107, 353, 1989.

71. D.J. Apple, N. Mamalis, K. Loftfield, J.M. Googe, L.C. Novack, D.K. Van-Norman, S.E. Brady, and R.J. Olson, "Complications of IOLs: Historical and Histopathological Review," Surv. Opthalmol., 29, 1, 1984.

72. E.P. Goldberg, F.M. Hofmeister, M. Yalon, S. Ida, J. Stacholy, P. Martin, A. Yahiaoui, and J.W. Sheets, "Hydrophilic Surface Modification of IOL Implants to Reduce Surgical and Post Operative Ocular Tissue Trauma," The Academy of Surgical Research Meeting, Boston, 1988.

73. E.P. Goldberg, F.M. Hofmeister, M. Yalon, J.W. Sheets, J. Stacholy, P. Martin, A. Ito, A. Yahiaoui, and R. Robinson, "Tissue Protective Properties of Permanent Hydrophilic Surface Modification Of PMMA: Iris Abrasion and Endothelium Damage Studies," 2nd American International Congress on Cataract, IOL and Refractive Surgery Meeting, Washington DC, 1989.

74. S.D. Bruck, "Macromolecular Aspects Of Biocompatible Materials--A Review," J. Biomed. Mater. Res., 6, 173, 1972.

75. J.M. Seeger, and N. Klingman, "Improved In Vivo Endothelialization of Prosthetic Grafts by Surface Modification with Fibronectin," J. Vasc. Surg., 8, 476, 1988.

76. T.A. Horbett, P.K. Weathersby, and A.S. Hoffman, "Hemoglobin Adsorption to Three Polymer Surfaces," Thromb. Res., 12, 319, 1978.

77. A.S. Hoffman, "Principles Governing Biomolecule Interactions at Foreign Interfaces," J. Biomed. Mater. Res. Symp., 5, 77, 1974.

78. S.R. Hanson, L.A. Harker, B.D. Ratner, and A.S. Hoffman, "In Vivo Evaluation of Artificial Surfaces with a Nonhuman Primate Model of Arterial Thrombosis," J. Lab. Clin. Med., 95, 289, 1980.

79. C.M. Jackson, and Y. Nemerson, "Blood Coagulation," Ann. Rev. Biochem., 49, 765, 1980.

80. H.J. Weiss, "Platelet Physiology and Abnormalities of Platelet Function," N. Eng. J. Med., 293, 580, 1975.

81. J.J. Sixma, "Platelet Coagulant Activities," Thromb. Haemostas., 40, 163, 1978.

82. O.D. Ratnoff, "The Role Of Haemostatic Mechanisms," Clin. Haematol., 10, 261, 1981.

83. A.P. Kaplan, M. Silverberg, J.T. Dunn, and G. Miller, "Mechanisms for Hageman Factor Activation and Role of HMW Kininogen as a Coagulation Cofactor," Ann. N.Y. Acad. Sci., 370, 253, 1981.

85. P.N. Walsh, and J.H. Griffin, "Platelet-coagulant Protein Interactions in Contact Activation," Ann. N. Y. Acad. Sci., 370, 241, 1981.

86. H.Y.K. Chuang, and S.P. Mitra, "Adsorption and Reactivity of Human Prothrombin to Artificial Surfaces," J. Biomed. Mater. Res., 18, 695, 1984.

87. R.F.A. Zwaal, "Membrane and Lipid Involvement in Blood Coagulation," Biochim. Biophys. Acta, 515, 163, 1978.

88. R.F.A. Zwaal, and H. C. Hemker, "Blood Cell Membranes and Haemostasis," Haemostasis, 11, 12, 1982.

89. A.D. Bangham, "A Correlation Between Surface Charge and Coagulant Action of Phospholipids," Nature, 192, 1197, 1961.

90. J.D. Andrade, "Surface Chemistry and Physics" in Surface and Interfacial Aspects of Biomedical Polymers ,Vol. 1, p. 4, Plenum Press, Inc., New York, 1985.

91. Din-Guo Chen, "Synthesis and Characterization of GeO_2-SiO_2 Waveguides," Ph.D. Dissertation, University of Florida, August 1991.

92. F.M. Hofmeister, "Biosurface Properties of Ocular Implant Polymers," M.S. Thesis, University Of Florida, 1988.

93. S. Reich, M. Levy, A. Meshorer, M. Blumenthal, M. Yalon, J. W. Sheets, and E.P. Goldberg, "Intraocular Lens- Endothelial Interface: Adhesive Force Measurements," J. Biomed. Mater. Res., 18, 737, 1984.

94. Z. Selinger and Y. Lapidot, "Synthesis of Fatty Acid Anhydrides by Reaction with Dicyclohexylcarbodiimide," Journal of Lipid Research , 7, p.174, 1966.

95. E. Bare and D. Buchnea, "Synthesis of Saturated and Unsaturated L-α-Lecithins," Can. J. Biochem. Physiol., 37, 953, 1959.

96. E. Cubero Robles and D. Van Den Berg, "Synthesis of Lecithins by Acylation of O-(sn-Glycero-3-Phosphoryl) Choline with Fatty Acid Anhydrides", Biochim.Biophys. Acta, 187,.520, 1969.

97. S.L. Regen, A. Singh, G.Oehme,and M.Singh, "Polymerized Phosphatidylcholine Vesicles. Synthesis and Characterization," J. Am.Chem. Soc., 104, 791, 1982.

98. O. Nishi, " Removal of Lens Epithelial Cells by Ultrasound in Endocapsular Cataract Surgery," Ophthalmic Surgery, 18, No.8, 577, August 1987.

99. O. Nishi, "Intercapsular Cataract Surgery with Lens Epithelial Cell Removal. Part I: Without Capsulorhexis," J. Cataract Refract. Surg., 15, 297, May 1989.

100. O. Nishi, "Fibrinous Membrane Formation on the Posterior Chamber Lens During the Early Postoperative Period," J. Cataract Refract. Surg., 14, 73, January 1988.

101. D.T. Clark and A. Dilks, "ESCA Applied to Polymers. XV. Radio Frequency Glow Discharge Modification of Polymers Studied by Means of ESCA in Terms of Direct and Radiative Energy Transfer Model," J. Polym. Sci. Polym. Chem. Ed., 15, 2321, 1977.

102. C M. Cunanan, N. M. Tarbaux, and P. M. Knight, "Surface Properties of Intraocular Lens Materials and Their Influence on In Vitro Cell Adhesion," J.Cataract Refract Surg., 17, 767, November 1991.

103. M. Szycher, Ed., Biocompatible Polymers, Metals, and Composites, Technomic Publishing Co., Lancaster, Pa., 1983.

104. J.A. Hayward, A.A. Durrani, C.J. Shelton, D.C. Lee, and D. Chapman, "Biomembranes as Models for Polymer Surfaces. III. Characterization of a Phosphorylcholine Surface Covalently Bound to Glass," Biomaterials, 17, 126, 1986.

BIOGRAPHICAL SKETCH

Jung-Hua Steven Kuo was born August 21, 1959, in Tainan, Taiwan. In 1982, he graduated from the National Central University with a B.S. degree in chemical engineering. After serving in the Army for two years, he worked for Formosa Plastics Corporation as an assistant engineer for 2 years.

He began his graduate studies at the University of Alabama, in the spring 1986 and earned a master's degree in chemical engineering in 1988. He then entered at the University of Florida in August 1989. Since then, he has worked to complete the requirements necessary to obtain his doctorate degree in materials science and engineering.

He served as a graduate research assistant in the Department of Materials Science and Engineering, University of Florida, and was a member of American Chemical Society and the Society for Plastics Engineers.

I certify that I have read this study and that in my opinion it conforms to acceptable standards of scholarly presentation and is fully adequate, in scope and quality, as a dissertation for the degree of Doctor of Philosophy.

Eugene P. Goldberg, Chairman
Professor of Materials Science and Engineering

I certify that I have read this study and that in my opinion it conforms to acceptable standards of scholarly presentation and is fully adequate, in scope and quality, as a dissertation for the degree of Doctor of Philosophy.

Anthony B. Brennan
Assistant Professor of Materials Science and Engineering

I certify that I have read this study and that in my opinion it conforms to acceptable standards of scholarly presentation and is fully adequate, in scope and quality, as a dissertation for the degree of Doctor of Philosophy.

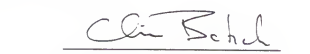

Christopher D. Batich
Professor of Materials Science and Engineering

I certify that I have read this study and that in my opinion it conforms to acceptable standards of scholarly presentation and is fully adequate, in scope and quality, as a dissertation for the degree of Doctor of Philosophy.

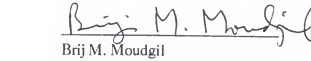

Brij M. Moudgil
Professor of Materials Science and Engineering

I certify that I have read this study and that in my opinion it conforms to acceptable standards of scholarly presentation and is fully adequate, in scope and quality, as a dissertation for the degree of Doctor of Philosophy.

Randolph S. Duran
Associate Professor of Chemistry

This dissertation was submitted to the Graduate Faculty of the College of Engineering and to the Graduate School and was accepted as partial fulfillment of the requirements for the degree of Doctor of Philosophy.

December, 1992

Winfred M. Phillips
Dean, College of Engineering

Madelyn M. Lockhart
Dean, Graduate School